Review of Rotor Loads Prediction With the Emergence of Rotorcraft CFD

Anubhav Datta
Assistant Research Scientist
Alfred Gessow Rotorcraft Center

Mark Nixon
Chief of Loads and Dynamics
U.S.Army Research Labs, NASA Langley

Inderjit Chopra
Professor and Director, Alfred Gessow Rotorcraft Center
Department of Aerospace Engineering
University of Maryland

ABSTRACT

This paper reviews the state of the art in helicopter rotor loads prediction using Computational Fluid Dynamics (CFD) and Computational Structural Dynamics (CSD) coupling. The application of CFD to rotorcraft problems has evolved, over the period 1990 to 2005, as a viable means to improve the aerodynamic modeling used in rotorcraft comprehensive analyses (CA). CFD/CSD coupling has the potential to meet the long term objective of a coupled rotor-fuselage analysis that can predict accurate loads and vibration at all critical flight conditions without empirical or semi-empirical inputs. This paper reviews the capabilities and limitations of current CFD analyses to capture the key aerodynamic phenomena driving critical rotor loads: wake, dynamic stall and tip transonic effects. Recent initiatives in CFD/CSD coupling, targeted to improve predictions of rotor loads, are discussed. The high speed (155 kts) forward flight condition of the UH-60A BlackHawk is studied as a test case. The flight condition falls in a critical high vibration regime, where the mechanisms of rotor vibratory loads were not clearly understood. Significant improvements in fundamental understanding and prediction of vibratory loads at this flight condition has been recently demonstrated by researchers using CFD/CSD coupling. The physical mechanisms involved, and the role of CFD in improving predictions is explained.

INTRODUCTION

The importance of rotor loads evolves from the rotorcraft design need to provide structures that are at minimum weight for the anticipated load conditions. Dynamic loads from rotor blades transmit throughout the aircraft, and is the dominant consideration in subcomponent design. Dynamic loads are *predicted* for a new system using previous experience, experimental data, and analysis. An analysis which can accurately *calculate* the loads over a wide range of flight conditions, without significant empirical input and corrections based on experimental data, provides the greatest flexibility and efficiency. The goal of the aeromechanics community is to develop such a capability. It will: (1) reduce the costs and risks associated with the development and testing of new rotor systems, and (2) generate new designs which reduce loads, vibration, noise, enhance performance, and extend the rotary wing flight envelope. An explosion in computational power over the last decade has provided an impetus for accelerated growth of this technology.

Presented at the 31st European Rotorcraft Forum, September 13-15, Florence, Italy, Europe 2005

Previous reviews

There have been several significant survey and workshop papers containing assessments of analysis capabilities to predict blade loads. Bousman and Mantay (Ref. 1) provided a comprehensive review of loads research over the period 1974 to 1987, using the 1973 AGARD Milan meeting and the 1974 hypothetical rotor comparison by Ormiston (Ref. 2) as the key occurrence initiating the time period. More recently in 1998, Hansford and Vorwald (Ref. 3) compared vibratory hub load predictions from eight state-of-art aeroelastic analyses with the Lynx flight test data. These reviews focus on a time frame when lifting line aerodynamics was the practical extent to which aerodynamic models could be used. Reference 4 first provided a systematic assessment of CFD methods for airloads prediction. The CFD codes used were based on potential flow equations that could not account for many viscous and compressibility effects. Predicted pitching moments, when included into the coupled CSD analysis, mostly diverged the solution procedure. Even though the approach was largely unsuccessful at improving predictions beyond the lifting-line analyses, it opened an opportunity into CFD implementation that is expected to grow dramatically in future. The study also provided significant insights into flow phenomena that must be treated with CFD, if it is to be applied to rotary-wing aeroelasticity.

A review of rotary-wing aeroelasticity, from historical trends to current state of art to future trends, was performed by Friedmann *et al* (Refs. 5–7) between 1999 to 2004. The focus in these reviews was on aeroelastic stability and active vibration control. The aerodynamic models reviewed were lifting-line models. The focus of the present study is on loads, and the emphasis is on CFD-based aerodynamic models. In reference 7, Friedmann identified coupling between CFD and rotor structural dynamics, as a key future research area with major pay-offs in the prediction of rotor loads. The intent of this paper is to review the growth and current status of this area.

There have been limited reviews on the application of CFD for capturing rotorcraft flows. Survey articles by McCroskey (Ref. 8), and Srinivasan and Sankar (Ref. 9), both in 1995, have assessed efforts to capture rotor flows up to that time. In 2000, Hariharan and Sankar (Ref. 10), reviewed the computational techniques for CFD based wake capturing using Navier-Stokes analysis. In the same year, Egolf, Wake and Berezin (Ref. 11), reviewed the wake simulation and modeling studies, using both lifting-line and CFD approaches, specifically undertaken at the United Technologies Corporation.

Dynamic stall, which limits the operating envelope via control system and servo loads, has been treated in several survey papers. Experimental investigations of dynamic stall was reviewed by Carr and Chandrasekhara in 1996 (Ref. 12). Numerical investigations using CFD was reviewed by Ekaterinaris and Platzer (Ref. 13) in 1997.

In the present paper, the focus is not exclusively on flow phenomena, but on its impact on rotor loads via CFD/CSD coupling. A historical review of CFD/CSD coupling was presented in 1997 by Lee, Saberi and Ormiston (Ref. 14). Significant developments in coupling efforts have taken place since then. The objective of the review presented in this paper, is to bring the reader up to date with the state of the art in rotorcraft CFD/CSD coupling. CFD capabilities, their potential benefits, current limitations, and on-going research are summarized in the context of rotor loads prediction at the critical flight conditions.

Critical flight conditions for loads

Two critical flight conditions occur in level flight (Ref. 15). They are the highest vibration regimes: (1) low speed transition (around 40 kts for the UH-60A) and (2) high speed forward flight (above 150 kts for the UH-60A). The rotor flow field in the first regime is characterized by wake induced loadings in the first and fourth quadrants. The rotor flow field in the second regime is characterized by tip compressibility effects on the advancing side, between the first and second quadrants. The two high vibration regimes translate directly to high operating and maintenance costs, and reduced crew and system performance for critical missions.

The limiting design loads, on the other hand, occur during maneuvers under high load dynamic stall conditions, e.g. during symmetrical pull up and diving turns (Ref. 16). Wake, compressibility and dynamic stall all play important roles. Reference 17 showed, that there exist high altitude, moderate speed level flight conditions, where the dynamic stall cycles are similar to those occurring in high load maneuvers. Together with the low speed and high speed conditions, the high altitude level flight condition forms three important regimes. In each of these regimes, one out of the three key aerodynamic phenomenon are more dominant than the others, and is therefore ideally suited for validating the analysis methods separately. For predicting design loads in maneuvering flight, it is necessary to begin with these level flight regimes, understand the mechanisms behind vibratory loads in each, and predict them accurately.

The cause of rotor vibratory loads at low speed - the intertwining of tip vortices, is well recognized (Refs. 15, 18–20), although not well predicted for all rotor configurations. Similarly, the basic phenomenon of dynamic stall under high loading, although not satisfactorily pre-

dicted, is well understood (Ref. 21). The mechanism of vibratory loads at high speed, on the other hand, was not clear until recently. As summarized by the AHS organized Lynx helicopter workshop (Ref. 3), predicted vibratory hub loads at high speed differed greatly from one analysis to another, and all showed errors of more than 50% with test data, especially in phase (figure 1). A significant drawback at high speed was the prediction of unsteady transonic pitching moments near the blade tip. Incorrect pitching moments produce erroneous elastic twist which feed into the blade lift, and then into the vortex wake, making it difficult to validate the different components of rotor analysis separately.

In 2002, convincing evidence of improved high speed loads prediction using CFD/CSD coupling was presented at the UH-60A BlackHawk Loads workshop, and later reported by Datta et al (Ref. 22) and Potsdam, Yeo and Johnson (Ref. 23). The methodology used to calculate the results in reference 22 has been extended, and new results formulated. The test data have also been recently corrected. The modified results are presented here. Predictions from reference 22 and 23 are compared for consistency. They represent the current state of art.

Scope of the present paper

The paper is organized into two major sections. The first section, reviews the following: (1) key aerodynamic mechanisms that need to be captured by CFD for successful prediction of critical blade loads, (2) current capabilities and drawbacks of CFD in capturing these mechanisms, and (3) status of rotorcraft CFD/CSD coupling for prediction of airloads and structural loads.

The second section demonstrates the recent progress made, using CFD/CSD coupling, in resolving the long standing problems of articulated rotor aeromechanics at high speed: advancing blade lift phase, under-prediction of pitch link load, and prediction of vibratory lift. The UH-60A airloads data is used for this purpose. The fundamental mechanisms are systematically identified, the unique contribution of CFD demonstrated, and CFD/CSD coupling performed to improve prediction of vibratory loads.

For the purpose of review, *rotor loads* refer to the internal loads supported by a rotor blade. Thus, the topic includes both the aerodynamic loading and the structural dynamics of the rotor system. The *oscillatory loads* refer to 1/rev and higher harmonics. The *vibratory loads* refer to those harmonics which can contribute to the fixed-system fuselage vibration. For a 4-bladed rotor, they are (3,4,5)/rev, (7,8,9)/rev, then (11,12,13)/rev and so on. In general 3/rev and higher harmonics are termed vibratory harmonics.

In this review, the loads prediction research is organized into four categories: (1) aerodynamic modeling, (2) structural dynamic modeling, (3) solution procedures and (4) CFD/CSD or comprehensive analysis (CA) coupling methods.

The aerodynamics modeling is subdivided into the key areas of unique flow phenomena: (a) dynamic stall, (b) wake-induced inflow, (c) blade-tip effects, and (d) fuselage flow effects. The structural dynamic modeling briefly discusses the rotor and fuselage models. Solution procedures discuss CSD loads calculations and reduced order CFD methods.

AERODYNAMIC MODELING

The rotor aerodynamic model consists of two parts: the first part is the excitation which causes the airloads, the second part is the airload response of the airfoil (pressure and the viscous drag).

The first part is due to the relative motion of the airfoil with respect to air, i.e., the section angle of attack variation. The section angle of attack variation requires the blade deformations, the air velocities, and the wake induced velocities at the section. The blade deformations depend on structural response and trim control angles, the air velocity depends on flight speed, gust field, fuselage flow, and aircraft trim attitudes, and the wake induced velocities due to the vortex wake from all the blades (*far wake*). The second part involves the calculation of unsteady airfoil response. It depends on the airfoil shape, boundary layer, compressibility, shock-boundary layer interactions, 3D tip effects, dynamic stall and the local trailed and shed vorticity behind the blade (*near wake*).

Out of these two parts, the aerodynamic calculation supplies the following two components: (1) far wake and its induced velocity at a section and, (2) the unsteady pressure response of the airfoil.

The goal of first-principles based CFD is to capture both. A CFD analysis which captures both can be called a multi-bladed CFD. A CFD analysis that focuses only on the second component can be called a single-bladed CFD. Thus, compared to a single-bladed CFD, a multi-bladed CFD has the additional challenge of capturing the far wake.

Depending on the type of fluid dynamic equations used by the CFD solver, e.g., potential, Euler, or Navier-Stokes (NS), there are limitations for capturing the key rotor flow physics. In the following subsections, a discussion is provided for each of the following flow phenomena: far wake, dynamic stall, blade tip effects and fuselage flow effects. The first and the last are related to the calculation of airfoil excitation, the remaining two are related

to the airfoil response. The first three are key to the prediction of blade loads. The fourth, fuselage flow effects, is more important for predicting fuselage airloads but can affect blade loads at inboard radial stations. Each discussion contains a brief description of the flow phenomenon, a brief description of the flight regime where the flow phenomenon is a major consideration, a review of past and current analytical models, and a review of CFD methods being used or being considered to provide a physics-based model of the flow phenomenon.

Far wake

Capturing the main rotor vortex wake remains the most challenging objective for rotorcraft CFD. Unlike a fixed-wing, where the tip vortices are convected downstream, the vortices from the rotor blades interact with the following blades and their vortices, over several turns. To convect over one turn, a tip vortex has to traverse a distance of around 120 chords without artificial dissipation. This involves an enormous computational cost with present Euler or Navier-Stokes (NS) solvers, as discussed below. It remains a challenge to preserve the vortex velocity profiles with the fidelity required to accurately compute Blade-Vortex Interaction (BVI) loads. On the other hand, even though the vortex velocity profiles are dissipated, as long as the circulation is reasonably preserved, the dominant vibratory airloads (3-5/rev, for a 4-bladed rotor) can be captured.

The bound circulation produced by lift along the blade span trails vorticity that is proportional to the spanwise changes in lift. The spanwise gradient is generally highest at the tip, and so the trailed vortices tend to roll up into a strong vortex near the tip. The time rate of change in blade lift also influences the wake, and results in shed vorticity with streamwise variation in strength. In general, the shed vorticity effects are relatively local and are contained within the near wake immediately behind each blade. The rotor far wake, consisting of the trailed vortices from all blades, has a significant influence on performance, dynamic loads, and noise levels.

In hover, the dynamic loads are less important due to symmetric flow conditions. Power and figure of merit are accurately captured by CFD. On the other hand, the BVI phenomena, is not accurately captured. BVI induced wake migration (transfer of vorticity from one tip vortex to another), miss distance and wake turbulence interactions govern the tip thrust loading in hover. Current CFD calculations fail to capture these phenomena precisely and over predict thrust loading at the tip (Ref. 24). Wake effects on dynamic loads are strongest at transition speeds ($0.10 <$ advance ratio $\mu < .15$). The phenomenon of tip vortex intertwining produces the dominant vibratory loads, 3-5/rev, for a 4-bladed rotor. Multiple BVI phenomenon at this flight condition produces higher frequencies of blade loads. At very high speeds, the wake becomes less important as it is convected downstream from the rotor more rapidly. However, inter-blade wake interactions are still strong enough so that the vibratory loads cannot be predicted accurately without a detailed knowledge of the rotor wake. In maneuvering flight, the rotor wake is further complicated by its unsteady and sometimes unstable character. Thus, the wake is important at all flight conditions.

To accurately capture the wake, the following phenomenon must be predicted for all the rotor blades: (1) formation of a vortex at the blade tip, (2) roll up of the inboard vortex sheet into one or more strong vortices (3) convection of these vortices over several revolutions, (4) viscous diffusion of the vortices, and (5) effect of BVI on the blades and on the vortex structure. The term *CFD wake capture* is subsequently used in this paper to describe CFD methods which try to calculate all of the above four phenomenon.

Review of early CFD efforts:

Early CFD efforts to model rotorcraft flows involved inviscid, irrotational, single equation flow solvers. They were fundamentally incapable of predicting vortical flows. The focus was on improving lifting-line models by capturing transonic shocks. Caradonna and Ipsom (Ref. 25) first extended the unsteady *conservative small disturbance* equation to calculate rotor flows. Among other researchers who further developed this method were Caradonna and Phillipe (Ref. 26), Phillipe and Chattot (Ref. 27), and Caradonna, Desopper and Tung (Ref. 28). These formulations are known as Transonic Small Disturbance (TSD) formulations. *Full potential nonconservative* formulations, applied to rotor flows during the same time, better predicted shocks near the tip (Refs. 29–33). Subsequent development of the *full potential conservative* formulations improved prediction of unsteady shocks. The fixed wing formulation laid by Bridgeman, Steger and Caradonna (Ref. 34) was extended to rotor flows by Sankar and Prichard (Ref. 35), Strawn and Caradonna (Ref. 36), and Bridgeman, Strawn and Caradonna (Ref. 37). These formulations are known as full potential rotor (FPR) formulations. The potential equations could handle mild shocks in an isentropic manner and included viscosity using near wall corrections. Fundamentally, they were incapable of capturing vortical flows. The vortices could be imposed externally as potential jumps with prior knowledge of the wake geometry. For example, Strawn and Caradonna (Ref. 36) used measured wake geometry from the Caradonna and Tung hover experiments (Ref. 38), while Egolf and Sparks (Ref. 32) used a prescribed wake geometry.

In the late 1980s and 90s *Euler* and *Navier-*

Stokes(NS) formulations began to be applied to rotor problems. The Euler equations are a simplification of the NS equations for inviscid, non-conducting flows, with the advantage that the CFD grid can be sized to resolve surface geometry rather than viscous scales, a difference of approximately a factor of ten. The NS equations, on the other hand, are important to model the viscous effects governing the roll up mechanism. Conceptually, both Euler and NS equations have the capacity to model vortical flows. The problem is the very high level of grid refinement necessary to convect the vortices to distances necessary for prediction of BVI. While a CFD analysis is capable of capturing the key physics of vortex formation, sheet roll up and viscous diffusion (in case of NS), numerical diffusion arising out of the discretization process prevents the convection of the vortices. The free wake models, on the other hand, convect the vortices accurately, while relying on semi-empirical models for roll up and diffusion. The development of free wake models have been successfully exploited by CFD researchers attempting to combine the best of both formulations. Thus, researchers have used free wake to convect the vortices into the far wake, while using Euler equations (Refs. 39, 40), or Navier-Stokes equations (Refs. 41–44) for resolving the flow near each blade. Before discussing CFD wake capture, the free vortex methods are briefly summarized.

Summary of Free Wake Models:

Vortex dominated flows can be treated using an Eulerian approach or a Lagrangian approach. CFD methods solve the flow field using an Eulerian approach. Here, body fixed grids are used to discretize the flow equations, and the flow quantities are solved at a given point fixed with respect to the body. For high Reynolds number flows, where the vortical region is very thin, the Eulerian approach requires a very high grid resolution to capture the structure of the vortical region. The Lagrangian approach, ignores the structure of the vortical region, assuming it to be small compared to the other dimensions of the problem. It sets up *markers* in form of surfaces or lines representing the centroid surface of the vortex sheets, assigns vorticity to each marker, and solves for their free convection in space. As long as the marker positions are accurately computed, the inflow induced at a blade section is assumed to be accurate. These methods are called Vortex Lattice, Vortex Blob or Free Wake methods for incompressible flows, and Vortex Embedding methods for compressible flows. These methods provide an efficient and successful means of convecting the trailed vortices.

The free wake methods assume irrotational and incompressible (i.e. potential) flow with all of the vorticity concentrated into discrete filaments, and treat vortex diffusion and convection separately. The wake wake geometry is computed based on the free-stream velocity plus the induced velocities of the wake filaments free to move in space based on the Lagrangian fluid equation of motion. The solution procedure is often initiated using prescribed geometry models, e.g. Egolf and Landgrebe (Ref. 45) and Beddoes (Ref. 46). The free wake geometry calculations adopt different numerical techniques which can be broadly classified into relaxation methods (for periodic solution) and time-accurate methods. The relaxation methods include - constant vorticity contour method by Quackenbush and Wachspress (Ref. 47), pseudo-implicit predictor-corrector method by Bagai and Leishman (Ref. 48), the general free wake geometry method by Johnson (Ref. 49) and more recently a refinement of the later in the form of the multiple trailer with consolidation method (Ref. 50). Time accurate free wake methods have been developed recently by Bhagwat and Leishman (Ref. 51), which capture the wake dynamics in maneuvering flight as well as flow instabilities like the vortex ring state. As mentioned before, none of these models capture the roll-up mechanism in the wake without semi-empirical inputs. This is because the *markers* have to be judiciously allocated depending on the topology of the vortical flow region (for example, single rolled up tip vortex, dual vortices, multiple trailer models) before they are allowed to convect. Thus, vortex roll up, merging, or interaction with fuselage cannot be predicted automatically without re-allocation of markers.

CFD Wake Capture:

Early efforts similar to CFD wake capture can be traced back to Steinhoff and Ramachandran (Ref. 52), Ramachandran, Tung and Caradonna (Ref. 53) and Ramachandran et al (Ref. 54). These studies used the full potential formulation as in references 33 and 36, mentioned earlier. However, unlike those references, where the wake geometry was incorporated from measurements or a prescribed wake model, these studies calculated the geometry as part of the compressible solution. Note that the markers defining the vortex sheets still had to be allocated a-priori. Thus, these were vortex embedding methods. It was nevertheless a significant improvement, and the methodology implemented in a code known as HELIX-I, a compressible potential flow solver, and had considerable success in predicting hover flows. It was later extended to forward flight as HELIX-II.

Subsequently, researchers have used similar approaches to model the far field using Lagrangian approach, while calculating the details of near field using Eulerian methods (Euler or NS). Examples of such work are Moultan, Hafez and Caradonna (Ref. 55), Berezin and Sankar (Ref. 56), Berkmann et al (Ref. 57), Bangalore, Moulton and Caradonna (Ref. 58), Yang et al (Ref. 59) and Moulton, Wenren and

Caradonna (Ref. 61). These formulations are classified as *hybrid formulations*, as they are a combination of Eulerian and Lagrangian approaches of treating vortical flows. Formulations, which use the same approach, but different solvers in near and far field, can be termed *hybrid type formulations* to distinguish them from the above category.

CFD wake capture, using Euler analyses for the entire flow field was studied by Chen and McCroskey (Ref. 62) and Kramer, Hertel and Wagner (Ref. 63). NS analyses were used by Srinivasan *et al* (Ref. 64), Srinivasan, Raghavan and Duque (Ref. 65), Srinivasan and Baeder (Ref. 66) and Srinivasan and McCroskey (Ref. 67). As mentioned earlier, both Euler and NS solvers failed to convect vortices over one turn, a minimal requirement for rotorcraft problems, without an almost complete dissipation of their velocity profiles. The dissipation is artificial, and arises out of numerical discretization of the flow equations. Researchers continue to address this fundamental problem in four ways:

(i) finer grids in vortical flow regions

(ii) higher order discretization schemes

(iii) vorticity confinement technique

(iv) vorticity transport method

The first two approaches keep the fluid equations unchanged, and modify the computational mesh. The next two approaches modify the fluid equations. These approaches are discussed below.

Finer Grids in Vortical Flow:

All previous Euler and NS examples used a structured grid system wrapped around each blade and into the far field. Even though, *grid redistribution* methods have been studied (Ref. 68), these single block structured grids are limited in their ability for localized mesh refinements. Refinements using structured grids tend to create excess grid points in regions which are not necessary, for example in regions were there is no significant vorticity. In addition, multiple bodies with relative motion (e.g. rotor-fuselage problem) are difficult to handle with this approach. Strawn and Barth (Ref. 69) used *unstructured grids* for targeted grid subdivision in the regions of vortical flow in hover. It is easy to add or delete cells in the vortical flow regions of interest using unstructured grids. However, the exact location of the vortical flow regions are not known a-priori. They have to be identified as the solution progresses and the grids re-adapted to maintain a high density in the vortical flow region. This is called grid adaptation. Park, Nam and Kwon (Ref. 70) have used unstructured grids with adaptation for wake capture in forward flight.

In general, adaptation and management is relatively difficult with unstructured grids. The *chimera method* pioneered by Steger, Dougherty and Benek (Ref. 71) and later expanded by Benek *et al* (Ref. 72) enables localized mesh refinements while still using structured grids. It is a system of overset or overlapping meshes with a proper methodology for inter-mesh information transfer. Each mesh can be generated independently based on the grid requirements of the flow region it covers, and then over-layed, without the need to join in a common boundary. In addition, one set of grid can be wholly embedded within another set of grid with different density, giving rise to a system of *embedded grids*. Chimera methods are extensively used for multibladed CFD wake capture (Refs. 73–77). Modern CFD/CSD coupling use chimera methods extensively, as discussed later.

The solution adaptive, localized grid refinement techniques are still not enough to preserve the tip vortex structure with acceptable resolution. Strawn and Djomehri (Ref. 24) have studied the effect of grid resolution in capturing the wake of a four bladed rotor in hover. Compared to a forward flight case, the rotating-blade NS equations in hover, with steady blade deformations, can be converted to a steady state problem (Ref. 43), and is less expensive to begin with. The sectional airloads were grid independent, but showed an over-prediction near the tip, which was related to inaccurate prediction of the BVI miss distance. It was shown, that with 10.6 million(M) grid points and 1,120 processor-hours (ph), roughly two revolutions of the tip vortex could be captured. And with 64M grid points and 15,500 ph, roughly four revolutions of the tip vortex could be captured. However, there were no experimental velocity profile data to study the vortex dissipation error. Neither of these simulations were in reality of sufficient resolution to capture the actual vortex velocity profiles. The finest off-body grid spacings (0.6 chords away from the airfoil surface) were 0.05 chord and 0.1 chord respectively. The tip vortex core size itself is in general of the order of 0.1 chord. Wake et al (Refs. 78, 79) have studied the convection of a model vortex and shown that, with a 5th order accurate model, at least 14 points are required within the vortex core, in order to convect it over one rotor revolution with minimal diffusion of strength and structure. The requirement on the number of points within the vortex core can be reduced by using higher order discretization schemes.

Higher Order Discretization Schemes:

Several methodologies have been studied to build high fidelity, low numerical dissipation, higher order schemes. They are, essentially nonoscillatory (ENO) (Refs. 80, 81), dispersion relation preserving (DRP) (Ref. 82) and projected MUSCL (Ref. 68) schemes. Hariharan and Sankar (Ref. 81) showed, using

fixed wing calculations, that with a 7th order scheme, it is possible to preserve a tip vortex over 1-2 revolutions using only 5 points across its core, compared to a 5th or 3rd order scheme which required 10 and 20 points respectively. The overset wake mesh used, had to be adapted at the same time, to track the vortex and keep the required number of points within its rotational core. The drawback of higher order schemes is that they are not compact, i.e., to construct a solution at a point, information from a large number of neighboring cells are required which in turn requires wider grid overlaps between overset meshes. This makes parallel processing of large flow fields more difficult. Compact higher-order schemes like the Discontinuous Galerkin (DG) finite element method (see Cockburn et al (Ref. 83) for the method) use information only from a given cell and its neighbors, by solving for both flow properties and their gradients. Boelens et al (Ref. 84) have used the DG method with adaptive unstructured grids for wake capture in forward flight. The method applies to Euler equations.

In addition to the problem of non-compactness of the higher order schemes, there are contradictions between the order of accuracy and the spectral resolution capability of a scheme (see Lele (Ref. 85), Tam and Webb (Ref. 86)). In this context, Tang and Baeder (Ref. 68) have shown that it is possible to achieve more than 5th order ENO accuracy with only a 3rd order scheme. Note that the higher order schemes are effective only in combination with some form of grid adaptation or refinement technique. This is simply because, in order to ensure a given number of grid points in the vortical flow region, the location of the vortical flow region must be tracked. Thus, the problem becomes quickly complicated when more than one vortices from multiple blades have to be tracked in forward flight, where the wake geometry is not as simple as it is in hover.

Vorticity Confinement Technique:

Developed by Steinhoff et al (Refs. 87–89), and Dietz (Ref. 90), vorticity confinement methods try to confine the vorticity within a narrow region so that coarse grids, and lower order schemes can be used. The method adds a term, called the confinement term, to the momentum part of the fluid equations (Euler or NS), which forces vorticity back towards the local maximum of the vortical region. The term appears as a velocity correction to be applied to the basic solution at each time step. Accurate determination of the confinement term, however, is problem dependent. In addition, the confinement terms have to be turned off : (i) for regions where viscous effects are dominant and contribute to real vortex diffusion, and (ii) in regions where the grid density is already high enough to prevent numerical diffusion.

Vorticity Transport Method:

The Vorticity Transport Method was proposed by Brown et al (Refs. 91, 92). The fundamental idea is that instead of solving the fluid equations (mass and momentum conservation) for primitive variables (velocity and pressure), the flow equations are recast into a vorticity conservation form. Thus the flow solution conserves vorticity effectively independent of grid resolution. However, there is no mechanism to prevent spatial smearing of vorticity (analogous to dissipation of the velocity profiles inside a vortex), which is important for capturing BVI loads. The vorticity conservation equation is formulated assuming incompressibility, which is an acceptable assumption for the wake, but not for near blade flows. Thus, it is an attractive scheme for a *hybrid type formulation*, where the near blade flow is solved using NS, and the far wake solved using Vorticity Transport Method.

Dynamic Stall

Dynamic stall is an unsteady flow separation phenomenon that occurs on a heavily loaded rotor (operating at high thrust or high altitude). The rotor blades can encounter dynamic stall on the retreating blade because of high angle of attack, and on the advancing blade because of shock induced leading-edge separation. Dynamic stall generates high oscillatory and vibratory torsion loads on the blades and the swash-plate servos, and limits the helicopter operating envelope in high-load and high-speed conditions. Improving dynamic stall characteristics is the key to producing higher forward speed capabilities for heavily loaded rotor systems. Predicting dynamic stall is necessary for initial sizing and stall flutter calculations.

Physical Understanding of Dynamic Stall:

Numerous experiments have revealed the general sequence of events that characterize a fully developed dynamic stall phenomenon. For an airfoil pitching up, a progressive trailing edge separation due to flow reversal in the boundary layer, is accompanied by the formation of a leading edge vortex. The onset of a critical leading edge pressure triggers a leading-edge separation where the vortex detaches and starts moving downstream. This phenomenon of vortex detachment generates a strong pitching moment stall. However, as long as the vortex traverses over the airfoil, the lift does not stall and continues to increase. The lift stalls when the vortex leaves the trailing edge. At this time, the pitching moment reaches its maximum negative value. A period of progressive flow re-attachment follows as the airfoil pitches down. During this time one or more weaker vortices can be shed from the upper surface, creating additional fluctuations in lift and pitching moment. This sequence of

events leads to large hysteresis loops in airloads when plotted versus the angle of incidence.

Dynamic stall modeling in present comprehensive analyses uses semi-empirical models like the UTRC Method 1970, the Beddoes Time-Delay Method 1976, Gangwani's Method 1982 (all reviewed in reference 21), the Boeing-Vertol gamma function method 1973 (Ref. 93), Johnson's Method 1969 (Ref. 94), the Leishman-Beddoes Method 1986 (Ref. 95), ONERA EDLIN (Equations Differentielles Linearires) model 1990 (Ref. 96) and the ONERA BH (Bifurcation de Hopf) model 1998 (Ref. 97). Predictions from different models are in general similar (Ref. 98), but correlation with test data show errors, as expected with empirical models.

Before reviewing CFD methods for dynamic stall prediction, the key physics that need to be captured must be identified. Experimental investigations which have provided fundamental understanding of the key physics are:

(a) Carr et al (Ref. 99), McCroskey (Ref. 100) and McAlister et al (Ref. 101) under 2D subsonic conditions (Mach numbers around 0.3, Re up to 4M, SC1095, HH-02, NACA 0012 airfoils);

(b) Lorber and Carta (Ref. 102) under 2D high subsonic conditions;

(c) Piziali (Ref. 103) for 3D wing under subsonic conditions (Mach numbers around 0.3, Re around 1.95M, NACA 0015 airfoil);

(d) Lorber (Ref. 104) and Lorber et al (Ref. 105) for 3D wing at high subsonic conditions, with focus on the effects of compressibility, sweep, and wing geometry (Mach numbers up to 0.6, SSC-A09 airfoil)

(e) VanDyken and Chandrasekhara (Refs. 106, 107), with focus on compressibility effects on 2D stall (Mach numbers up to 0.45, Re up to 4M using boundary layer trips, NACA 0012 airfoil).

Carr and Chandrasekhar (Ref. 12) have reviewed experimental techniques and dynamic stall investigations up to 1996. Subsequent research have revealed newer and more complex mechanisms, and generated more detailed data sets for dynamic stall. For example, Chandrasekhara, Wilder and Carr (Ref. 108) have identified competing interactions between laminar separation bubble, supersonic flow and shocks that determine stall onset at low and moderate Reynolds numbers. Flow effects associated with compressibility were determined experimentally in reference 109 using heat-flux gauges on an oscillating 6-in NACA 0012 airfoil. The influence of shock on the separation bubble dynamics accelerates the events that lead to bursting and separation, and lowers the angle of attack at which dynamic stall occurs. The measurements show that while the dynamic stall onset varies significantly with the compressibility of the flow, the re-attachment process is similar. The surface shear stresses measured during the separation and reattachment processes, provide excellent data for correlation with CFD analysis. The significant influence of 3D effects has been demonstrated experimentally in reference 110 using a finite rectangular wing undergoing oscillatory motion. This study included three wing planforms: a straight rectangular wing, a swept tip, and a delta wing. Results of the study showed that deep dynamic stall could be achieved on inner portions of the wing while the influence of tip vortices limited the severity of dynamic stall near the tip region.

The key physics which need to be captured for dynamic stall predictions are: (1) lag in leading-edge pressure response due to unsteady motion, delaying stall onset, (2) lag in boundary layer response, (3) mechanisms of stall initiation and (4) stall sequence with re-attachment. Category 3 involves the influence of laminar separation bubble, local supersonic flow, turbulent transition, shock-turbulence interaction and the effect of 3-dimensionality on each of these phenomena. Category 4 involves the influence of local supersonic flow conditions governing the leading edge vortex shape and movement, and the large scale unsteadiness associated with the formation and collapse of eddies.

CFD Methods:

CFD computation of unsteady flows, in general, can be handled at several levels. In increasing order of capability, they are: (1) inviscid/incompressible (potential flow) solution using panel methods, (2) viscous boundary-layer methods for incompressible flows, (3) viscous-inviscid interaction (VII) methods, and (4) Navier-Stokes method. A potential flow solution captures the lag in leading-edge pressure response accurately for airfoils of arbitrary geometry. It cannot capture any other phenomena. The boundary-layer methods can be used to model the lag in boundary layer response, and to predict the stall onset. Typically, the boundary layer grows much faster compared to the pressure response, and therefore the unsteady effects of the boundary layer can be neglected. A steady-state boundary layer calculation with an unsteady panel code provides a good estimate of the boundary layer development. The boundary layer calculation requires empirical criteria for laminar to turbulent transition, both for predicting the transition onset and the transition length. Such criteria exist only for steady flows at high Re numbers. There are no experimental measurements for developing such

criteria for unsteady flows. Even for steady flows, such criteria do not exist at lower Re numbers (around 1M) where, flow separates before transition to turbulence and then attaches once it is turbulent, so that the transition occurs inside a separation bubble. In spite of these drawbacks, the unsteady boundary layer methods can still predict boundary layer solutions as accurately as NS methods (Ref. 111), and the stall onset (Ref. 112). They cannot, however, predict separated flows which characterize the post stall behavior. The VII methods can be used for predicting separated flows under post stall conditions.

A VII formulation can be obtained by extending the unsteady boundary layer calculations to separated flows as in Cebeci et al (Ref. 113). A preferred alternative is to solve NS equations (viscous) for the near-field and couple it with potential or Euler solutions (inviscid) in the far field to reduce computational cost. Unlike in the case of wake capture, where near field usually refers to 10 chords around the blade, here in the VII approach it means a fraction of the chord length. The main idea behind using this approach is grid point savings (Ref. 114) while predicting separated flows as accurately as full NS (Ref. 13).

For rotorcraft problems, the typical Re range of interest is from 1 to 6M (flight and wind tunnel). The freestream Mach numbers encountered during stalled flight can be as high as 0.7 to 0.8 on the advancing blade and 0.2 to 0.4 on the retreating blade. The associated angle of attack variations are around 4 ± 4 degrees and 10 ± 10 degrees respectively. Typical reduced frequencies are of the order 0.05 to 0.15. Even for incident Mach numbers of 0.3, local leading edge Mach numbers reach sonic and supersonic levels at such high angles of attack (Ref. 108). A viscous flow consists of a laminar to turbulent transition, with or without a laminar separation bubble. There is no theory to predict transition. The problem of transition can be bypassed to some extent for rotorcraft flows, which occur above Re of 1M, rendering the boundary layer fully turbulent in most cases of practical interest. The challenge therefore, lies mainly in the prediction of fully turbulent flows with massive separation.

Turbulent flows involve 3D, nonlinear, unstable motion of eddies. The eddies exist in a wide range of spatial and temporal scales. The higher the Re, the wider this range. Conceptually, the NS equations can resolve all these scales, but the computational speed and storage required to capture all these scales of motion are impractical. For very low Re, where the range of spatial and temporal scales are relatively narrow, and for very simple geometries, direct NS (DNS) simulations have been performed where the eddies have been resolved down to the Kolmogorov scale. A coarser approach is to stop at higher scales, i.e. resolve eddies which are at comparatively larger scales, and leave the remaining smaller unresolved eddies to sub-grid turbulence models. These large eddy simulation (LES) methods are still very expensive for rotorcraft application, but they have enormous potential in improving stall predictions. This is because, the unresolved smaller eddies generally behave in a statistically universal way, the larger eddies play a key role in the stall phenomena.

The current state-of-the-art in NS method is the use of Reynolds Averaged Navier-Stokes (RANS) models. In RANS, all flow quantities are broken into mean motions and turbulent fluctuations. The dynamics of all eddies are ignored, but their effect on the mean motion is retained via turbulence models. The turbulence models have no physical time dependency. The turbulence models affect the mean motions via the Reynolds Stress terms. The turbulence model generates approximation of the stress terms relating them to the known flow properties, while producing sufficient number of equations to *close the system*. The model can be a simple algebraic model like Baldwin-Lomax (Ref. 115) or RNG (Ref. 116). It can be an ODE based model like Johnson and King (Ref. 117), also called a half equation model. Or, it can involve solution of complete field PDEs for the parameters of turbulence. Depending on the number of PDEs, there are one equation models like Baldwin-Barth (Ref. 118) and Spalart-Allmaras (Ref. 119); two equation models like $k - \epsilon$ (Ref. 120), $k - \omega$ (Ref. 121), and modifications of the latter like the Baseline (BSL $k - \omega$) and Shear Stress Transport (SST $k - \omega$) (Ref. 13). Current CFD/CSD coupling methods have used Baldwin-Lomax, Baldwin-Barth and Spalart-Allmaras models.

CFD Predictions:

The state of art in RANS capability to predict dynamic stall have been investigated by several researchers. These include the effects of compressibility, boundary layer model (laminar vs. turbulent), turbulence models and grid resolution effects. The effects of compressibility were studied using laminar boundary layers by Sankar and Tassa (Ref. 122), Visbal and Shang (Ref. 123) and Choudhury and Knight (Ref. 124). Studies more relevant to rotorcraft flows are those using turbulent boundary layers. One of the early investigations were by Sankar and Tung (Ref. 125). Subsequently, Patterson and Lorber (Ref. 126) showed reasonably good validation of Sikorksy SSC-A09 airfoil dynamic stall at Mach number 0.2, Re of 2M, and reduced frequency of 0.1. The algebraic Baldwin-Lomax model was used. The algebraic model was understood to be inadequate to simulate massively separated flows, but using the two equation $k - \epsilon$ model, did not improve predictions as expected (Ref. 127). Compared to deep stall, light stall is more challenging to predict, especially for capturing the

correct pitching moment loops. The pitching moment loops determine torsion damping and are key to the prediction of stall flutter (Ref. 128). In deep stall the airfoil is always in the post static stall regime. In light stall the airfoil moves in and out of the static stall regime. 2D light stall predictions of NACA 0012 are shown in references 127, 129–131. All predictions depend heavily on the turbulence models used.

Srinivasan, Ekaterinaris and McCroskey (Ref. 132) performed a systematic study of NACA 0015 2D light and deep dynamic stall at Mach 0.3 and Re 1.95M, investigating the effects of turbulence model and grid refinements. Results were validated with tripped fully turbulent experimental data from reference 103. One conclusion was that the one equation models better predicted deep stall compared to algebraic models. This was because the algebraic models needed a boundary layer thickness, which is undefined for massively separated flows. However, predictions from different one equation models showed significantly different results. The same test case was repeated by Ekaterinaris and Menter (Ref. 133), and Ko and McCroskey (Ref. 134) comparing one and two equation turbulence models. Results from one and two equation models were similar. Both predicted an oscillatory flow behavior during the down-stroke of the deep dynamic stall, which could be traced to vortical structures near the trailing edge. It was recognized that the experimental data smoothed the oscillations because of averaging over several cycles. The NACA 0012 test case, discussed before, also showed improvement with a single equation turbulent model. However, for this test case, the boundary layer was not tripped during experiment, to force a fully turbulent layer. References 133 and 135 have shown improved prediction using transition models, instead of assuming a fully turbulent flow.

Recently Sankar et al (Ref. 136) have validated the NACA 0015 2D test cases examining three numerical schemes (Georgia Tech RANS, ONERA RANS, and an ONERA RANS-Potential flow VII scheme), grid density, numerical viscosity and transition. None of the methods accurately captured the pitching moment stall onset and hysteresis loops. It was found, that a coarse grid produced similar predictions as reference 132, while a more refined grid produced less satisfactory results. Predictions were sensitive to the transition model and numerical viscosity of the schemes. Thus, accurate prediction of even a 2D light dynamic stall at low Mach numbers with RANS analysis remains a challenge.

Advanced CFD Methods:

The development of turbulence models for RANS, i.e., closure models for improved prediction of turbulence, continues to be an area of research, but as discussed in reference 137, there are several limitations to these models. Many models are based on linear eddy-viscosity theory. They are therefore limited by an inability to account for turbulence anisotropy and are frame indifferent (independent of imposed system rotation). Full second-moment closures (SMC) can model the anisotropy, but have been limited in use due to high computational expenses and numerical stiffness. The common feature of each closure model is the need to define an empirical wall-correction in order to integrate the governing set of equations all the way to the wall, and this moves CFD away from first principles modeling. Nonlinear near-wall eddy-viscosity models, continue to be developed in an attempt to develop closure models that are internally consistent, predict stabilization due to system rotation, and are capable of modeling anisotropic turbulence 137. As detailed in reference 138, the problem is inherent in the construction of RANS turbulence models, which ensemble averages all scales of the unsteady motion.

Application of LES methods for Reynolds numbers that are typical of full-scale rotorcraft is still not within reach. Because of the high computational cost of LES methods, researchers interested in turbulence modeling for aerospace applications have considered solution schemes that are a hybrid between RANS and LES methods (Refs. 138, 139). The detached eddy simulation (DES) model is one of the most popular forms of this approach. Nelson and Nichols (Ref. 140) compared hybrid RANS/LES solutions to experimental results from the compressible mixing layer experiment of Samimy and Elliot (Ref. 141). This study showed that hybrid RANS/LES models provide LES quality results, and a radical improvement over the RANS models from which they are derived. These methods were extended in reference 141 to several turbulence flow problems, with Reynolds numbers in the millions range, and computational requirements that were on the same order as RANS solutions alone. One test case was an oscillating 2D NACA 0015 airfoil, for which results indicated development of small-scale vortical structures in the near wake using the hybrid solution that were not present in the RANS solution. In general, the hybrid RANS/LES models appear to be promising for eventual application to the dynamic stall problem.

Shock induced boundary layer separation plays a key role in dynamic stall under compressible flow conditions (Ref. 108). Even under an incident Mach number of 0.35, dynamic stall at high angles of attack, as is the case on the retreating blades, occur under a locally supersonic flow, which means that the leading edge vortex has to evolve and convect under an external supersonic flow. In general, shock boundary layer interaction is an area (Ref. 142), not well-predicted by RANS equations. Recently LES methods have been developed to improve

the computation of flows with shocks (Ref. 143). Validation of the model was conducted for the case of a supersonic compression ramp flow (Re = 1685), with good agreement obtained between DNS and LES results. The LES results were achieved at a fraction of the cost for DNS (0.5%). Direct application in rotorcraft problems is still very costly, even with parallel implementation.

Nonetheless, CFD solutions that model the proper flow physics from first principles must be pursued, and methods developed, to incorporate these higher fidelity schemes as embedded flows within a larger rotor computation domain.

Blade-Tip Effects

Blade tip effects refer to 3-dimensional flow effects induced by the finiteness of the rotor blade. They include: (1) steady and unsteady effects of the near wake, (2) spanwise flow associated with the tip vortex roll up, (3) progressive tip vortex formation that modifies the chord-wise pressure distribution at the tip and (4) steady and unsteady transonic effects like compressibility relief, movement of shock location and shock-boundary layer interaction.

The near wake consists of shed and trailed vorticity consistent with the azimuthal and span-wise gradient of bound circulation on the blade. The effect of near trailed vorticity is incorporated by lifting-line or lifting-surface models, modified to account for reverse flow, incident yawed flow and 2D airfoil properties. The effect of shed wake is incorporated, either directly using a vortex-lattice model or via an unsteady aerodynamic model. The unsteady models, like the Leishman-Beddoes semi-empirical model, offer greater scope in that they account for viscous effects, compressibility effects, flow separation and dynamic stall. A comprehensive review of the state of the art in lifting-line models can be found in Johnson (Ref. 144).

The span-wise flow associated with tip vortex roll up, chordwise pressure fluctuation caused by tip vortex formation, and the unsteady transonic effects are not captured by lifting-line models. Unsteady transonic effects near the blade tip are a key phenomenon at high forward speeds (Ref. 15). They produce large oscillatory torsion and pitch link loads. For articulated rotors, and rotors which are flexible in torsion, the unsteady moments near the tip produce large elastic twist deformations which affect blade lift via the azimuthal velocity variation (Ref. 145). For modern rotors with high twist, the tip on the advancing side operates at a negative lift at high-speed, and this negative loading produces additional effects on vortex wake roll up.

Recent application of the RANS flow solver TURNS coupled to the elastic blade model of UMARC have significantly improved the transonic unsteady pitching moment predictions near the blade tip of the UH-60A (Ref. 22). Similar tip effects have been reported by Potsdam et al (Ref. 23) with the RANS flow solver OVERFLOW coupled to the elastic blade models of CAMRAD II and RCAS. The most significant improvement from the lifting-line models was noted to be the transonic pitching moments. TURNS used a single blade simulation with free wake input from a Lagrangian wake model. OVERFLOW adopted an overset mesh technique for complete wake capture using four blades. Similar predictions show that the error in tip pitching moments arise not from the wake roll up but from the 3D unsteady transonic effects. The details of these analyses and results are described later.

Fuselage Flow Effects

Airflow around the fuselage in forward flight can produce an up-flow through the rotor disk plane on the forward sections of the azimuth, and a down-flow on the aft sections. The far wake geometry is distorted by the fuselage. The effect is more pronounced at lower speeds when a large part of the rotor downwash interacts with the fuselage. The fuselage upwash is by itself a 1/rev influence on blade loads. However, the effect of fuselage on the wake may provide a nonlinear inflow resulting in higher harmonic blade loads.

Free wake models used in lifting-line comprehensive analyses, ignore the effect of fuselage on the wake distortion. Experimental studies (Ref. 146) indicate that the wake convects with approximately the same skew angle as that predicted by the free wake models,with or without the fuselage. The Lynx workshop (Ref. 3) showed that even though fuselage upwash models improved 3 and 4/rev flap loads, the enhancements were marginal within the context of lifting-line models. At the time, the problem of high speed airloads were of more pressing concern. As CFD begins to resolve the fundamental discrepancy at high speed (tip pitching moments), secondary effects like that of fuselage upwash is becoming important for refined airload predictions. Recently, Potsdam et al (Ref. 23) examined the effect of the fuselage on the UH-60A blade airloads at high-speed (155 kts, $\mu = 0.368$). CFD was used to capture the complete rotor-fuselage interactional flowfield using overset meshes. The effect was not significant, the primary improvement was in the near root (22.5% R) pitching moments in the reverse flow region. Apart from this study, there is little published research on the effect of rotor-fuselage interactional flow on blade loads.

Compared to the effect of fuselage on the rotor loads, the effect of the *rotor on the fuselage* loads is important for fuselage vibration in low speed flight. Here, the surface-wake interactions caused by the rotor tip vortices impinging directly on the tail boom/rear-fuselage gener-

ate significant pressure fluctuations at the blade passage frequency (Leishman and Bi 147). Capturing these unsteady pressure fluctuations, pre-impingement and during impingement, require extremely accurate rotor wake geometry upto several turns. The post-impingement interactions, on the other hand, are dominated by the viscous effects of the fuselage-surface. A recent rotor-body interactional aerodynamics study by Wachspress et al (Ref. 148) uses a free wake model for the rotor and a potential flow model for the fuselage. The free wake model preserves the tip vortices accurately and predicts the pre-impingement and impingement pressure fluctuations well. The problem in prediction, as expected, was that of capturing post-impingement pressure fluctuations dominated by viscous effects. Navier-Stokes codes (Ref. 149) are expected to improve post-impingement predictions, but miss the pre-impingement phenomena due to artificial dissipation of the vortices.

In general rotor-fuselage interactional studies studies can be classified into three categories depending on the fidelity of the rotor model : (1) rotor modeled as an actuator disk (Refs. 150–153), (2) rotor modeled using lifting-line or lifting-surfaces with a Lagrangian free wake (Ref. 148) and (3) rotor modeled using CFD plus a lagrangian free wake, or direct CFD wake capture (Refs. 23, 70, 154, 155). A detailed discussion on modern rotor-fuselage interactional studies is beyond the scope of the present paper.

STRUCTURAL DYNAMICS

A brief summary of modern structural dynamics analyses of the main rotor blades is presented in this section. A brief discussion on rotor-fuselage coupled dynamics is provided next followed by a description of solution procedures. Fuselage dynamics is not critical for blade loads, except for certain teetering rotor configurations, but essential for the calculation of fuselage loads and vibration.

Rotor blade model

The structural dynamic equations of nonlinear, coupled, isotropic Euler-Bernoulli beams were derived in references 156–160. By retaining the second-order effects of elastic motion in the kinetic and strain energy terms, and by adding the nonlinearities (up to second order) in extension and torsion produced by bending, *almost-exact* beam models can be developed. They are accurate up to moderate bending deflections of 15% (Ref. 161). Such a structural model is used later in the example test case. For larger bending deformations, the nonlinearities can be handled in two ways: (1) the so called *geometrically exact* theories (Refs. 162–164) and, (2) multibody type formulations, as described later (Refs. 161, 165).

In the 1990's there was an emphasis on improving cross-section analyses to account for anisotropy produced by composite materials. Research in composite blade modeling has been reviewed in great detail by several survey papers, for example, Hodges in 1990 (Ref. 166), Jung, Nagaraj and Chopra in 1999 (Ref. 167) and Friedmann in 2003 (Ref. 6). A detailed discussion on this topic is not the focus of this paper. The basic idea has been to perform a linear or non-linear 2D cross-sectional analysis, uncoupled from the 1D non-linear beam theories mentioned above, with the goal of obtaining the cross-sectional elastic constants and warping. It has been shown using asymptotic methods that such uncoupling assumptions hold true for most cases for rotor blades (Ref. 168). The cross-sectional elastic constants defining the stress-strain relation are fully coupled. For low frequency dynamic behavior, a *classical analysis* with a single shear strain measure (as in the case of isotropic beams) can be reasonably accurate, as long as the coupled elastic constants are calculated properly (Ref. 169). For higher accuracy, as required for rotor analysis, the strain vector can include two additional strains to account for the transverse shears, or one additional strain to account for the Vlasov or restrained warping. The success of the model depends more on the accuracy of the elastic constants than the number of strain measures (Ref. 170). There are several methods for extracting these constants. They are: engineering methods that work well for certain type of cross-sections (Ref. 171), mixed force-displacement formulation (Ref. 172), asymptotic methods which yield closed form solutions for thin walled beams (Refs. 173–175), and finite element methods based on St. Venant's principle (Ref. 176) or based on the asymptotic methods (Refs. 168, 177). The last two references provide a generalized treatment, where the cross-sectional equations and the 1D blade equations are rigorously reduced from 3D elasticity theory. Advanced geometry formulations with structural sweep, droop and pretwist (Refs. 178, 179) have also been extended to include composite modeling (Refs. 175, 180).

Examples of finite element cross-section analyses are Variational Asymptotic Beam Section Analysis, VABS (Ref. 168) and Saint-V code (Ref. 176). Validation of these analyses codes show modeling accuracy on the same level as 3D finite element methods (Refs. 181, 182). The mixed force-displacement formulation of Jung, Nagaraj and Chopra (Ref. 172) has been used to predict results as accurate as finite element based analyses. The key point is: with the technology level for cross-section analyses available today, the section properties required to operate any comprehensive code can be obtained reli-

ably. The dynamics of the blade can then be accurately predicted, subject to proper modeling of the boundary conditions. The latter remains a challenging task because of nonlinearities associated with the root end of the blades, the prime examples of which are lag dampers and control systems.

Gandhi and Chopra (Refs. 183, 184) first incorporated an elastomeric lag damper in a rotor comprehensive analysis. The goal was to study the effects of lag damper on aeromechanical stability. The model was an analytical one. Finite element based damper models have also been developed, such as by Smith et al (Ref. 185). In general, the difficulties with modeling lag dampers are numerous, and are described in references 186 and 187. Non-linearities associated with temperature, amplitude, and frequency of these structures create unknown parameters and reduce prediction accuracy of the blade models. Calculation of the chord-wise response and loads can be greatly improved with advanced nonlinear lag damper models (Ref. 188).

The challenge of modeling complex boundary conditions can be handled in a generalized manner using multibody type structural formulations. Conventional rotor formulations of the structural dynamic equations exploit the topology of a helicopter rotor system to simplify the derivation of the governing equations. This leads to a loss of expand-ability of the analysis. For example, to model detailed control system linkages at the root, swash-plate assembly, inter-blade or hub-blade components like dampers, or for developing a fully coupled rotor-fuselage system, active flap-blade system, the dynamic equations must be re-derived. A small increase in the scope of analysis, therefore, involves the entire analysis, which becomes progressively harder with each new feature. Moreover with each new feature, the same model which is now expressed by a different set of equations, must be revalidated. The strength of multibody formulations is that they increase the scope of structural analysis without having to re-derive and re-validate the equations with each additional feature.

Using multibody formulations, large deformation problems can be handled while still using second-order nonlinear beam theory (i.e., without using geometrically exact theories). This is done by simply breaking up the rotor blade into multiple bodies each undergoing only moderate deformations. This technique is employed in comprehensive rotor analysis codes like CAMRAD II (Ref. 161) and RCAS (Ref. 165). Each beam element undergoes only a moderate deformation in its own frame, while the total deformation is obtained by adding to it the end contribution of the adjoining parent element as a rigid motion.

DYMORE (Ref. 164) and MBDyn (Ref. 189) are examples of generalized multi-body structural codes. The versatility of these codes lie in their topology independent formulation, in that they can be used to model any structure, rotating or non-rotating. This versatility stems from an approach radically different from other rotorcraft codes, in that the motion of all bodies are referred directly to a single global inertial frame, avoiding the assumption of any hierarchical frame structure. This is made possible by letting the structural components have finite displacements and rotations, and by implementing the algebraic constraint equations explicitly.

Multi-body formulations can be used to simulate models of complex control linkages and couplings at the root end (important for gimballed rotors) using simpler, validated, lower-level structural elements like beams, plates, and rigid bars with appropriate constraints. Usually these methods are geared to solve the full non-linear finite element equations using time-marching schemes (due to the presence of algebraic constraint equations). The application of multibody dynamics has enabled modeling systems that provide difficulty using classical methods, e.g. rotorcraft engage/disengage operation (Ref. 190), tiltrotor inter-blade/hub kinematic couplings (Ref. 191) and integration with active controls and hydraulic systems (Refs. 192, 193). These modeling options have significantly enhanced the scope of rotor structural simulation for design purposes.

The importance of detailed boundary condition modeling, on the accuracy of predicted blade sectional loads remains to be well understood.

Fuselage dynamics

Wind tunnel tests show, that fuselage dynamics can significantly affect blade loads for two-bladed teetering rotors (Ref. 194). For higher blade numbers and more conventional hubs, there has not been clear experimental evidence of fuselage dynamics affecting rotor loads. On the other hand, the vibration level at any fuselage station require accurate fuselage dynamics.

Rotor-fuselage dynamic coupling for aeromechanical stability prediction is well developed (see review by Chopra, Ref. 195). For loads prediction, researchers generally presume the hub is fixed and ignore the fuselage dynamics entirely. The subject of coupling rotor and airframe has in the past been an active area of research. One technique commonly used is known as *impedance matching* (Ref. 196). This is a loosely coupled technique, where the load and displacement fields at the interface between the rotor system and the fuselage are matched. As with any superposition method, the technique can only capture the linear effects of the rotor-airframe interaction.

A fully coupled set of nonlinear rotor-fuselage dynamic equations were formulated for the AH-1G teetering rotor helicopter in references 197 and 198. The fuse-

lage model was progressively refined in these studies from a stick model, to a 3D airframe model, to a 3D model including difficult components. The last study, which included a free wake analysis, showed that the coupled main rotor pylon roll mode had a significant contribution (26%) in the 2/rev vibration (blade passage frequency) at the pilot seat. The study confirmed the significant influence of elastic fuselage modeling on the 1/rev chord bending moments. Compared to two bladed systems, there are fewer studies on multi-bladed systems, probably because the effects tends to be small. Reference 199 examined the response of a BO-105 type four-bladed hingeless rotor with a fully coupled rotor-fuselage dynamic formulation and quasi-steady aerodynamics. The inclusion of fuselage dynamics had a minor effect on the blade loads.

Most comprehensive rotorcraft analyses in use today have the capability of building and developing a sophisticated fuselage dynamics model and properly coupling it to the rotor system. Such is the case with CAMRAD II, RCAS, and UMARC (Ref. 200). The primary drawback of these methods, as mentioned in the blade modeling section before, is that the formulation of the equations is a cumbersome task. In addition, often, as in the case of reference 200, the rigid body motions of the fuselage are assumed to be small. This may affect the accuracy of prediction during large angle maneuvers.

Recently, multibody analyses have begun to be applied to rotor-fuselage dynamics. The fuselage model is still reduced to a few modes for practical computational costs. The rigid motion of the fuselage can be large, and is handled using the concept of *floating frames* (Ref. 201). The elastic motion remains small. The choice of a suitable modal basis for representing the fuselage dynamics is crucial for retaining the topology independence of the formulation, and for coupling the fuselage modal coordinates with the physical coordinates of the rotor system (Ref. 202).

SOLUTION PROCEDURES

The governing structural dynamic equations can be solved for blade response using harmonic balance (Ref. 203), Floquet theory (Ref. 204), finite element in time (Ref. 205) (for steady-state response), or using time-marching (for transient response). Traditionally, to reduce computational cost, the spatial degrees of freedom are reduced by using normal modes. For moderate deformation problems, normal modes extracted about a mean deformed geometry, do not significantly compromise the accuracy of the solution. Accuracy is an issue for large deformation problems (Ref. 206).

The sectional loads are frequently calculated using two approaches: (1) deflection or curvature method and (2) force summation method. In the curvature method (also called modal method if the deflection is obtained using normal modes), the loads at a given section are determined by the elastic motion induced curvature and structural properties at that section. If there is a radial step change in structural properties, e.g. bending stiffness, or a concentrated loading, e.g. damper force, then there should be a corresponding step change in curvature, to keep the physical loads continuous. With a small number modes or shape functions this discontinuity cannot be captured. Moreover, the curvature method gives zero load on an element without elastic degrees of freedom. A force summation method rectifies the above deficiencies. It is a force balance method which obtains the section loads from the difference between the applied forces and the inertial forces acting on the blade on one side of the section. The forces used for this purpose must be exactly same as those used for solving the structural dynamic equations, otherwise inconsistent loads are obtained. For example, the bending moments at a pure hinge would not be identically zero. With lesser number of modes, the force summation method better captures the effects of concentrated loading and radial discontinuities of structural properties. However, with increase in number of modes the curvature method and the force summation method must approach the same solution.

Solution of the fluid dynamic equations, for the most advanced CFD analyses, remain a challenge due to the high computational expense of LES and DNS methods. Formal reduced order modeling (ROM) and proper orthogonal decomposition (POD) are techniques that are being investigated to reduce the computational cost of CFD simulations. These methods are analogous to modal reduction techniques of structural dynamics. Applications of such reduction methods on unsteady flows are provided in references 207 and 208, for transonic flows in reference 209, and for compressible flows in reference 210. It is expected that some form of ROM/POD may be employed to improve blade loads prediction capabilities under complex aerodynamic phenomena such as dynamic stall.

ROTORCRAFT CFD/CSD COUPLING

The first step in obtaining an aeromechanical solution in level flight is to trim the helicopter. For unsteady maneuvers, it is a starting point. For steady flight, trim must be simultaneously achieved alongside converged airloads and blade loads. Johnson (Ref. 212) summarized several trim options in level flight. The trim option used

in the example case study later is the free flight propulsive trim. The rotor control angles, the tail rotor collective and the fuselage lateral and longitudinal attitude angles are obtained to maintain three forces and three moments equilibrium about the vehicle center of gravity.

Coupling Procedure

CFD/CSD coupling methods are a topic of current research. At present, coupling is accomplished in two ways : (1) loose or weak coupling, and (2) tight or strong coupling. In loose coupling, airloads and blade deformations are transferred between CFD and CSD once every rotor revolution. In tight coupling, the information exchange is per time step. The efficiency of the different methods must be evaluated at the same trim state.

The loose coupling method or the *delta* method was proposed by Tung, Caradonna and Johnson in 1986 (Ref. 213). Here, a TSD code was coupled with CAMRAD comprehensive analysis. The comprehensive analysis supplied trim capability, in addition to the CSD model. Only the lift was coupled, within a specified region in the advancing side. The far wake inflow, and blade deformations were incorporated as angle of attack changes in the blade. Subsequent refinements, which comprised of extending coupling to the entire azimuth, was carried out by Strawn and Tung (Ref. 214) using the FPR code. FPR-CAMRAD loose coupling validation with AS-330 Puma flight test data (Ref. 215) did not show any significant improvement in airload prediction from lifting-line models. The FPR code was later refined by Strawn and Bridgeman (Ref. 216) with marginal effect on airload prediction. This lack of improvement in airload prediction can be traced to the fact that the pitching moments were not coupled in these efforts. An attempt to couple the pitching moments led to divergence in the torsion dynamics (Ref. 215). Kim, Desopper and Chopra (Ref. 217) coupled a TSD code with UMARC comprehensive analysis. Here too, torsion divergence was a problem and had to be avoided, by using a combination of CFD and lifting-line pitching moments in the coupling process. The problem of torsion divergence led early researchers to suggest that the loose coupling procedure might be inadequate when torsion dynamics is included. It is now recognized that the reasons for the earlier failure was not the coupling procedure, but inaccurate pitching moment prediction (Ref. 14). This was partly due to the inability of the CFD codes to resolve the transonic compressibility effects accurately, and partly due to inaccurate grid velocities away from the blade surface which were not consistent with the physical deformation of the blade. In recent years, the loose coupling method has been applied to obtain stable and converged Euler and NS solutions, by Altmikus (Ref. 218), Servera, Beaumier and Costes (Ref. 219), Pahlke and Berend van der Wall (Ref. 220), Datta and Sitaraman et al (Ref. 22) and Potsdam, Yeo and Johnson (Ref. 23). They are discussed in more detail later.

Early tight coupling efforts were by Alonso et al (Ref. 221), Bauchau and Ahmad (Ref. 222) and Lee, Saberi and Ormiston (Ref. 14). Reference 222 coupled DYMORE with OVERFLOW. The trim control angles were prescribed. Reference 14 coupled 2GCHAS (predecessor of RCAS) with the FPX code (a refined version of FPR code) and obtained a trim solution. The torsion divergence problem was traced to inaccurate pitching moments, and was resolved using finer time steps in FPX. The predicted airloads, after a successful trim solution was reached, were almost identical to the earlier FPR-CAMRAD loose coupling results for the Puma airloads. A similar conclusion has been reached in recent years by Altmikus et al (Ref. 218). The two coupling methods generate the same airloads at high speed, after reaching the same trim state. The trim state is easily achieved in loose coupling. Trim requires a greater computational cost with current implementations of tight coupling. On the other hand, tight coupling has the potential to provide stability solutions which is difficult in the case of loose coupling. Note that CFD, unlike lifting-line models, do not provide aerodynamic sensitivity coefficients which can be readily used for stability analysis.

Both the coupling methods, can be handled by two CFD and CSD codes using an interface, without the need for modifying the original codes. The time accuracy in each can be handled independently of the other. This idea has been described as the *partitioned procedure approach* in reference 223. A CFD/CSD analysis where the fluid and structural equations are coupled during formulation and integrated in time together is a higher fidelity approach, beyond today's capability.

Compared to loose coupling, tight coupling enables the coupling of a pure CSD code to a CFD code. Loose coupling with a pure CSD analysis is an ill-posed problem. A pure CSD code does not contain response dependent aerodynamic damping. For example, for a teetering rotor, with the first flap frequency at 1/rev and no structural damping, the problem cannot be solved. The CFD airloads when imposed on the structure produces resonance at 1/rev. The real airloads contain the response dependent damping terms and when imposed on the structure produces a zero 1/rev aerodynamic hinge moment. When the response is unknown the aerodynamic hinge moment will not be zero. Loose coupling with a comprehensive analysis renders the problem well-posed. Here, the aerodynamic damping coefficients from a lifting-line calculation are retained. The CFD airloads are imposed on the structure as a correction to the lifting-line airloads. The final converged airloads are entirely the CFD airloads, and are independent of the lifting-line

airloads used.

A useful approach in CFD/CSD coupling would be to perform a loose coupling for trim, response and loads. Then using the prescribed trim angles perform a tight coupling. The response and loads, upon convergence of the tight coupling, must be identical to the loose coupling solution. However, using tight coupling, a stability or transient solution can be obtained by imposing an airload disturbance at any azimuth location and re-integrating the CFD/CSD equations in time.

CFD/CSD coupling: State of Art

This section provides an overview of the CFD/CSD coupling studies performed in recent years. The focus is on methods in which the CFD and CSD include the following capabilities: (1) CFD accounts for the rotor wake, (2) CFD includes time-varying flexible blade deformations in flap, lag and torsion, (3) CSD calculates blade dynamics using the CFD airloads, and (4) the coupling incorporates a trim mechanism.

In recent years, rotorcraft CFD have been successfully used for acoustic predictions. The focus there is on the prediction of shock induced High Speed Impulsive (HSI) noise and BVI induced low speed descent noise. Significant efforts in this area by researchers in Europe, Japan, Korea and the US are described in references 70, 77, 84, 224–226. The CFD in these efforts all use full wake capture, can incorporate flexible blade deformations in principle, and optionally perform trim calculations. However, these studies are focused on aerodynamics, and do not calculate CSD response to the CFD airloads. The studies validate airloads and acoustic predictions with Operational Loads Survey (OLS) rotor (Refs. 227, 228), the HART/HART II tests (Ref. 229), and the HELINOISE (Ref. 230) and HELISHAPE program (Ref. 219). The trim conditions and blade deformations, were measured during these wind tunnel tests, and could be prescribed during the CFD calculations.

Yang *et al* (Ref. 59) have computed CSD response to CFD loads in forward flight. The NS solver incorporated a prescribed or free wake model for far wake inflow. Flexible blade deformations and trim was accounted for. Elastic twist however, a key deformation at high speed, was prescribed from the model UH-60A DNW test measurements (Ref. 60), along with the rotor trim angles.

Recent CFD/CSD coupling methods which calculate CFD, CSD and trim consistently are as follows.

1. HOST with WAVES (2000 (Ref. 219)) and HOST with FLOWer (2002 (Ref. 218))
2. INROT with DYNROT (2002 (Ref. 223))
3. S4 with FLOWer (2004 (Ref. 220)
4. UMARC with TURNS (2004 (Ref. 22))
5. CAMRAD II and RCAS with OVERFLOW-D (2004 (Ref. 23)).

The first name in each represent the CSD or CA code, the second is the CFD code. The first three initiatives are part of a collaborative research effort in Europe involving the Office National d'Etudes et de Recherches Aerospatiales (ONERA) at Chatillon, the Institute of Aerodynamics and Fluid Technology (DLR), and the Institute of Aerodynamics and Gasdynamics (IAG) at the University of Stuttgart. The next two are part of a collaborative effort organized by the National Rotorcraft Technology Center (NRTC) in the US. The European efforts use the ONERA 7A, 7AD rotor wind tunnel test data for validation. The US efforts use the UH-60A Black Hawk flight test data for validation. The first three focus on high speed airloads. The fourth focuses on both high speed airloads and structural loads. The last, focuses on airloads, but at all three critical level flight conditions (as well as hover).

All of the above initiatives can be considered landmark. The key message from the first three initiatives is that CFD/CSD loose coupling and tight coupling both produce the same airloads, when the rotor is trimmed to the same state. The fourth and the fifth initiatives, captured for the first time, the unsteady transonic pitching moments near the tip of the UH-60A blades, predicted the phase of vibratory lift harmonics correctly, and resolved the advancing blade lift phase problem in high speed flight. (At the time of publication of these references, there appeared to be a residual phase error of around 14 degrees, which was later confirmed to be an azimuthal error in flight test data). Additionally, the fourth, showed the effect of CFD coupling on structural loads. It resolved the correct peak to peak pitch-link load and torsion bending moment. The fifth, in addition to high speed airload improvement, demonstrated: (i) the potential of RANS CFD in capturing dynamic stall in high altitude flight, and (ii) that the vortex velocity profile dissipation error need not be a critical impediment to predicting low frequency vibratory airloads (3-5/rev) at the wake dominated transition flight.

With the exception of WAVES, which is an Euler code, all the other CFD codes are RANS codes. The OVERFLOW-D results were obtained used Baldwin-Barth turbulence model. Others used algebraic models like Baldwin-Lomax.

The INROT and DYNROT coupling does not account for rotor trim, but it is not a fundamental limitation of the scheme, and is included in the discussion here as it is a recent tight coupling initiative that accounts for all other key physics. The details of the initiatives are discussed next.

HOST-WAVES and HOST-FLOWer:

HOST with FLOWer and HOST with WAVES coupling (Ref. 218), have examined both loose and tight coupling methods consistently (i.e., under the same trim conditions). HOST is an Eurocopter flight mechanics simulation tool which supplies the CSD and trim modules. The FLOWer (developed at IAG, DLR) and WAVES (developed at ONERA) codes are four bladed CFD codes with full wake capture. FLOWer solves Euler or RANS equations with overset or chimera mesh. Each blade has a single block grid embedded in a background cartesian mesh. The elastic deformations are introduced by an algebraic grid deformation method. The WAVES is an Euler code. Instead of overset meshes, it uses a multiblock structured grid system to model all four blades. Each block around each blade has coincident nodes with those from its neighboring blades. The blade deformations are accounted for using a deforming grid technique (Ref. 231). FLOWer and WAVES were run in the Euler mode and showed similar airload predictions. Coupling with HOST code was performed using both strong and weak coupling. Both showed same final results for trim and airloads. Neither of the Euler codes showed any significant improvement in the prediction of airloads compared to lifting-line models.

S4-FLOWer:

A similar coupling study was performed by Pahlke and Berend van der Wall (Ref. 220) using S4 (DLR rotor simulation code) for CSD and trim, and FLOWer for CFD. FLOWer is used in the NS form, and a modified version from that reported in the previous coupling initiative. Compared to the Euler coupling performed above, the airload prediction using the NS coupling, produced significant differences. For the 7A rotor, the NS coupling brought predicted pitching moment and lift closer to test data. However, for the 7AD rotor, the change produced an improvement in lift but not in pitching moment. The predicted blade twist were different in either case, thus it is not clear whether the differences stem from response calculation or Euler/NS calculations. One of the goals of the following example case study would be therefore to compare Euler and NS airloads using the same deformations and far wake.

INROT-DYNROT:

INROT and DYNROT by Pomin and Wagner is a tight coupling (Ref. 223). The trim angles are prescribed from a lifting-line CA solution using HOST. INROT solves the RANS equations. A time-dependent transformation of the flow equations from the physical domain to the computational domain is used to permit arbitrary rigid and elastic motion of the rotor blades. Like OVERFLOW-D and FLOWer, INROT uses overset or chimera mesh to capture the wake using a four bladed simulation, except that in this case the background mesh is cylindrical, not cartesian. The near body grids solves RANS. The background grid, in which the near body grids are embedded, solves the Euler equations. DYNROT supplies the CSD model which at present follows a geometrically linear Timoshenko beam formulation. CSD/CFD coupling is performed using an implicit-implicit tight coupling scheme developed by Hierholz and Buchtala.

UMARC-TURNS:

UMARC and TURNS coupling is reported in reference 22. Both airloads and structural loads at high speed were compared with lifting-line results and with the UH-60A flight test data. The Transonic Unsteady Rotor Navier Stokes (TURNS) code was developed by by Srinivasan and Baeder et al (Refs. 64, 66). The aeroelastic blade deformations are incorporated (Sitaraman et al, Ref. 232) by moving the grid points to conform to the surface geometry of the deformed blade and calculating the space and time metrics at each time step. A single block mesh constructed around the blade captures the near wake. The far wake is calculated by a free wake method (Bagai-Leishman free wake) and incorporated into the CFD solution using the *Field Velocity Approach*. It is a way of modeling unsteady flows via grid movement (Ref. 233). UMARC comprehensive analysis supplies the CSD, trim and lifting-line airloads for loose coupling. The CSD model was separately validated using measured airloads. The lifting-line comprehensive analysis is validated in reference 145.

CAMRAD II and RCAS - OVERFLOW-D:

In CAMRAD II and RCAS coupling with OVERFLOW-D (Ref. 23), CAMRAD II and RCAS supplies the CSD, trim and lifting-line airloads. The OVERFLOW-D originates from the OVERFLOW code.

The OVERFLOW code was developed for fixed wing by Buning et al (Ref. 234). It was extended by Meakin et al (Ref. 235) to incorporate domain connectivity algorithms for arbitrary motions between vehicle components and off-body solutions, using structured overset meshes. The overset mesh system can then be efficiently exploited for parallel computations (Ref. 236). This code is known as OVERFLOW-D. Earlier, Ahmad and Duque (Ref. 74) exploited the overset mesh technique and domain connectivity algorithm to prescribe rigid blade motions and study rotor flows in forward-flight. The flow solver, however was not OVERFLOW. The first rotary wing version of OVERFLOW was initialy demonstrated by Ahmad, Duque and Strawn in 1996 and later improved upon by

the same researchers in reference 77. The method assumed rigid motions in flap and pitch. The method was extended to include full flexible deformations in flap, lag and torsion and incorporated in OVERFLOW-D by Potsdam et al (Ref. 23). It was this version of OVERFLOW-D that has been coupled with CAMRAD II and RCAS.

Each blade is surrounded by a local grid, within a progressively coarser set of cartesian background grids. The background meshes captures the far wake inflow. The finest background grid spacing is 0.1 chord. Thus the individual vortices, important for BVI loading, are dissipated (because this requires at least 10-15 points within the vortex core which itself is of the order of 0.1 chord). However their circulation strengths appeared to be well preserved to capture the vibratory blade loads. This was clearly demonstrated in the transition flight regime where the tip vortex intertwining dominated vibrator loads were captured as accurately as free wake models. The dynamic stall cycles in high altitude flight were captured well in the retreating side. However, significant discrepancies remained in the prediction of advancing blade lift, and vibratory lift. The CSD and CA modules of CAMRAD II and RCAS have been widely validated and is not discussed here (Refs. 161, 237).

PREDICTION OF UH-60A ROTOR LOADS AT HIGH SPEED

The objective in this section is to study improved rotor loads prediction at high speed using CFD/CSD loose coupling. The approach taken, is to isolate the physics of structural dynamics and aerodynamics from the coupled aeroelastic problem, and then bring them back together.

In the first section, the flight test *measured airloads* and damper load are imposed on the structure to calculate structural loads. The goals are to: (1) validate the structural model, and (2) once validated, obtain a set of blade deformations which, in absence of flight test measured deformations, form a reasonable basis to validate aerodynamic models. The key message from this section is that a second order accurate non-linear beam theory (Refs. 156, 157) is sufficiently accurate to predict the correct vibratory airloads at high speed. Deficiencies are noted in higher harmonics of torsion loads and chord bending moments (4/rev and higher).

In the second section, the *prescribed deformations* obtained above are used to validate lifting-line, NS and Euler models. There are several key conclusions here. First, inaccurate vibratory airloads is an aerodynamic problem, not a structural dynamic problem. Second, elastic twist and a refined wake are important. Elastic twist is driven largely by tip transonic pitching moments, which the lifting-line models fail to capture. Third, the pitching moments for the UH-60A are accurately captured by both Euler and NS solvers.

In the third section coupled UMARC-TURNS predictions of airloads, blade loads and pitch link load are obtained from first principles. The airload predictions are compared with published CAMRAD II-OVERFLOW/D coupling results. The test data used are the azimuthally corrected data from Flight 85 (nominal vehicle weight coefficient, $C_W/\sigma = 0.0783$), Counter 34 (high speed, 155 kts, $\mu = 0.368$) of the UH-60A Airloads Program. The key conclusion here, is that the problem of lift phase, vibratory lift and peak-to-peak pitch link load is resolved. However, the improvement is not enough to resolve flap bending moment phase. The source of this problem is still not understood.

Brief review of high speed flight problem

Lifting-line predictions show significant discrepancies in the prediction of vibratory loads, at high speed (see figure 1), even though both airloads and structural loads show consistent patterns for a large number of helicopters (Refs. 238, 239). The problems of advancing blade negative lift phase and under-prediction of pitch link load, were identified by Bousman as two fundamental deficiencies in articulated rotor aeromechanics (Ref. 15).

Lim and Anastassiades (Ref. 241) had identified the problem of advancing blade negative lift phase for the UH-60A flight test using CAMRAD and 2GCHAS comprehensive analysis. For illustration, figure 2 compares predicted airloads for the UH-60A at high speed, from three comprehensive analyses. The drop in the predicted lift on the advancing side leads the flight test data by a phase error of around 30 degrees. Datta and Chopra (Ref. 145) showed that the lift phase problem is not limited to the negative lift near the tip but stems in general from inaccurate prediction of vibratory lift at all radial stations, as shown in figure 2. Recently in 2004, Yeo and Johnson (Ref. 242) compared high speed air loads with CAMRAD II predictions for five articulated rotor configurations: H-34 full scale in wind tunnel, SA 330 Research Puma full scale in flight, SA 349/2 full scale in flight and the UH-60A full scale in flight. Except for the Research Puma, all rotors showed varying degrees of similar lift phase error. The tip shapes varied from straight, trapezoidal to swept, the rigid pretwist varied from low to high. Model-scale UH-60A data obtained from DNW wind-tunnel tests show similar advancing blade lift phase at high-speed, as measured in the full-scale helicopter (Ref. 243). Because both full-scale helicopters and model-scale rotors show the same discrepancy, it is therefore possible to rule out fuselage aerodynamics, dynamics, side slip angles, full scale non-linear lead-lag damper dynamics or bifilar modeling as

possible sources of error. The model rotor did not have bifilars or non-linear lag dampers.

Pitching moment predictions, for all the rotors, including the Research Puma was poor. The pitching moments determine elastic twist deformations which directly affect the blade lift as a contributing component of the angle of attack. Torok and Berezin (Ref. 245) had shown using the DNW model test data, that the lift on the advancing blade is dominated by elastic twist deformation. Lifting-line pitching moments from comprehensive codes are inaccurate, as shown in figure 2, particularly at the outboard stations where unsteady transonic 3D effects play a key role in high speed flight. Torok and Goodman (Ref. 244), had shown earlier, that even with correct pitching moments, predicting elastic twist is a challenging problem. Thus, accurate prediction of lift and pitching moment are related to each other via the accuracy of structural response calculation. The intent in this study is to decouple these two effects.

Validation of UMARC CSD model

Measured airloads, damper load and control angles are are used to validate the structural model. The non-linear coupled flap-lag-torsion equations, used in the present study, are based on references 156 and 157, and extended to include bending nonlinearities (up to second order) in axial elongation and elastic twist. The damper force is imposed on the structure as a set of concentrated forces and moments. The pitch link is modeled as a linear spring-damper system using the measured root torsion spring stiffness value of 1090 ft-lbs/deg (Ref. 246). The elastomeric bearing stiffness and damper are modeled as linear springs and dampers in flap, lag and torsion. The first eight structural modes are used for the present study. Converged blade loads were obtained using eight modes during comprehensive analysis. The periodic blade response is calculated directly using finite element in time.

Sensitivity of the measured airloads problem:

The measured airloads problem is ill-posed because the airloads are fixed and do not change in response to blade deformations. For example, the problem cannot be solved for a rotor with fundamental flap frequency 1/rev, and zero structural damping. Ideally, with perfect knowledge of measured airloads, the 1p component of the aerodynamic hinge moment would be identically zero. Therefore the 1/rev flap response would be undefined. This is because, at resonance, the damping force is equal and opposite to the exciting force and they are both included within the measured air loads. In practice, errors in measurements produce a non-zero 1/rev aerodynamic hinge moment which drive the rotor response to infinity. For non-zero structural damping, the response is not infinite but the accuracy of the measured airloads required for a reasonably accurate response solution is extremely high. The point is: the measured airloads problem is highly sensitive to small errors in airloads as well as small changes in rotor parameters. For example, increasing the first torsion frequency from below 4/rev to above 4/rev (due to uncertainty in pitch link stiffness) changes the phase of 4/rev torsion response by 180 degrees. This is not the case for a coupled solution with damping, where the pitch link stiffness has no significant effect on the torsion loads (Refs. 246, 22).

Error in 1/rev flapping:

The measured airloads, when imposed on the structure produce an error in 1/rev flap response. This stems from measurement errors and explained as follows. Out of all the harmonics of the aerodynamic hinge moment, the 1/rev component is small, and is generated as a residual of counter acting inboard and outboard 1/rev lift forces. The 1/rev lift forces are large, but they are mutually 180 degree out of phase. This is required to generate a low steady hub moment in trimmed level flight. This radial balance between the inboard and outboard normal forces determine the phase of the 1/rev aerodynamic hinge moment. The radial balance is easily destroyed by a small errors in measurement at any one radial station. In addition, interpolation over stations where the measurements are unknown contribute to this error. It appears that the phase error in calculated root flap angle stems from such unavoidable errors in the measured air loads. The problem was recognized by Frank Harris, clarified by Bobby Matthews and investigated in great detail by Ormiston (Ref. 237) (participants of the UH-60A Workshop). The rememdy is to use a 4% critical damping in first flap mode, as done by Datta *et al* (Ref. 22). The 4% damping happens to be the amount required to offset the error. Note that the damping is required only for generating an accurate *prescribed deformation* set from the measured airloads. For a fully coupled comprehensive analysis, the calculated airloads are consistent and no artificial damping is necessary.

Structural Loads:

The predicted flap bending moments are compared with test data in figure 3. Predictions show the correct peak-to-peak and higher harmonic variation. The torsion bending moments and the pitch link load are shown in figure 4. Predictions are good in the advancing side but are less satisfactory in the retreating side. This is due to errors in the 5/rev loads as shown in figure 5. Out of all the harmonics of elastic torsion, 1-3/rev are important for airloads. 1/rev produces 2/rev lift through the azimuthal velocity variation. 2/rev and 3/rev are the signif-

icant contributors to vibratory lift, of which 2/rev is the largest. Prediction of 1-3/rev elastic torsion shows satisfactory trends in magnitude and phase. Figure 6 shows predicted chord bending moments. The damper force has a significant effect on the chord-wise moments up to 50% R. The effect is dominant on the low frequency harmonics, 1-3/rev. The predicted phase of all harmonics show satisfactory correlation with test data. Discrepancies exist in the magnitude of prediction. Out of the vibratory harmonics, the 3/rev prediction is good, 4/rev is under-predicted and 5/rev is over-predicted. 1 and 2/rev harmonics show the right trends but are under-predicted at the mid-span stations. The chordwise deformation, however, do not have a significant impact on the vibratory airloads. The deformation set obtained above, provides an reasonable basis to validate and compare aerodynamic models.

Validation of Lifting-line, Euler and Navier-Stokes models

Three types of airload models are compared: lifting-line, NS and Euler. The control angles are obtained by performing a lifting-line comprehensive analysis with measured pitching moments. This produces a set of control angles consistent with the large elastic twist deformations. The flight test control angles, and if used directly, produces a non-physical negative stall in the advancing side. The blade deformations and control angles are held fixed for the different airload models. Therefore, the steady and 1/rev components of normal force are removed for comparison with test data. The CFD calculations are single blade simulations. The near wake is captured. The far wake inflow is obtained from the free wake calculations in the lifting-line model. Thus CFD and lifting-line solutions are compared for same deflections, controls and far wake inflow.

The lifting-line model combines a Weissinger-L type near wake (Ref. 247), Bagai-Leishman pseudo-implicit free wake, Leishman-Beddoes 2D unsteady model, and CFD generated 2D airfoil property tables. The 2D CFD tables agree well with test airfoil tables, as shown by Smith et al (Ref. 248) with small differences in the transonic regime (Mach 0.8).

The free wake models, as discussed earlier, require assumptions of wake roll up. Three roll up models are investigated - (i) tip vortex, (ii) moving vortex and, (iii) dual peak. All wakes use 15 degrees discretization angle and 2 turns. In the tip vortex model, the maximum bound circulation outboard of 50% span is assumed to fully roll up from the tip of the swept elastic axis at all azimuth locations. In the moving vortex model, the vortex rolls up inboard in the azimuths of negative lift, and is trailed from the zero bound circulation cross-over point. This is a simple way to model a roll up process occurring inboard in the azimuths of negative lift. In the dual peak model, a vortex of negative strength is trailed from the tip in the azimuths of negative lift. The possibility of a negative vortex in the tip region was suggested by Hooper (Ref. 239). The strength of the negative vortex is equal to the maximum negative circulation attained near the blade tip. The positive vortex continues trailing from the zero bound circulation cross-over point, with strength equal to the sum of the maximum bound circulation occurring outboard of 50% blade radius and the maximum negative circulation occurring near the blade tip.

The top views of the tip and moving vortex geometries in figure 7, shows that the advancing blade interactions with the wake trailed from the two preceding blades (B3 and B4) occur at different radial locations depending on the roll up model. The dual peak wake geometries are shown in figures 8(a) and 8(b). Figure 9 shows predicted lift using the lifting-line models. Compared to the comprehensive analysis predictions (figure 2), all wake models show improved advancing blade lift phase and vibratory lift near the tip (96.5% R). This is due to accurate 1/rev and 2/rev elastic twist affecting 2/rev and 3/rev blade lift. Accurate torsion alone is not sufficient at a relatively inboard station (77.5% R). The moving vortex and dual peak wake models improve the phasing of the vibratory harmonics significantly inboard. A marginal improvement using dual peak shows that the key phenomenon behind the generation of vibratory lift at the inboard stations is the positive trailed vortex moving inboard, not the negative vortex trailed from the tip. The predictions show, that even at high speed, the mechanism of wake roll up is an important contributor to vibratory lift.

The CFD model used is a version of the TURNS research code modified by Sitaraman and Baeder, as discussed earlier. A single block C-H grid is constructed around the UH-60A rotor blade. A relatively coarse mesh using 133 points in the wrap around direction, of which 99 are on the airfoil surface, 43 points in the normal direction and 43 points in the span-wise direction are used. The azimuthal step size is 0.5 degrees. The spacing at the blade surface in the normal direction is 5×10^{-5} chords for viscous computations and the outer boundaries are 10 chords away from the blade surface. The details of the scheme and grid and time independence studies are described in Sitaraman *et al* (Ref. 232). The free stream boundary condition used in reference (Ref. 232) have been subsequent modified to characteristic boundary conditions (Ref. 22). Figure 10 compares CFD predictions with lifting-line. All three use the moving vortex model. The inboard vibratory impulse at 77.5% R is again well captured by CFD. The Euler analyses shows the same prediction as NS. Even though the waveform

is slightly different in the advancing side, with accurate twist, and a refined wake model, all three models show similar lift prediction. For the pitching moments, the CFD predictions offer a significant improvement compared to the lifting-line model (Figure 11). CFD calculations better capture the unsteady waveform on the advancing blade at the outboard stations. Again, the near wall viscous effects do not appear to play a significant role for the UH-60A blades, as both Euler and NS calculations show the same trends.

CFD/CSD loose coupling

The goal of the CFD/CSD coupling is to improve unsteady transonic pitching moment predictions at high speed. This improves elastic twist prediction, which, in presence of a refined wake model, generates the correct vibratory lift harmonics. A loose coupling method is adopted with a propulsive trim solution. The CSD and CFD models remains same as those validated in the previous two sections.

The predicted normal forces by UMARC-TURNS loose coupling are shown in Figure 12. Predictions using the tip vortex model show the effect of improved pitching moments alone. The result is relevant for rotors which do not produce negative lift near the tip at high speed, e.g. the SA 349/2 Gazelle. Predictions using the moving vortex model show the effect of refined wake in addition to improved pitching moments. This result is relevant for rotor which produce significant negative lift near the tip. With the refined wake, predictions outboard remain similar. Prediction inboard at 77.5% R, as expected, show improvement in the impulsive waveform on the advancing side.

Figure 13 summarizes the contribution of CFD in improving the prediction of high speed lift. The spanwise distribution of predicted lift harmonics are compared in magnitude and phase between CFD and lifting-line predictions. Both use the same moving vortex free wake model. The key contribution of CFD is in the phase of 3 and 4/rev lift harmonics. Compared to the lifting-line predictions, the fundamental trends in the phase of vibratory lift harmonics appear to be in place. Improved prediction of 2,3 and 4/rev harmonics can be traced back to, as explained before, improved 1, 2 and 3/rev elastic twist prediction. The predicted pitching moments, which drive elastic twist, are shown in figure 14. The unsteady moments at the outboard stations are well captured in peak to peak and in waveform. The effect of wake is not significant, except in the second quadrant near the tip. The waveform at 77.5% R show a relatively large error compared to other radial stations. The unknown flight test trim tab setting, which spans across this stations, could be a possible source of error.

The predicted 1-10/rev torsion bending moment at 30% R, and the pitch link load are shown in Figure 15. Figure 15(a) and (b) shows prediction from UMARC lifting-line analysis. The loose coupling, as shown in (c) and (d), shows an improvement in the waveform. As in the case of measured airloads, figure 4, predictions in the retreating blade are not satisfactory. It is marginally improved by the damper load, but deficiencies remain in the prediction of higher harmonics.

Unlike torsion bending moments, predicted flap bending moments do not show any significant improvement in phase (figure 16). Figure 17 shows that the phase and the peak-to peak magnitude of the flap bending moments depend on the accuracy of the 1-3/rev harmonics. The flap bending moment harmonics (1-5/rev) are shown in figure 18. Lifting-line predictions, corresponding to airloads in figure 2, are compared with CFD predictions corresponding to airloads in figures 12 and 13. Predictions using measured airloads are shown as an upper limit for aerodynamic improvement. Compared to the lifting-line model, the phase of all three vibratory harmonics are significantly improved by CFD coupling. The magnitude of 3/rev and 5/rev remain similar, 4/rev is improved. The phase of 1,2 and 3/rev harmonics, which dominate the total flap bending moment phase, show improved spanwise trends. However, a constant azimuthal phase error of approximately 15 degrees remain all along the span. The reason for this discrepancy is not understood at present.

Figure 19 summarizes the fundamental improvement achieved by CFD/CSD coupling in the prediction of high speed airloads. It compares the same flight test airloads as in figure 2, this time with predictions from two state of the art CFD/CSD loose coupling methods. Pitching moment at 77.5% R is replaced with 86.5% R, because of a trim tab uncertainty at the former station. The steady difference at 96.5% R is an error in the test data. The couplings use different structural models and different far wake methods, but both capture the outboard pitching moments satisfactorily. And therefore, both show consistent and improved prediction of advancing blade lift phase and vibratory lift harmonics.

CONCLUSIONS

A review of rotor loads research was presented with focus on the emerging CFD tools. The state of the art in rotorcraft CFD/CSD coupling was reviewed for trimmed aeroelastic loads solution in forward flight. The high speed forward flight of the UH-60A was studied as a test case to demonstrate the most significant, recent contribution of CFD to rotor aeromechanics. The key conclusions of the review is summarized as follows.

1. The key improvement provided by CFD is in the prediction of transonic unsteady pitching moments at high-speed forward flight. Predictions appear to be satisfactory from both NS and Euler codes, for the UH-60A, with or without direct capture of the far wake. Accurate prediction of transonic pitching moments resolves the problem of advancing blade lift phase, vibratory lift and peak-to peak pitch link load.

2. The phase of the flap bending moment at high speed remains unresolved. This is an aerodynamic problem because, imposing the flight test measured airloads on the CSD model, generate improved bending moment predictions compared to a CFD/CSD solution. The higher harmonic pitch link loads remain unresolved. This is a structural dynamic problem because, imposing flight test airloads on the CSD retains similar inaccuracy as the CFD/CSD solution.

3. In transition flight, direct capture of the far wake using RANS appears to be acceptable for prediction of vortex *induced* vibratory loads at lower frequencies (3-5/rev). However, the state of the art in wake capture is not mature enough for the prediction of higher harmonic BVI loads. Even for a relatively simple steady state hover problem, grid dependent numerical dissipation makes it difficult to convect the vortex velocity profiles over one revolution. Overset RANS with adaptive grid refinement in vortical flow regions, higher order discretization schemes, vorticity confinement and the vorticity transport methods are being investigated. The accuracy of these methods must be consistently compared and validated with wake velocity profile measurements to establish their relative merits and computational costs.

4. In high altitude flight, prediction of dynamic stall appears to be a significant fundamental difficulty. RANS predictions have recently shown the potential for capturing the deep dynamic stall cycles occuring at this flight condition. There is limited study in CFD predictions of 3D dynamic stall, even though reliable data exists for both thick (NACA 0015) and thin (SC1095) airfoil wings. The key deficiency lies in RANS turbulence models. LES type solutions, which can be obtained at a fraction of DNS solutions (e.g. 0.5%) still remain prohibitively expensive for high Reynolds number flow. However, LES, hybrid RANS/LES methods, Reduced Order Modeling with Proper Orthogonal Decomposition techniques, and adaptive mesh techniques are promising avenues.

5. CFD/CSD loose coupling is a robust and stable method to obtain trimmed steady state aerolelastic response solutions. For aerolelastic stability, transient response, and unsteady maneuvers, a tight coupling method is required. In their current form of implementation, the tight coupling algorithms require a higher computational cost for rotor trim (e.g. 2.5 times loose coupling). Under steady conditions, however, airload predictions from both methods are same. Thus, for stability and transient loads a loose coupling can be performed as the first step. The trim controls can then be simply prescribed for a tight coupling calculation.

ACKNOWLEDGMENTS

The authors acknowledge the support provided by the National Rotorcraft Technology Center with Dr. Yung Yu as technical monitor and all participants of the UH-60A Black Hawk Air loads Workshop organized by U.S.Army/NASA Ames. The CFD analyses used in the coupled results shown in the paper have been developed by Jayanarayanan Sitaraman and James Baeder. Their active collaboration has been the key to improving blade loads prediction using CFD/CSD coupling. The ongoing research effort is a collaborative enterprise between all participants of the Air loads Workshop. The authors thank Jim Duh, Alan Egolf and Charles Berezin of Sikorsky Aircraft Corp., Bobby Mathews, Bruce Charles and Ram Janakiram of Boeing Company, Robert Ormiston, Willium Bousman, Mark Potsdam, Wayne Johnson and Hyeonsoo Yeo (Army/NASA), and Franklin Harris for providing key insights, test data and comparison of predictions.

References

[1] Bousman. W.G. and Mantay, W.R., "A Review of Research in Rotor Loads," NASA/Army Rotorcraft Technology Conference, NASA Ames Research Center, March 1987.

[2] Ormiston, R.A., "Comparison of Several Methods for Predicting Loads on a Hypothetical Helicopter Rotor," NASA SP-352, 1974.

[3] Hansford, R. E., Vorwald J., "Dynamics Workshop On Rotor Vibratory Loads Prediction," *Journal of the American Helicopter Society*, Vol. 43, (1), January 1998, pp 76-87.

[4] Bousman, W.G., Young, C., Toulmay, F., Gilbert, N. E., Strawn, R. C., Miller, J. V., Maier, T. H., Costes, M. and Beaumier P., "A Comparison of Lifting-Line and CFD Methods with Flight Test Data from a Research

Puma Helicopter," NASA TM 110421 USAATCOM TP 96-A-008, October 1996.

[5] Friedmann, P. P., and Hodges, D. H., "Rotary Wing Aeroelasticity," *Journal of Aircraft*, Vol. 40, No. 6, 2003.

[6] Friedmann, P. P., "Renaissance of Aeroelasticity and Its Future," *Journal of Aircraft*, Vol. 36, No. 1, 1999.

[7] Friedmann, P. P., "Rotary-Wing Aeroelasticity : Current Status and Future Trends," *AIAA Journal*, Vol. 42, No. 10, 2004.

[8] McCroskey, W. J., "Wake Vortex System of Helicopters," AIAA 95-0530, Reno, NV, January 1995.

[9] Srinivasan, G. R., and Sankar, L. N., "Status of Euler and Navier-Stokes CFD Methods for Helicopter Applications," AHS Aeromechanics Specialist Meeting, October 1995.

[10] Hariharan, N., and Sankar, L. N., "A Review of Computational Techniques for Rotor Wake Modeling," AIAA 2000-0114, Reno, NV, January 2000.

[11] Egolf, T., A., Wake, B. E., and Berezin, C., "Recent Rotor Wake Simulation and Modeling Studies at United Technologies Corporation," AIAA 2000-0115, Reno, NV, January 2000.

[12] Carr, L. W., and Chandrasekhara, M. S., "Compressibility effects on dynamic stall," *Prog. Aerospace Sci.* 32, pp. 523-573.

[13] Ekaterinaris, J. A., and Platzer, M. F., "Computational Prediction of Airfoil Dynamic Stall," *Prog. Aerospace Sci.*, Vol. 33, pp. 759-846, 1997.

[14] Lee, C. S., Saberi, H., Ormiston, R. A., "Aerodynamic and Numerical Issues for Coupling CFD into Comprehensive Rotor Analysis," Proceedings of the American Helicopter Society 53rd Annual Forum, 1997, pp. 1068-1087.

[15] William G. Bousman, "Putting the Aero Back Into Aeroelasticity," 8th Annual ARO Workshop on Aeroelasticity of Rotorcraft Systems, University Park, PA, October, 1999.

[16] Bousman, W. G., "A Qualitative Examination of Dynamic Stall from Flight Test Data,", American Helicopter Society 53rd Annual Forum, Virginia Beach, VA, April 1997.

[17] Kufeld, R., M., Bousman, W., G., "High Load Conditions Measured on a UH-60A in Maneuvering Flight,", American Helicopter Society 51th Annual Forum, Forth Worth, TX, May 1995.

[18] William G. Bousman, T. Maier, "An Investigation of Helicopter Rotor Blade Flap Vibratory Loads," American Helicopter Society 48th Annual Forum Proceedings, Washington D.C., June 1992.

[19] Elliot, J. W., Althoff, S. L., Sailey, R. H., "Inflow Measurements made with a Laser Velocimeter on a Helicopter Model in Forward Flight," Vols. I and II, Rectangular Blades - Advance Ratios of 0.23 and 0.30, NASA TM 100542, 100543, April 1988.

[20] Miller, R. H., Ellis, S. C., Dadone, L., "Effects of Wake Migration during Roll-up on Blade Air Loads," *Vertica*, Vol. 30, No. 1, 1989, pp. 1-15.

[21] Leishman, Gordon J., Principles of Helicopter Aerodynamics, Cambridge University Press, 2000.

[22] Datta, A., Sitaraman, J., Chopra., I, and Baeder, J., "Analysis Refinements for Prediction of Rotor Vibratory Loads in High-Speed Forward Flight," American Helicopter Society 60th Annual Forum, Baltimore, MD, June 2004.

[23] Potsdam, M., Yeo, Hyeonsoo, Johnson, Wayne, "Rotor Airloads Prediction Using Loose Aerodynamic/Structural Coupling," Presented at the American Helicopter Society 60th Annual Forum, Baltimore, MD, June 7-10, 2004.

[24] Strawn, R. C., and Djomehri, M. J., "Computational Modeling of Hovering Rotor and Wake Aerodynamics," *Journal of Aircraft*, Vol. 39, No. 5, pp. 786-793, October 2002.

[25] Caradonna, F. X., Isom, M. P., "Subsonic and Transonic Potential Flow over Helicopter Rotor Blades," *AIAA Journal*, No. 12, Dec. 1972, pp. 1606-1612.

[26] Caradonna, F. X., and Phillippe, J. J., "The Flow Over a Helicopter Blade Tip in the Transonic Regime,", *Vertica*, Vol. 2, April 1978, pp. 43-60.

[27] Phillippe, J. J., and Chattot, J. J., "Experimental and Theoritical Studies on Helicopter Blade Tips at ONERA," 6th European Rotorcraft Forum, Bristol, England, Paper 46, September 1980, pp. 16-19.

[28] Caradonna, F. X., Desopper, A., and Tung, C., "Finite Difference Modeling of Rotor Flows Including Wake Effects,", 8th European Rotorcraft Forum, Aix-en-Provence, France, Paper 2.7, August 1982.

[29] Arieli, R. and Tauber, M. E., "Computation of Subsonic and Transonic Flow about Lifting Rotor Blades," AIAA Paper 79-1667, August 1979.

[30] Chang, I-Chung and Tung, C., "Numerical Solution of the Full-Potential Equation for Rotors and Oblique Wings using a New Wake Model," AIAA Paper 85-0268, January 1985.

[31] Chang, I-Chung, "Transonic Flow Analysis for Rotors, Part 2, Three-Dimensional, Unsteady, Full-Potential Calculations," NASA TP 2375, 1985.

[32] Egolf, T. A., Sparks, S. P., "Hovering Rotor Airload Prediction Using a Full-Potential Flow Analysis with Realistic Wake Geometry," American Helicopter Society 41st Annual Forum, May 1985, pp. 515-530.

[33] Egolf, T. A., Sparks, S. P., "A Full Potential Rotor Analysis with Wake Influence using an Inner-Outer Domain Technique," American Helicopter Society 42nd Annual Forum, June 1986.

[34] Bridgeman, J. O., Steger, J. L., and Caradonna, F. X., "A Conservative Finite-Difference Algorithm for the Unsteady Transonic Potential Equation in Generalized Coordinates," AIAA Paper 82-1388, August 1982.

[35] Sankar, L. N., and Prichard, D., "Solution of Transonic Flow past rotor blades using the Conservative Full Potential Equation," AIAA 85-5012, October 1985.

[36] Strawn, R. C., and Caradonna, F. X., "Conservative full potential model for unsteady transonic rotor flows," *AIAA Journal*, Vol. 25, No. 2, February 1987, pp. 193-198.

[37] Bridgeman, J. O., Strawn, R. C., and Caradonna, F. X., "An Entropy and Viscosity Corrected Potential Method for Rotor Performance Prediction," American Helicopter Society 44th Annual Forum, June 1988.

[38] Caradonna, F. X., and Tung, C., "Experimental and Analytical Studies of a Model Helicopter Rotor in Hover," NASA TM-81232 or USAAVRADCOM TR-81-23, Sept. 1981.

[39] Chen, C. L., McCroskey, W. J., and Ying, S. X., "Euler Solution of Multi-bladed Rotor Flow," *Vertica*, Vol. 12, No. 3, 1988, pp. 303-313.

[40] Sankar, L. N., Wake, B. E., and Lekoudis, S. G., "Solution of the Unsteady Euler equations for fixed and rotor wing configurations," *Journal of Aircraft*, Vol. 23, No. 4, April 1986, pp. 283-289.

[41] Agarwal, R. K., and Deese, J. E., "Navier-Stokes Calculations of Hovering Rotor Flowfields," AIAA Paper 88-0106, 1988.

[42] Wake, B. E., and Sankar, L. N., "Solution of Navier-Stokes Equations for the flow over a rotor blade," *Journal of the American Helicopter Society*, April 1989.

[43] Chen, C. L., McCroskey, W. J., and Obayashi, S., "Numerical solutions of forward flight rotor flows using an upwind method," *Journal of Aircraft* Vol. 28, June 1991, pp. 374-380.

[44] Smith, M. J., and Sankar, L. N., "Evaluation of a Fourth-Order Compact Operator Scheme for Euler, Navier-Stokes Simulations of a Rotor in Hover," AIAA Paper 91-0766, January 1991.

[45] Egolf, T. A., Landgrebe, A. J., "Helicopter Rotor Wake Geometry and its influence in Forward Flight, Vol. 1 - Generalized Wake Geometry and Wake Effects in Rotor Airloads and Performance," NASA CR-3726, October 1983.

[46] Beddoes, T. S., "A Wake Model for High Resolution Airloads," Proceedings of the 2nd International Conference on Basic Rotorcraft Research, Traingle Park, NC, 1985.

[47] Wachspress, D. A., Quackenbush, T. R., Boschitsch, A. H., "First-Principles Free-Vortex Wake Analysis For Helicopters and Tiltrotors," Presented at the American Helicopter Society, 59th Annual Forum, Phoenix, AZ, May 6-8, 2003.

[48] Bagai, A., Leishman, J.G., "Rotor Free-Wake Modeling using a Pseudo-Implicit Technique - Including Comparisons with Experiment," *Journal of the American Helicopter Society*, Vol. 40, No. 3, July 1995, pp. 29-41.

[49] Johnson, W., "A General Free Wake Geometry Calculation For Wings and Rotors," Presented at the American Helicopter Society 51st Annual Forum, Fort Worth, Texas, May 9-11, 1995.

[50] Johnson, W., "Influence of Wake Models on Calculated Tiltrotor Aerodynamics," American Helicopter Society Aerodynamics, Acoustics, and Test and Evaluation Technical Specialist Meeting Proceedings, San Francisco, CA, January 2002.

[51] Bhagwat, M. J., Leishman, J. G., "Rotor Aerodynamics During Maneuvering Flight Using a Time-Accurate Free-Vortex Wake," *Journal of American Helicopter Society*, Vol. 48, No. 3, July 2003.

[52] Steinhoff, J. S. and Ramachandran, K., "A Vortex Embedding Method for Free Wake Analysis of Helicopter Blades in Hover", *Vertica*, Vol. 13, 1999.

[53] Ramachandran, K., Tung, C., and Caradonna, F. X., "Rotor Hover Performance Prediction Using a Free-Wake, Computational Fluid Dynamics,", *Journal of Aircraft*, Vol. 26, No. 12, 1989, pp. 1105-1110.

[54] Ramachandran, K., Moffitt, R. C., Owen, S. J., and Caradonna, F. X., "Hover Performance Prediction using CFD," American Helicopter Society 50th Annual Forum, June 1994.

[55] Moultan, M. A., Hafez, M. M. and Caradonna, F. X., "Zonal Procedure for predicting the hover performance of a helicopter," *ASME Journal*, Volume 184, 1984

[56] Berezin, C. R., and Sankar, L. N., "An Improved Navier-Stokes/Full Potential Coupled Ananlysis for Rotors," *Mathematical Computational Modeling*, Vol. 19, No. 3/4, 1994, pp. 125-133.

[57] Berkmann, M. E., Sankar, L. N., Berezin, C., and Torok, M. S., "A Navier-Stokes/Full Potential Free Wake Method for Rotor Flows," AIAA-97-0112.

[58] Bangalore, A. K., Moulton, M. A., and Caradonna, F. X., "The Development of an Overset/Hybrid Method for Rotorcraft Applications", AHS Specialists' Meeting for Rotorcraft Aerodynamics and Aeroacoustics, Williamsburg, Virginia, Oct. 27-30, 1997.

[59] Yang, Z. Sankar, L.N., Smith, M.J., and Bauchau, O., "Recent Improvements to a Hybrid Method for Rotors in Forward Flight," *Journal of Aircraft*, Vol. 39, No. 5, Oct 2002.

[60] Peter F. Lorber, "Aerodynamic Results of a Pressure-Instrumented Model Rotor Test at the DNW," *Journal of the American Helicopter Society*, Vol. 38, No. 3, July 1993, pp. 26-34.

[61] Moulton, M.A., Wnren, Y., and Caradonna, F.X., "Development of an Overset/Hybrid CFD Method for the Prediction of Hovering Performance," Proceedings of the 53rd Annual Forum of the American Helicopter Society. Virginia Beach, VA, May 1997.

[62] Chen, C. L. and McCroskey, W. J., "Numerical Simulation of Helicopter Multi-Bladed Rotor Flows," Paper AIAA-88-0046, January 1988.

[63] Kramer, E., Hertel, J., and Wagner, S., "Computation of Subsonic and Transonic Helicopter Rotor Flow Using Euler Equations," *Vertica*, Vol. 12, No. 3, 1988, pp. 279-291.

[64] Srinivasan, G. R., Baeder, J. D., Obayashi, S. and McCroskey, W. J., "Flowfield of a Lifting Rotor in Hover - A Navier-Stokes Simulation," *AIAA Journal*, Vol. 30, No. 10, 1992, pp. 2371-2378.

[65] Srinivasan, G. R., Raghavan, V., and Duque, E. P. N., "Flow-field Analysis of Modern Helicopter Rotors in Hover by Navier-Stokes Method," American Helicopter Society-Royal Aeronautical Society International Technical Specialists Meeting on Rotorcraft Acoustics and Rotor Fluid Dynamics, Philadelphia, Oct. 1991

[66] Srinivasan, G. R. and Baeder, J. D., "TURNS : A Free-Wake Euler/Navier-Stokes Numerical Method for Helicopter Rotors," *AIAA Journal* Vol. 31, No. 5: Technical Notes, May 1993, pp. 959-962.

[67] Srinivasan, G. R., and McCroskey, W. J., "Navier-Stokes Calculations of Hovering Rotor Flowfields," *Journal of Aircraft*, Vol. 25, No. 10, October 1988, pp. 865-874.

[68] Tang, L., and Baeder, J. D., "Improved Euler Simulation of Hovering Rotor Tip Vortices with Validation," American Helicopter Society 55th Annual Forum, Montreal, Canada, May 1999, Vol. 2, pp. 1934-1948.

[69] Strawn, R. C., and Barth, T. J., "A Finite-Volume Euler Solver for Computing Rotary-Wing Aerodynamics on Unstructured Meshes," American Helicopter Society 48th Annual Forum, Washington D. C., June 1992, Vol. 1, pp. 419-428.

[70] Park, Y. M., Nam, H. J., and Kwon, O. J., "Simulations of Unsteady Rotor-Fuselage Interactions Using Unstructured Adaptive Meshes," American Helicopter Society 59th Annual Forum, Phoenix, Arizona, May 6-8, 2003, pp. 1441-1446.

[71] Steger, J. L., Dougherty, F. C., and Benek, J. A., "A Chimera Grid Scheme," Advances in Grid Generation, K. N. Ghia, U. Ghia, Eds., *ASME FED-5*, pp. 59-69, 1983.

[72] Benek, J. A., Donegan, T. L., and Suhs, N. E., "Extended Chimera Grid Embedding Scheme with Application to Viscous Flows," AIAA Paper 87-1126, AIAA 19th Fluid Dynamics, Plasma Dynamics and Lasers Conference, Honolulu, HI, June 9-11, 1987.

[73] Duque, E. P. and Srinivasan, G. R., "Numerical Simulation of a Hovering Rotor Using Embedded Grids," American Helicopter Society 48th Annual Forum, Washington D. C., June 1992, Vol. 2, pp. 429-445.

[74] Ahmad, J., and Duque, E. P. N., "Helicopter Rotor Blade Computation in Unsteady Flows using Moving Overset Grids," *Journal of Aircraft*, Vol. 33, No. 1, pp. 54-60, Jan-Feb. 1996.

[75] Duque, E. P. N., "A Structured/Unstructured Embedded Grid Solver for Helicopter Rotor Flows," American Helicopter Society 50th Annual Forum, June 1994.

[76] Ahmad, J. U., and Strawn, R. C., "Hovering Rotor and Wake Calculations With an Overset-Grid Navier-Stokes Solver," American Helicopter Society 55th Annual Forum, Montreal, Canada, May 1999, Vol. 2, pp. 1949-1959.

[77] Strawn, R. C., Duque E. P. N., and Ahmad, J., "Rotorcraft Aeroacoustics Computations with Overset-Grid CFD Methods," *Journal of the American Helicopter Society*, Vol. 44, No. 2, April 1999.

[78] Wake, B. E., and Choi, D., "Investigation of Higher Order Upwinded Differencing for Vortex Convection," *AIAA Journal*, Vol. 34, pp. 332-337, 1995.

[79] Wake, B. E., Egolf, T. A., and Choi, D., "Resolution and Convection of Tip Vortex Using Higher-Order Methods," *Journal of Computational Physics.*

[80] Harten, A., Engquist, B., Osher, S., and Chakravarthy, C. R., "Uniformly High Order Accurate Essentially Non-oscillatory Schemes III," *Journal of Computational Physics*, Vol. 131, No. 1, 1997, pp. 3-47.

[81] Hariharan, N., and Sankar, L. N., "High-Order Essentially Nonoscillatory Schemes for Rotary-Wing Wake Computations," *Journal of Aircraft*, Vol. 41, No. 2, March-April 2004.

[82] Hall, C. M., and Long, L. N., "High-Order Accurate Simulations of Wake and Tip Vortex Flowfields," American Helicopter Society 55th Annual Forum, Alexandria, VA, May 1999.

[83] Cockburn, B., Karniadakis, G., and Shu, C. W., "An Overview of the Development of Discontinuous Galerkin Methods," Lecture Notes in *Computational Science and Engineering*, Vol. 11, Springer Verlag, 1999.

[84] Boelens, O. J., Van der Ven, Oskam, B., and Hassan, A. A., "Boundary Conforming Discontinuous Galerkin Finite Element Approach for Rotorcraft Simulations," *Journal of Aircraft*, Vol. 39, No. 5, 2002, pp. 776-785.

[85] Lele, S. K., "Compact Finite Difference Schemes with Spectral-like Resolution," *Journal of Computational Physics*, Vol. 103, 1992, pp. 16-42.

[86] Tam, C. K. W., and Webb, J. C., "Dispersion-Relation-Preserving Finite Difference Schemes for Computational Acoustics," *Journal of Computational Physics*, Vol. 107, 1993, pp. 262-281.

[87] Steinhoff, J. S., Yonghu, W., Mersch, T., and Senge, H., "Computational Vorticity Capturing - Application to Helicopter Rotor Flow," AIAA 30th Aerospace Sciences Meeting, January 1992.

[88] Wang, C. M., Bridgeman, J. O., Steinhoff, J. S., and Yonghu, W., "The Application of Computational Vorticity Confinement to Helicopter Rotor and Body Flows," American Helicopter Society 49th Annual Forum Proceedings, St. Louis, Missouri, May 1993.

[89] Wenren, Y. and Steinhoff, J., "Application of Vorticity Confinement to the Prediction of the Wake of Helicopter Rotors and Complex Bodies," AIAA Paper 99-3200, 1999.

[90] Dietz, W.E.,"Application of Vorticity Confinement to Compressible Flow," 42nd AIAA Aerospace Sciences Meeting and Exhibit, Reno, NV, Jan 2004.

[91] Brown, R. E., "Rotor Wake Modeling for Flight Dynamic Simulation of Helicopters, " AIAA Journal, Vol. 38, No. 1, 2000, pp. 57-63.

[92] Line, A.J. and Brown, R.E., "Efficient High-Resolution Wake Modelling Using the Vorticity Transport Equation," American Helicopter Society 60th Forum, Baltimore, MD, June 2004.

[93] Gormont, R. E., "A Mathematical Model of Unsteady Aerodynamics and Radial Flow for Application to Helicopter Rotors," USA AVLABS TR 72-67, May 1970.

[94] Johnson, W., "The Response and Airloading of Helicopter Rotor Blades Due to Dynamic Stall," ASRL TR 130-1, May 1970

[95] Leishman, J. G., Beddoes, T. S., "A Semi-Empirical Model for Dynamic Stall," *Journal of the American Helicopter Society*, July 1989, pp. 3-17.

[96] Petot, D., "Differential Equation Modeling of Dynamic Stall," La Recherche Aerospatiale, Number 1989-5 (Corrections dated October 1990).

[97] Truong, V. K., "A 2-D Dynamic Stall Model Based on a Hopf Bifurcation," Nineteenth European Rotorcraft Forum, Marseiles, France, September, 1998.

[98] Johnson, W., "Rotorcraft Aerodynamics Models for a Comprehensive Analysis," 54th Annual Forum of the American Helicopter Society, Washington DC, May 20-22, 1998.

[99] Carr, L. W., McAlister, K. W., and McCroskey, W. J., "Analysis of the Development of Dynamic Stall Based on Oscillating Airfoil Experiments," NASA TN D-8382, January 1977.

[100] McCroskey, W. J., "The Phenomenon of Dynamic Stall," NASA TM-81264.

[101] McAlister, K. W., Pucci, S. L., McCroskey, W. J., and Carr, L. W., "Experimental Study of Dynamic Stall of Advanced Airfoil Sections, Vol. II - Pressure and Force Data," NASA TM-84245, September 1982.

[102] Lorber, P. F. and Carta, F. O., "Airfoil Dynamic Stall at Constant Pitch rate and High Reynolds Number," *Journal of Aircraft*, Vol. 25, No. 6, pp. 548-556, June 1988.

[103] Piziali, R. A., "2-D and 3-D Oscillating Wing Aerodynamics for a Range of Angles of Attack Including Stall,", NASA TM 4632, USAATCOM Technical Report 94-A-011, September 1994.

[104] Lorber, P. F., "Compressibility Effects on the Dynamic Stall of a Three-Dimensional Wing," AIAA Paper 92-0191, AIAA 30th Aerospace Sciences Meeting, January 1992.

[105] Lorber, P. F., Carta, F. O. and Covino, A. F., "An Oscillating three-dimensional wing experiment: compressibility, sweep, rate, waveform and geometry effects on unsteady separation and dynamic stall," AIAA Paper 91-1795, June 1991.

[106] Van Dyken, R. D., and Chandrasekhara, M. S., "Leading-edge velocity field of an oscillating airfoil in compressible dynamic stall," AIAA Paper 92-0193.

[107] Chandrasekhara, M. S., and Van Dyken, R. D., "LDV Measurements in dynamically separated flows," *SPIE Proc. Laser Anemometry Adv. Appl.* 2052, pp. 305-312.

[108] Chandrasekhara, M. S., Wilder, M. C., and Carr, L. W., "Competing Mechanisms of Compressible Dynamic Stall," *AIAA Journal*, Vol. 36, No. 3, March 1998.

[109] Chandrasekhara, M.S. and Wilder, M.C., "Heat Flux Gage Studies of Compressible Dynamic Stall," 40th AIAA Aerospace Sciences Meeting and Exhibit, Reno, NV, Jan 2002.

[110] Coton, F.N., and Galbraith, R.A.McD., "An Examiniation of Dynamic Stall on an Oscillating Rectangular Wing," 21st Applied Aerodynamic Conference, Orlando, FL, June 2003.

[111] Ekaterinaris, J. A., Cricelli, A. S., and Platzer, M. F., "A zonal method for unsteady, viscous, compressible airfoil flows," *J. Fluids Struct.* 8, pp. 107-123.

[112] Jones, K. D. and Platzer, M. F., "A Fast Method for the prediction of dynamic stall onset on turbomachinery blades," ASME Paper 97-GT-101.

[113] Cebeci, T., Platzer, M. F., Jang, H. M., and Chen, H. H., "An inviscid-viscous interaction approach for the calculation of dynamic stall initiation of airfoils," *ASME J. Turbomachinery* 115(4), pp. 714-723.

[114] Tuncer, I. C., Ekaterinaris, J. A., and Platzer, M. F., "Viscous-inviscid interaction method for unsteady low-speed airfoil flows," *AIAA Journal*, Vol. 33, No. 1, pp. 151-154.

[115] Baldwin, B. S., and Lomax, H., "Thin Layer Approximation and Algebraic Model for Separated Turbulent Flows," AIAA Paper no. 78-257, 1978.

[116] Yakhot, V. and Orzag, S. A., "Renormalization group analysis of Turbulence 1 - Basic Theory," *Journal of Scientific Computing*, 1, pp. 1-36, 1986.

[117] Johnson, D. A., and King, L. S., "A Mathematically Simple Turbulence Closure Model for Attached and Separated Boundary Layers," *AIAA Journal*, 23, pp. 1684-1692, 1985.

[118] Baldwin, B. S. and Barth, T. J., "A One-equation Turbulence Transport Model for high Reynolds Number Wall-bounded Flows," NASA TM 102847.

[119] Spalart, P. R. and Allmaras, S. R., "A One-equation Turbulence Model for Aerodynamic Flows," AIAA Paper 92-0439, 1992.

[120] Jones, W. P. and Launder, B. E., "The Calculation of Low-Reynolds-Number-Phenomena with a two-equation model of turbulence," *International Journal of Heat and Mass Transfer*, 16, pp. 1119-1130.

[121] Wilcox, D. C., "Reassessment of the Scale-Determining Equation for Advanced Turbulence Models," *AIAA Journal*, 26(11), pp. 1299-1310, 1988.

[122] Sankar, L. N., and Tassa, W., "Compressibility effects of dynamic stall of a NACA 0012 airfoil," *AIAA Journal*, Vol. 19, No. 5, pp. 557-568, 1981.

[123] Visbal, M. R., and Shang, J. S., "Investigation of the flow structure around a rapidly pitching airfoil," *AIAA Journal*, Vol. 27, No. 8, pp. 1044-1055, 1989.

[124] Choudhuri, P. G., and Knight, D. D., "Effects of compressibility, pitch rate, and Reynolds number of unsteady incipient leading-edge separation on a pitching airfoil," *AIAA Journal* Vol. 32, No. 4, pp. 673-681, 1994.

[125] Sankar, L. N., and Tung, W., "Numerical Solution of unsteady viscous flow past rotor sections," AIAA Paper 85-0129.

[126] Patterson, M. T., and Lorber, P. F., "Computational and Experimental Studies of compressible dynamic stall," *J. Fluids Struct.*, 4, pp. 259-285, 1990.

[127] Wu, J. C., and Sankar, N. L., "Evaluation of three turbulence models for the prediction of steady and unsteady airloads," AIAA Paper 89-0609.

[128] Carta, F. O., and Lorber, P. F., "Experimental Study of the aerodynamics of incipient torsional stall flutter," *J. Propulsion Power* 3 (2), pp. 164-170, 1987.

[129] Rizetta D. P., and Visbal, M. R., "Comparative numerical study of two turbulence models for airfoil static and dynamic stall," *AIAA Journal*, 31, pp. 784-786, 1993.

[130] Dindar, M. and Kaynak, U., "Effect of turbulence modeling on dynamic stall of a NACA-0012 Airfoil," AIAA Paper 92-0027.

[131] Clarkson, J. D., Ekaterinaris, J. A., and Platzer, M. F., "Computational investigation of airfoil stall flutter," In H. M. Atassi (ed.), *Unsteady Aerodynamics, Aerocoustics and Aeroelasticity of Turbomachines and Propellers*, pp. 415-432, 1993, Springer, Berlin.

[132] Srinivasan, G. R., Ekaterinaris, J. A., and McCroskey, W. J., "Dynamic stall of an oscillating wing, Part 1: evaluation of turbulence models," *Comput. Fluids*, Vol. 24, No. 7, pp. 833-861, 1995.

[133] Ekaterinaris, J. A. and Menter, F. R., "Computation of oscillating airfoil flows with One- and Two-equation turbulence models," *AIAA Journal* Vol. 32, No. 12, pp. 2359-2365, 1994.

[134] Ko, S., and McCroskey, W. J., "Computations of unsteady separating flows over an oscillating airfoil," AIAA Paper 95-0312.

[135] Ekaterinaris, J. A., and Platzer, M. F., "Numerical investigation of stall flutter," *ASME J. Turbomachinery*, 118, pp. 197-203, 1996.

[136] Sankar, L. N., Zibi-Bailly, J., LeBalleur, J. C., Blaise, D., Rouzaud, O., and Rhee, M., "A Comparative Study of three methodologies for modeling dynamic stall," European Rotorcraft Forum, 2004.

[137] Reif, B.A. Pettersson, "A Nonlinear Eddy-Viscosity Model for Near-Wall Turbulence," AIAA-2000-0135, 1999.

[138] Nichols, R.H., Nelson, C.C., "Application of Hybrid RANS/LES Turbulence Models," 41st Aerospace Sciences Meeting and Exhibit, Reno, NV, Jan 2003.

[139] Spalart, P. R. and Allmaras, S. R., "A One-Equation Turbulence Model for Aerodynamic Flows", AIAA Paper 92-0439, January 1992.

[140] Nelson, C.C. and Nichols, R.H., "Evaluation of Hybrid RANS/LES Turbulence Models Using an LES Code," 16th AIAA Computational Fluid Dynamics Conference, Orlando, FL, June 2003.

[141] Samimy, M. and Elliot, G., "Effects of Compressibility on the Characteristics of Free Shear Layers," AIAA Journal, Vol. 28, No. 3, March 1990.

[142] Dolling, D. S., "50 Years of Shock-Wave/Boundary Layer Interaction Research: What Next?," AIAA J, Vol. 39, No. 8, pp. 1517-1531, August 2001.

[143] Kaenel, R. vo, Kleiser, L., Adams, N.A., and Vos, J.B., "Large-Eddy Simulation of Shock-Turbulence Interaction Using the Approximate Deconvolution Model in a Finite Volume Scheme," 16th AIAA Computational Fluid Dynamics Conference, Orlando, FL, June 2003.

[144] Johnson, W., "Recent Developments in Rotary-Wing Aerodynamic Theory," *AIAA Journal*, Vol. 24, No. 8, August 1986, pp. 1219-1245. '

[145] Datta, A., Chopra, I., "Validation and Understanding of UH-60A Vibratory Loads in Steady Level Flight," *Journal of the American Helicopter Society*, Vol. 49, No. 3, July 2004, pp 271-287.

[146] Gorton, S.A., Meyers, J.F., and Berry, J.D., "Velocity Measurements Near the Empennage of a Small-Scale Helicopter Model," American Helicopter Society 52nd Annual Forum, Washington, D.C., June 1996.

[147] Leishman, J. G., Bi, N., "Aerodynamic Interactions Between a Rotor and a Fuselage in Forward Flight," *Journal of the American Helicopter Society*, Vol. 35, No. 3, July 1990.

[148] Wachspress, D. A., Quackenbush, T. R., Boschitsch, A. H., "Rotorcraft Interactional Aerodynamics with Fast Vortex/Fast Panel Methods," *Journal of the American Helicopter Society*, Vol. 48, No. 4, October 2003.

[149] Bettschart, N., "Rotor Fuselage Interaction : Euler and Navier-Stokes Computations with an Actuator Disk," American Helicopter Society 55th Annual Forum Proceedings, Montreal, Canada, May 1999.

[150] Zori, L. A. J., Mathur, S. R., Rajagopalan, R. G., "Three Dimensional Calculations of Rotor-Airframe Interaction in Forward Flight," American Helicopter Society 52nd Annual Forum Proceedings, Washington D.C., June 1992.

[151] Duque, E., and Dimanlig, A., "Navier-Stokes Simulation of the RAH-66 Comanche Helicopter," American Helicopter Society Aeromechanics Specialists Conference Proceedings, San Francisco, California, January 1994.

[152] Berry, J. D., Letnikow, V., Bavykina, I., and Chaffin, M. S., "A Comparison of Interactional Aerodynamics Methods for a Helicopter in Low Speed Flight," NASA TM-1998-208420, AFDD TR-98-A-003, June 1998.

[153] Ruffin, S. M., O'Brien, D., Smith, M., Hariharan, N., Lee, J. D., Sankar, L., "Comparison of Rotor Airframe Interaction Utilizing Overset and Unstructured Grid Techniques," AIAA 42nd Aerospace Sciences Meeting and Exhibit, Reno, NV, January 2004.

[154] Narramore, J. C., Vadyak, J., and Strewsbury, G., "Navier-Stokes Computations of the Full V-22 Configuration Using Massively Parallel Computers," American Helicopter Society 52nd Annual Forum Proceedings, Washington D. C., June 1996.

[155] Boyd, D. D., Barnwell, R. W., and Gorton, S. A., "A Computational Model for Rotor-Fuselage Interactional Aerodynamics," 38th Aerospace Sciences Meeting and Exhibit, Reno, NV, January 2000.

[156] Hodges, D. H., and Dowell, E. H., "Nonlinear Equations of Motion for the Elastic Bending and Torsion of Twisted Nonuniform Rotor Blades," NASA TN D-7818, December 1974.

[157] Ormiston, R. A., Hodges, D. H., and Peters, D. A., "On the Nonlinear Deformation Geometry of Euler-Bernoulli Beams," NASA Technical Paper 1566, 1980.

[158] Kvaternik, Raymond G., Kaza, Krishna R. V., Nonlinear Curvature Expressions for Combined Flapwise Bending, Chordwise Bending, Torsion, and Extension of Twisted Rotor Blades, NASA TM X-73, 997, 1976.

[159] Rosen, A., Friedmann, P.P., "Nonlinear Equations of Equilibrium for Elastic Helicopter or Wind Turbine Blades Undergoing Moderate Deformation," Report UCLA-ENG 7718, University of California at Los Angeles, June 1977 (also NASA CR-159478, 1978)

[160] Johnson, W., "Aeroelastic Analysis for Rotorcraft in Flight or in a Wind Tunnel," NASA TN D-8515, 1977.

[161] Johnson, W., "Rotorcraft Dynamics Models for a Comprehensive Analysis," 54th Annual Forum of the American Helicopter Society, Washington D.C., May 20-22, 1998.

[162] Hodges, D.H., "A Mixed Variational Formulation Based on Exact Intrinsic Equations for Dynamics of Moving Beams," Int. J. Solids Structures, Volume 26, No. 11, 1990, pp. 1253-1273.

[163] Hodges, D. H., Patil, M. J., "Technical Note : Correlation of Geometrically-Exact Beam Theory with the Priceton Data," *Journal of the American Helicopter Society*, Vol. 49, No. 3, July 2004, pp 357-360.

[164] Bauchau, O. A., Kang, N. K., "A Multibody Formulation for Helicopter Structural Dynamic Analysis," *Journal of the American Helicopter Society*, Vol. 38, No. 2, April 1993.

[165] Hopkins, A. S., and Ormiston, R. A., "An Examination of Selected Problems in Rotor Blade Structural Mechanics and Dynamics", Proceedings of the 59th Annual Helicopter Society Annual Forum, Phoenix, AZ, May 2003.

[166] Hodges, D. H., "A Review of Composite Rotor Blade Modeling,", *AIAA Journal*, Vol 28, No. 3, 1990, pp. 561-565.

[167] Jung, S. N., Nagaraj, V. T., and Chopra, I., "Assessment of Composite Rotor Blade Modeling Techniques" *Journal of the American Helicopter Society*, Vol. 44, No. 3, 1999, pp. 188-205.

[168] Cesnik, C. E. S., "VABS: A New Concept for Composite Rotor Blade Cross-Sectional Modeling," *Journal of the American Helicopter Society*, Vol. 42, No. 1, Jan 1997, pp. 27-38.

[169] Hodges, D. H., Atilgan, A. R., Cesnik, C. E. S., Fulton, M. V., "On a Simplified Strain Energy Function for Geometrically Nonlinear Behavior of Anisotropic Beams,", Composites Engineering, Volume 2, Numbers 5-7, 1992.

[170] Volovoi, V. V., Hodges, D. H., Cesnik, C. E. S., and Popescu, B., "Assessment of Beam Modeling Methods for Rotor Blade Application," *Mathematical and Computer Modelling*, Vol. 33, No. 10-11, 2001, pp. 1099-1112.

[171] Smith, E. C., Chopra, I., "Aeroelastic Response, Loads, and Stability of a Composite Rotor in Forward Flight," *AIAA Journal*, Vol. 31, No. 7, July 1993.

[172] Jung, S. N., Nagaraj, V. T. and Chopra, I., "Refined Structural Model for Thin- and Thick-walled Composite Rotor Blades," *AIAA Journal*, Vol. 40, No. 1, 2002, pp. 105-116

[173] Berdichevsky, V. L, Armanios, E. A., and Badir, A. M., "Theory of Anisotropic Thin-Walled Closed-Section Beams," *Composites Engineering*, Vol. 2, No. 5-7, 1992, pp. 411-432.

[174] Volovoi, V. V. and Hodges, D. H., "Theory of Anisotropic Thin-Walled Beams," *Journal of Applied Mechanics*, Vol. 67, No. 3, 2000, pp. 453-459.

[175] Yuan, I., Friedmann, P. P., Venkatesan, C., "A New Aeroelastic Model for Composite Rotor Blades with Straight and Swept Tips," Proceedings of the 33rd AIAA/ASME/ASCE/AHS/ASC Structures, Structural Dynamics and Materials Conference, AIAA, Washington, DC, 1992, pp. 1371-1390.

[176] Kosmatka, J. B., "Extension-Bend-Twist Coupling Behavior of Nonhomogeneous Anisotropic Beams with Initial Twist," *AIAA Journal*, vol. 30, no. 2, 1992, pp. 519-527.

[177] Yu, W., Hodges, D. H., Volovoi, V. V. and Cesnik, C. E. S., "On Timoshenko-Like Modeling of Initially Curved and Twisted Composite Beams," *International Journal of Solids and Structures*, Vol. 39, No. 19, 2002, pp. 5101-5121.

[178] Celi, R., Friedmann, P. P., "Structural Optimization with Aeroelastic Constraints of Rotor Blades with Straight and Swept Tips," *AIAA Journal*, Vol. 28, No. 5, 1992.

[179] Kim, K. C., Chopra, I., "Aeroelastic Analysis of Helicopter Blades with Advanced Tip Shapes," *Journal of the American Helicopter Society*, Vol. 37, No. 1, Jan 1992.

[180] Ganguli, R., Chopra, I., "Aeroelastic Optimization of an Advanced Geometry Composite Helicopter Rotor," Annual Forum Proceedings of the American Helicopter Society, Vol. 2, 1995, pp. 965-984.

[181] Yu, W, Volovoi, V.V., Hodges, D.H., and Hong, X., "Validation of the Variational Asymptotic Beam Section (VABS) Analysis," *AIAA Journal*, Vol. 40, No. 10, 2002, pp. 2105-2112.

[182] Piatak, D.J., M.W. Nixon, and J.B. Kosmatka; Stiffness Characteristics of Composite Rotor Blades with Elastic Couplings, NASA TP-3641, ARL TR-1279, pp. 1-47, April, 1997.

[183] Gandhi, F., and Chopra, I., "An Analytical Model for Nonlinear Elastomeric Lag Damper and Its Effect on Aeromechanical Stability in Hover," *Journal of the American Helicopter Society*, Vol. 39, No. 4, 1994, pp. 59-69.

[184] Gandhi, F., and Chopra, I., "Analysis of Bearingless Main Rotor Aeroelasticity Using an Improved Time Domain Nonlinear Elastomeric Damper Model," *Journal of the American Helicopter Society*, Vol. 41, No. 3, 1996, pp. 267-277.

[185] Smith, E., Govindswamy, K., Beale, M. R., and Lesieutre, G., "Formulation, Validation and Application of a Finite Element Model for Elastomeric Lag Dampers," *Journal of the American Helicopter Society*, Vol. 41, No. 3, 1996, pp. 247-256.

[186] Tarzanin, F. J. and Panda, B., "Development And Application Of Nonlinear Elastomeric And Hydraulic Lag Damper Models," AIAA-1995-1449, Presented at the 36th SDM Conference, New Orleans, LA, April 1995.

[187] Brackbill, C.R., Lesieutre, G.A., Ruhl, L.E., and Smith, E.C., "Characterization and Modeling of the Low Strain Amplitude and Frequency Dependent Behavior of Elastomeric Damper Materials," AIAA-1998-1845, AIAA/ASME/ASCE/AHS/ASC Structures, Structural Dynamics, and Materials Conference and Exhibit, 39th, and AIAA/ASME/AHS Adaptive Structures Forum, Long Beach, CA, Apr. 20-23, 1998.

[188] Curtiss, H.C., Hong, S., Kothmann, B., and Keller, J., "Modeling the Inplane Motion of Rotor Blades," Presented at Fifth International Workshop on Dynamics and Aeroelastic Stability Modeling of Rotorcraft Systems, Rensselaer Polytechnic Institute, Troy, NY, Oct 1993.

[189] Ghiringhelli, G. L., Masarati, P., Mantegazza, P., Nixon, M. W., "Multi-Body Analysis of the 1/5 scale Wind Tunnel Model of the V-22 Tiltrotor," 55th Annual Forum of the American Helicopter Society, Montreal, Canada, May 25-27, 1999.

[190] Bottasso, C.L. and Bauchau., O.A. , "Multibody Modeling Of Engage And Disengage Operations Of Helicopter Rotors," *Journal of the American Helicopter Society*, 46(4):290-300, 2001.

[191] G.L. Ghiringhelli, P. Masarati, P. Mantegazza and M. W. Nixon, "Multi-Body Analysis of a Tiltrotor Configuration," 7th Conference On Nonlinear Vibrations, Stability, and Dynamics of Structures, July 26-30, 1998, Blacksburg, VA, USA (also published in the journal Nonlinear Dynamics, August 1999).

[192] G.L. Ghiringhelli, P. Masarati, P. Mantegazza and M. W. Nixon, "Multi-Body Analysis of an Active Control for a Tiltrotor," presented at the International Forum on Aeroelasticity and Structural Dynamics 1999, June 22-25, 1999, Williamsburg, VA, USA, pp. 149-158.

[193] P. Masarati, G.L. Ghiringhelli, M. Lanz, and P. Mantegazza, "Integration of Hydraulic Components in a Multibody Framework for Rotorcraft Analysis'," presented at the 26th European Rotorcraft Forum, Semptember 26-29, 2000, The Hague, The Netherlands.

[194] Lee, C.D. and White, J.A., "Investigation of the Effect of Hub Support Parameters on Two-Bladed Rotor Oscillatory Loads," NASA CR-132435, 1974.

[195] Chopra, I., "Perspectives in Aeromechanical Stability of Helicopter Rotors," *Vertica*, v 14, n 4, 1990, pp. 457

[196] Staley, J.A. and Sciarra, J.J., "Coupled Rotor/Airframe Vibration Prediction Methods, Rotorcraft Dynamics," NASA SP-352, 1974.

[197] Vellaichamy, S., Chopra, I., "Effect of Modeling Techniques in the Coupled Rotor-Body Vibration Analysis," In Proceedings of the 34th Structures, Structural Dynamics and Materials Conference and Adaptive Structures Forum, La Jolla, CA, April 1993.

[198] Yeo, H. and Chopra, I., "Coupled Rotor/Fuselage Vibration Analysis for Teetering Rotor and Test Data Comparison," *Journal of Aircraft*, Vol. 38, No. 1, Feb 2001.

[199] Cribbs, R.C., Friedmann, P.P., and Chiu, T., "Coupled Helicopter Rotor/Flexible Fuselage Aeroelastic Model for Control of Structural Response," AIAA Journal, Vol. 38, No. 10, Oct 2000.

[200] Yeo, H., Chopra, I., "Coupled Rotor/Fuselage Vibration Analysis Using Detailed 3-D Airframe Models," *Mathematical and Computer Modelling* 33 (2001) pp. 1035-1054.

[201] Shabana, A. A., "Flexible Multibody Dynamics: Review of Past and Recent Developments," *Multibody System Dynamics*, Vol. 1, 1997, pp. 189-222.

[202] Bauchau, O. A., Rodriguez, J., Chen, S., "Coupled Rotor-Fuselage Analysis with Finite Motions Using Component Mode Synthesis", *Journal of the American Helicopter Society*, Vol. 49, No. 2, April 2004, pp. 201-211.

[203] Johnson, W., *Helicopter Theory*, Princeton University Press, Princeton, New Jersey, 1980.

[204] Dugundji, J., Wendell, H., "Some Analysis Methods for Rotating Systems with Periodic Coefficients," *AIAA Journal*, Vol. 21, No. 6, June 1983.

[205] Panda, B., Chopra, I., "Dynamics of Composite Rotor Blades in Forward Flight," *Vertica*, Vol. 11, No. 1/2, January 1987.

[206] Bauchau, O.A. and Guernsey, D., "On The Choice Of Appropriate Bases For Nonlinear Dynamic Modal Analysis," *Journal of the American Helicopter Society*, 38:28-36, 1993.

[207] Thomas, J.P., Dowell, E.H., and Hall, K.C., "A Static/Dynamic Correction Approach for Reduced-Order Modeling of Unsteady Aerodynamics," 39th AIAA Aerospace Sciences Meeting and Exhibit, Reno, NV, Jan 2001.

[208] Willcox, K., "Unsteady Flow Sensing and Estimation via the Gappy Proper Orthogonal Decomposition," AIAA Flow Control Conference, Portland, Oregan, July 2004.

[209] LeGresley, P.A. and Alonso, J.J., "Dynamic Domain Decompositon and Error Correction for Reduced Order Models," 41st Aerospace Sciences Meeting and Exhibit, Reno, NV, Jan 2003.

[210] Bui-Thanh, T., Damodaran, M., and Willcox, K., "Aerodynamic Data Reconstruction and Inverse Design Using Proper Orthogonal Decomposition," *AIAA Journal*, August 2004.

[211] Saberi, H., Khoshlahjeh, M., Ormiston, R. A., Rutkowski, M. J., "Overview of RCAS and Application to Advanced Rotorcraft Problems," Presented at the AHS 4th Decennial Specialist's Conference on Aeromechanics, San Francisco, California, January 21-23, 2004.

[212] Johnson, W, "A Comprehensive Analytical Model of Rotorcraft Aerodynamics and Dynamics, Part I : Analysis Development," NASA TM-81182, June 1980.

[213] Tung, C., Cardonna, F.X., and Johnson, W.R., "The Prediction of Transonic Flows on an Advancing Rotor," *Journal of the American Helicopter Society*, Vol. 31, No. 3, July 1986.

[214] Strawn, R.C. and Tung, C., "Conservative Full Potential Model for Unsteady Transonic Rotor Flows," *AIAA Journal*, Vol. 25, No. 2, 1987 p 193-198.

[215] Strawn, R., C., Desopper, A., Miller, J., Jones, A., "Correlation of Puma Airloads - Evaluation of CFD Prediction Methods," Paper No. 14, 15th European Rotorcraft Forum, September 1989.

[216] Strawn, R. C., Bridgeman, J. O., "An Improved Three-Dimensional Aerodynamics Model for Helicopter Airloads Prediction," AIAA Paper 91-0767, AIAA 29th Aerospace Sciences Meeting and Exhibit, Reno, NV, January 1991.

[217] Kim, K. C., Desopper, A. and Chopra, I.,"Blade Response Calculations Using Three-Dimensional Aerodynamic Modeling," *Journal of American Helicopter Society*, Vol. 36, No. 1, p. 68-77, January 1991.

[218] Altmikus, A. R. M., Wagner, S., Beaumier, P., and Servera, G., "A Comparison : Weak versus Strong Modular Coupling for Trimmed Aeroelastic Rotor Simulation," American Helicopter Society 58th Annual Forum, Montreal, Quebec, June 2002.

[219] G. Servera, P. Beaumier, M. Costes, "A Weak Coupling Method between the Dynamics Code Host and the 3D Unsteady Euler Code Waves," 26th European Rotorcraft Forum, The Hague, Netherlands, Sept 2000.

[220] Pahlke, K. and Van Der Wall, B., "Progress in Weak Fluid-Structure-Coupling for Multibladed Rotors in High-Speed Forward Flight," ERF.

[221] Alonso, J. J., Sheffer, S. G., Martinelli, L., and Jameson, A., "Parallel Unsteady Simulation of the Flow Through a Helicopter Rotor in Hover Including Aeroelastic Effects," Proceedings First AFOSR Conference on Dynamic Motion CFD, Rutgers University, New Brunswick, June 1996.

[222] Bauchau, O., A. and Ahmad, J., U., " Advanced CFD and CSD Methods for Multidisciplinary Applications of Rotorcraft Problems," AIAA 6th Symposium on Multidisciplinary Analysis and Optimization, Seattle, WA, September 1996.

[223] Pomin, H. and Wagner, S. "Aeroelastic Analysis of Helicopter Rotor Blades on Deformable Chimera Grids," *Journal of Aircraft*, Vol. 41, No. 3, May-June 2004.

[224] Pahlke, K., Boniface, J. C., "A Detailed Comparison of DLR and ONERA 3D Euler Methods for Rotors in High Speed Forward Flight," 24th European Rotorcraft Forum, AE14, Marseilles, France, Sep. 1998.

[225] Akio, O., Aoyama, T., Saito, S., Shima, E., Yamakawa, E., "BVI Noise Predictions by Moving Overlapped Grid Method," American Helicopter Society 55th Annual Forum Proceedings, Montreal, Canada, May 25-27, 1999.

[226] Kondo, N., Nakamura, H., Aoyama, T., Saito, S., and Yamakawa, E., "Validation of a Helicopter Noise Prediction System," American Helicopter Society 56th Annual Forum Proceedings, Virginia Beach, Virginia, May 2-4, 2000.

[227] Sakowsky, P. C., and Charles, B. D., "Noise Measurement Test Results for AH-1G Operational Loads Survey," Vol I and II, Bell Helicopter Co. Rept. 299-099-831, Forth Worth, TX, Oct. 1976.

[228] Yu, Y. H., Tung, C., and Gallman, J., "Aerodynamics and Acoustics of Rotor Blade-Vortex Interactions," *Journal of Aircraft*, Vol. 32, No. 5, Oct. 1995, pp. 970-977.

[229] Splettstoeser, W. R., Kube, R., Wagner, W., Seelhorst, U., Boutier, A., Micheli, F., Mercker, E., and Pengel, K., "Key results from a higher harmonic control aeroacoustic rotor test (HART)," *Journal of the American Helicopter Society*, 1997, pp. 58-78.

[230] Splettstoeser, W. R., Niesl, G., Cenedese, F., Nitti, F., and Papnikas, D. G., "Experimental results of the European HELINOISE aeroacoustic rotor test," *Journal of the American Helicopter Society*, 1995, pp. 3-14.

[231] Boniface, J. C., Mialon, B., and Sides, J., "Numerical Simulation of Unsteady Euler Flow Around Multibladed Rotor in Forward Flight using a Moving Grid Approach," 51st Annual Forum of the American Helicopter Society, Forth Worth, TX, May, 1995.

[232] Sitaraman, J., Baeder, J. D., and Chopra, I., "Validation of UH-60 Rotor Blade Aerodynamic Characteristics using CFD," 59th Annual Forum of the American Helicopter Society, Phoenix, AZ, May 6-8, 2003.

[233] Paramesvaran, V. and Baeder, J. D., "Indicial Aerodynamics in Compressible Flow - Direct Computational Fluid Dynamic Calculations," *Journal of Aircraft*, Vol. 34, No. 1, January 1997, pp. 131-133.

[234] Buning, P., Chan, W., Renze, K., and Sondak, D., *OVERFLOW 1.6ap Users Manual*, NASA Ames Research Center, Feb. 1995.

[235] Meakin, R., "Composite Overset Structured Grids," *Handbook of Grid Generation*, edited by Thompson, J. F., Soni, B. K., and Weatherill, N. P., CRC Press, Washington, DC, 1999, pp. 11-1 to 11-19.

[236] Meakin, R. L., and Wissink, A. M., "Unsteady Aerodynamic Simulation of Static and Moving Bodies Using Scalable Computers," AIAA-99-3302, Proc. 14th AIAA Computational Fluid Dynamics Conf. Norfolk VA, July 1999, pp. 469-483.

[237] Ormiston, R. A., "An Investigation of the Mechanical Airloads Problem for Evaluating Rotor Blade Structural Dynamics Analysis", Presented at the AHS 4th Decennial Specialist's Conference on Aeromechanics, San Francisco, CA, January 21-23, 2004.

[238] W.G.Bousman, "Response of Helicopter Rotors to Vibratory Airloads," *Journal of the American Helicopter Society*, Vol. 35, No. 4, Oct, 1990, pp. 53-62.

[239] W.E.Hooper, "The Vibratory Airloading of Helicopter Rotors," Paper No.46, 9th European Rotorcraft Forum, Stresa, Italy, September, 1983.

[240] Leishman, J.G., "Validation of Approximate Indicial Aerodynamic Functions for Two-Dimensional Subsonic Flow," *Journal of Aircraft*, Vol. 25, No. 1, October 1, 1988.

[241] Lim, J. W., Anastassiades, T., "Correlation of 2GCHAS Analysis with Experimental Data," *Journal of the American Helicopter Society*, Vol.40, No. 4, October 1995, pp. 18-33.

[242] Yeo, H., Johnson, W., "Assessment of Comprehensive Analysis Calculation of Airloads on Helicopter Rotors," Presented at the American Helicopter Society 4th

Decennial Specialist's Conference on Aeromechanics, San Francisco, CA, January 21-23, 2004.

[243] Bousman, W. G., "A Note on Torsional Dynamic Scaling," *Journal of the American Helicopter Society*, Vol. 43, No. 2, April 1998, pp. 172-175.

[244] Torok, M. S. and Goodman, R. K., "Analysis of Rotor Blade Dynamics Using Model Scale UH-60A Airloads," *Journal of the American Helicopter Society*, Vol.39, No. 1, January 1994, pp. 63-69.

[245] Torok, Michael S. and Berezin, Charles R., "Aerodynamic and Wake Methodology Evaluation Using Model UH-60A Experimental Data," *Journal of the American Helicopter Society*, Vol.39, No. 2, April 1994, pp. 21-29.

[246] Kufeld, R. M., Johnson, W. "The Effects of Control System Stiffness Models on the Dynamic Stall Behavior of a Helicopter," American Helicopter Society 54nd Annual Forum Proceedings, Washington, D.C., May 20-22.

[247] J. Weissinger, "The Lift Distribution of Swept-Back Wings," National Advisory Committee for Aeronautics, Technical Memorandum No. 1120, 1942.

[248] Smith, M. J., Wong, T., Potsdam, M., Baeder, J., and Phanse, S., "Evaluation of CFD to Determine Two-Dimensional Airfoil Characteristics for Rotorcraft Applications," American Helicopter Society 60th Annual Forum, Baltimore, MD, June 7-10, 2004.

[249] Roe, P. L., "Approximate Riemann Solvers, Parametric Vectors, and Difference Schemes," *Journal of Computational Physics*, Vol. 43, No. 3, 1981, pp. 357-372.

[250] Vatsa, V. N., Thomas, J. L., and Wedan, B. W., "Navier-Stokes Computations of Prolate Spheroids at Angle of Attack," AIAA Paper 87-2627, August 1987.

[251] Jameson, A., and Yoon, S., "Lower-Upper Implicit Schemes with Multiple Grids for the Euler Equations," *AIAA Journal*, Vol. 25, No. 7, July 1987, pp. 929-935.

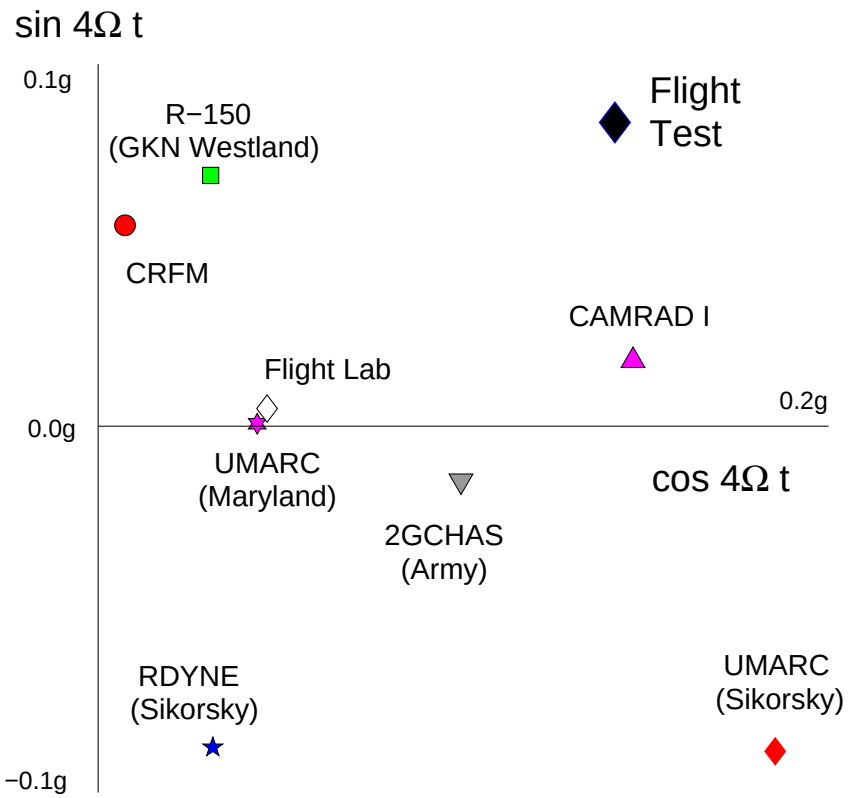

Figure 1: **Vibratory hub load predictions from eight aeroelastic codes compared with Lynx data, cockpit starboard location, high-speed steady level flight at 158 kts; Hansford and Vorwald (Reference 3)**

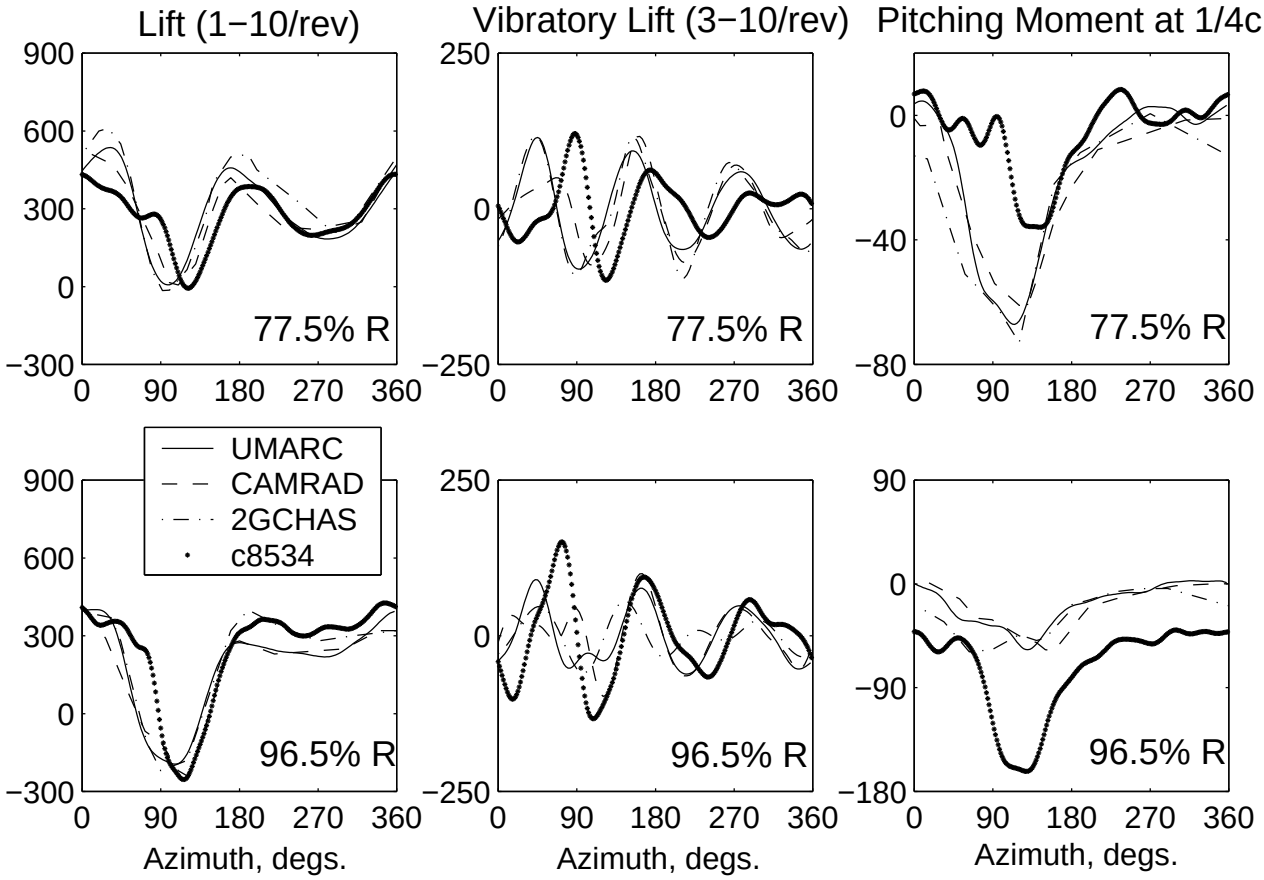

Figure 2: **State of art in predicted airloads using lifting-line comprehensive analyses; UH-60A flight 8534; high speed level flight, $\mu = 0.368$, $C_w/\sigma = 0.0783$; CAMRAD/JA and 2GCHAS from Lim (Reference 239)**

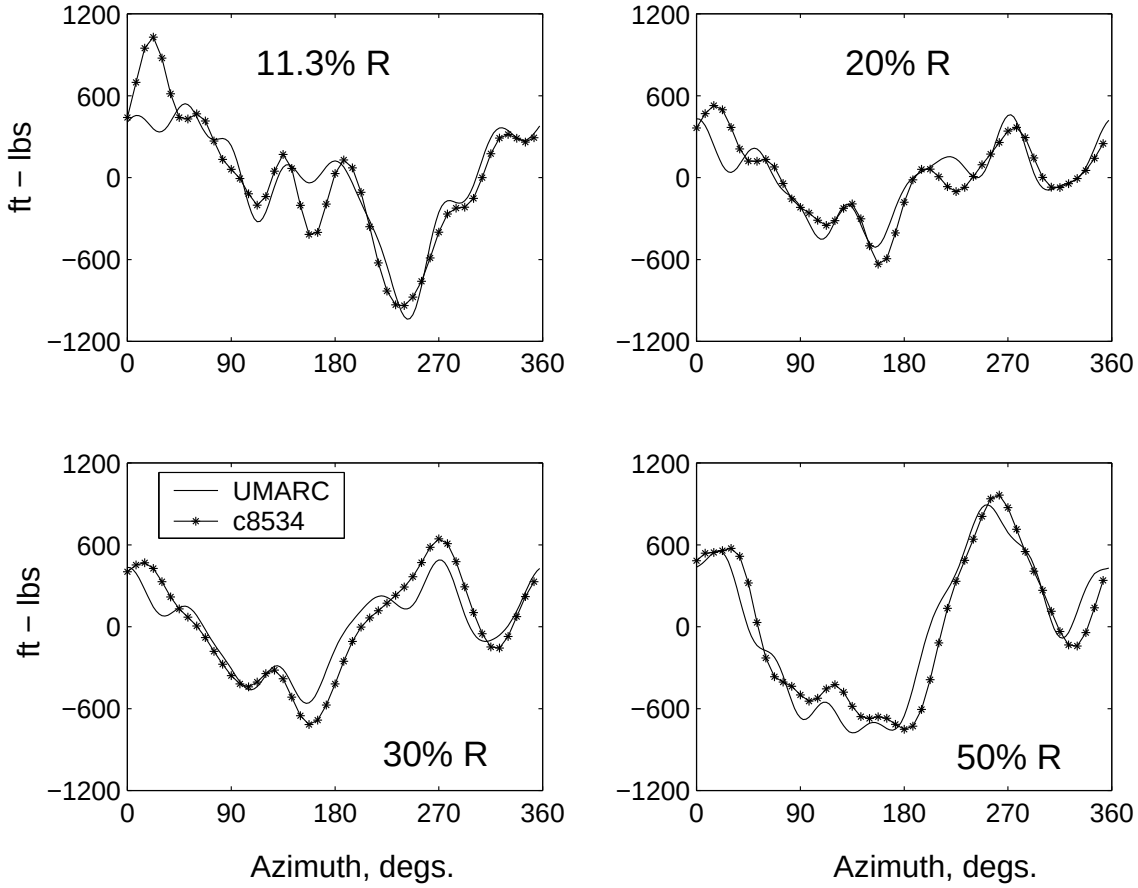

Figure 3: **Predicted and measured flap bending moments compared at four radial stations using airloads measured in flight test; UH-60A Flight C8534, $C_W/\sigma = 0.0783$, high-speed $\mu = 0.368$**

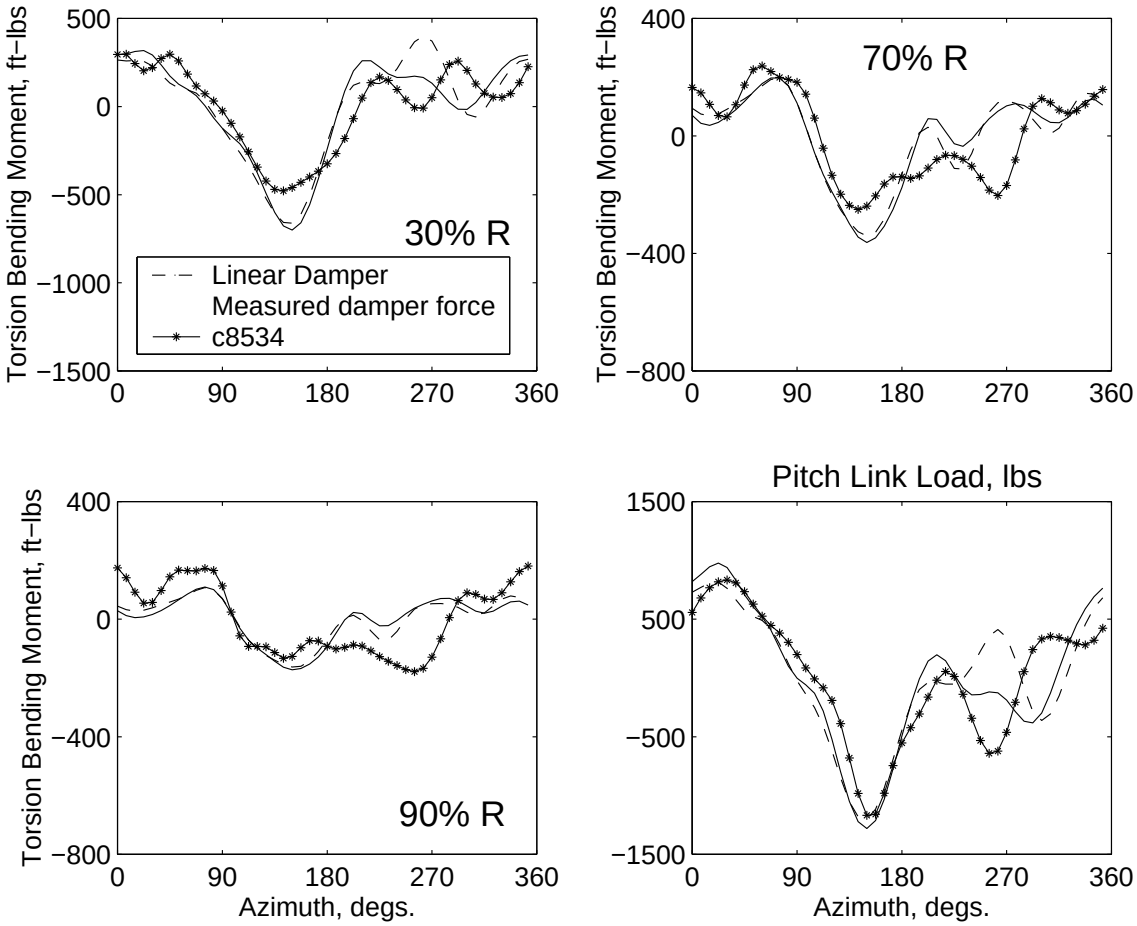

Figure 4: **Predicted and measured torsion bending moments and pitch link load for UH-60A; using airloads measured in flight test; UH-60A Flight C8534**

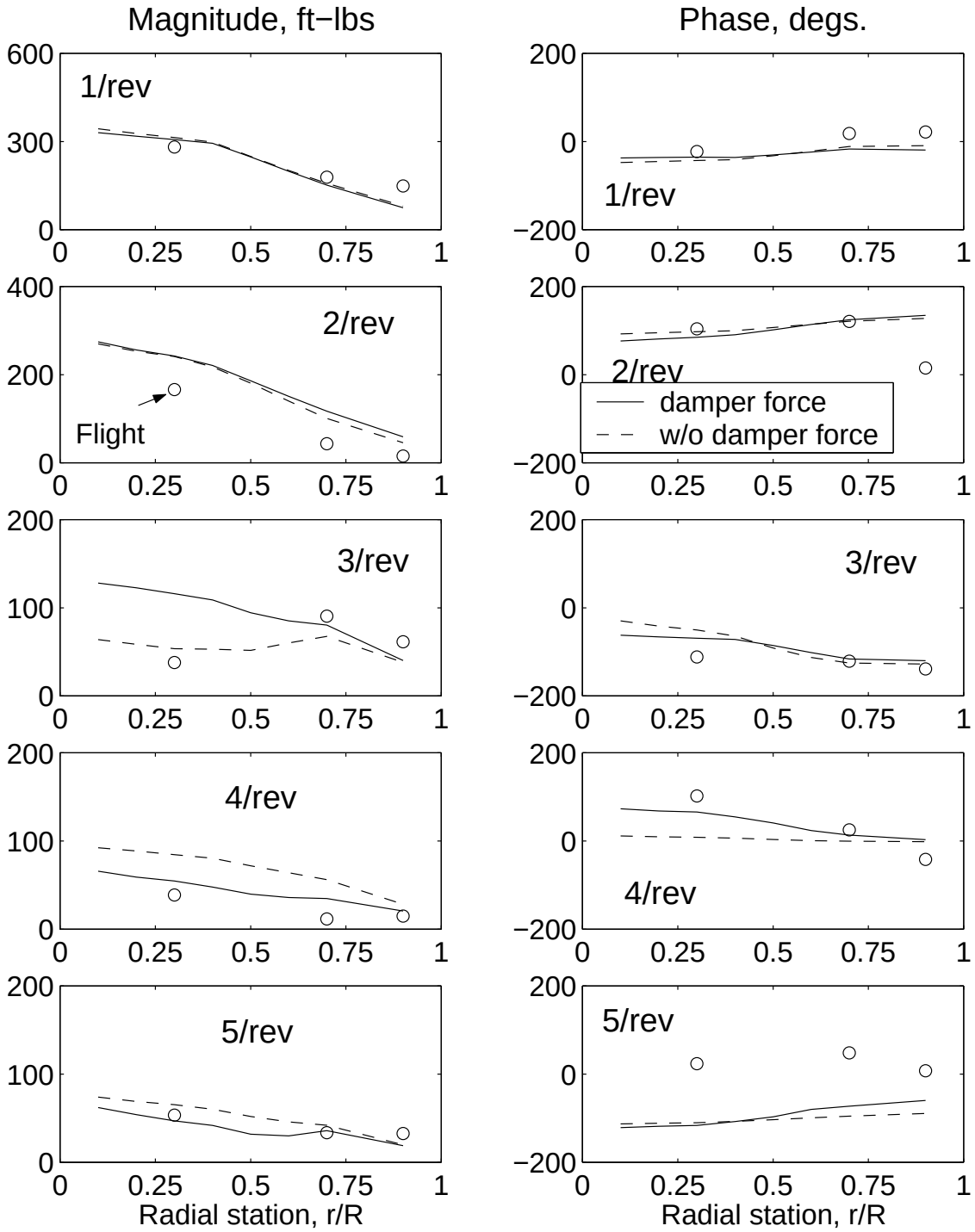

Figure 5: **Effect of measured lag damper force on the predicted torsion bending moment harmonics for UH-60A; using airloads measured in flight test; UH-60A Flight C8534**

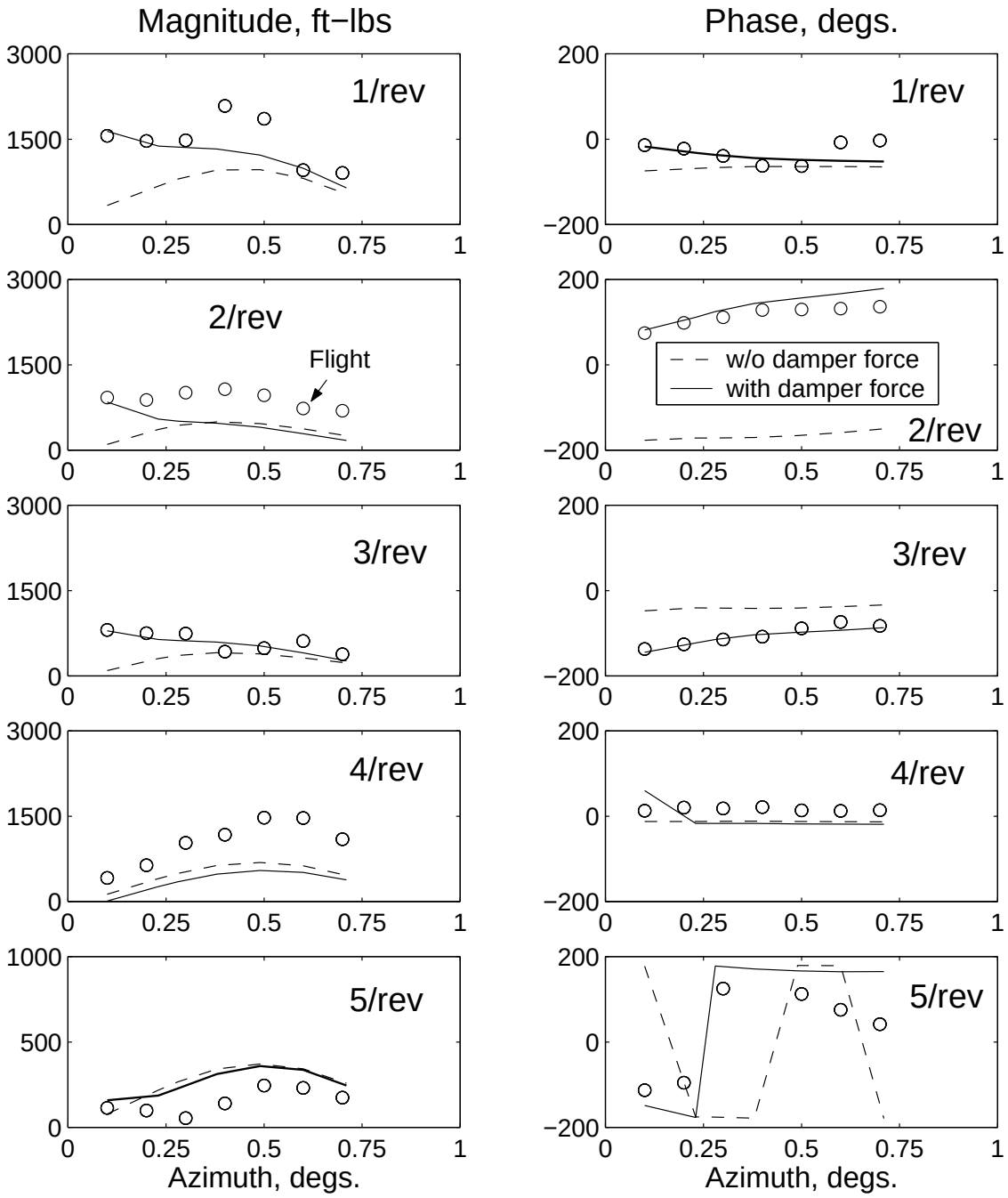

Figure 6: **Predicted and measured chord bending moments for UH-60A Black Hawk using measured air loads and damper load; UH-60A Flight C8534**

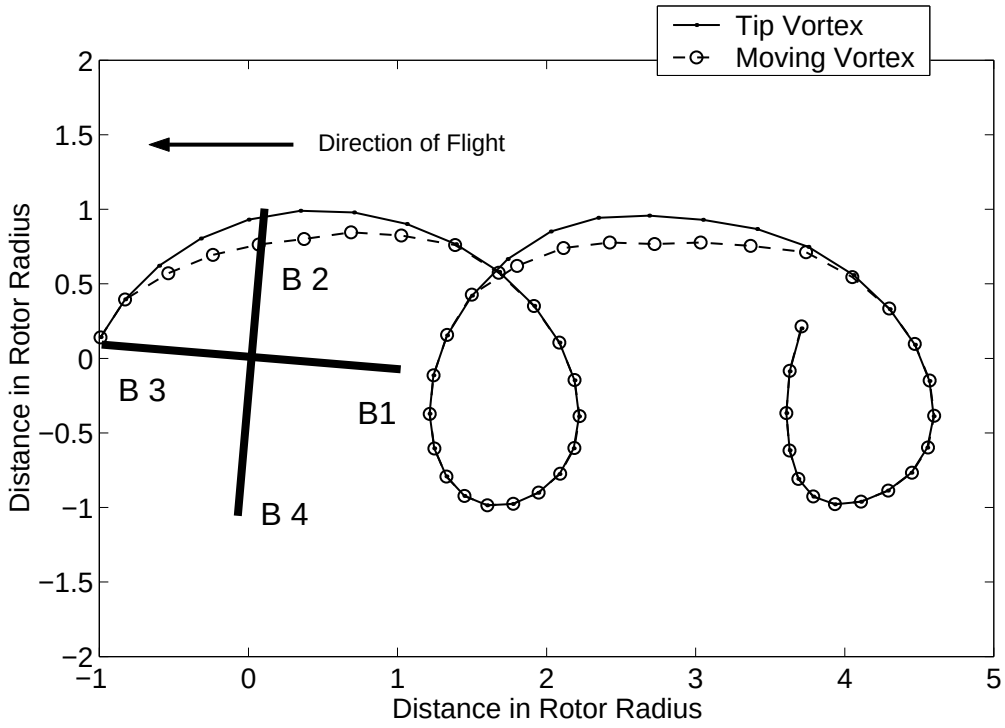

(a) Trailed vortex from Blade 3

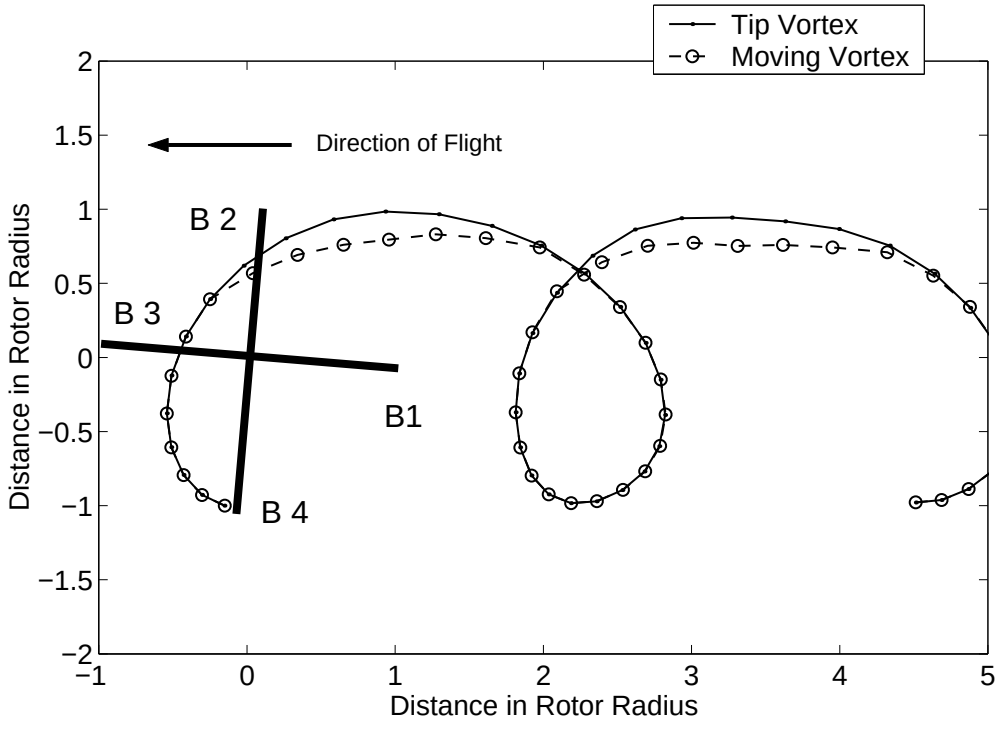

(b) Trailed vortex from Blade 4

Figure 7: **Top View of single peak tip and moving vortex free wake geometries; UH-60A Flight C8534**

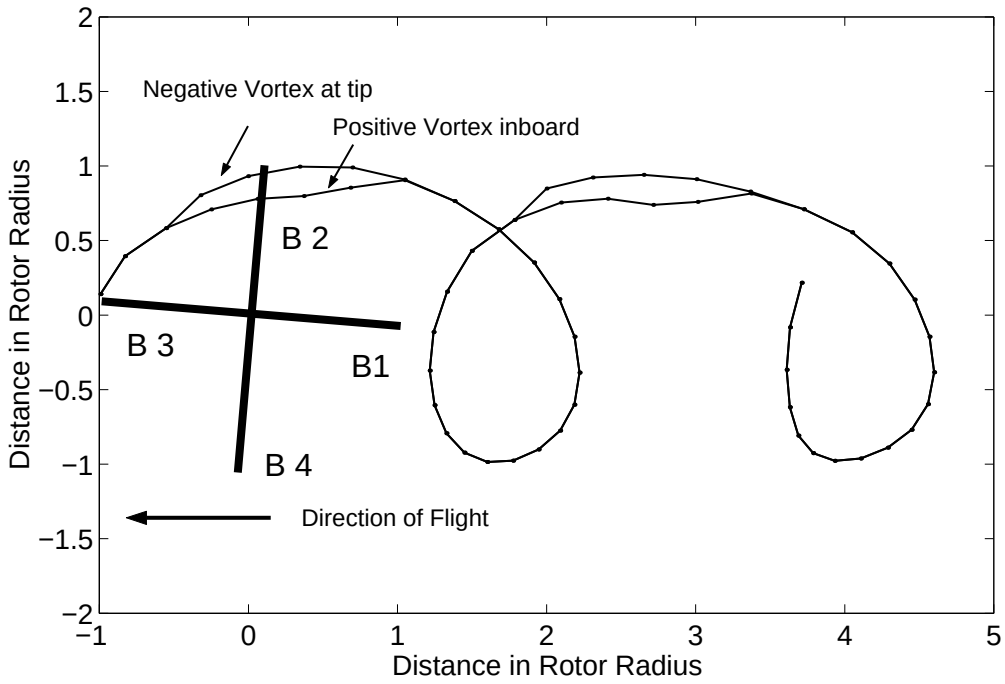

(a) Dual peak vortices from Blade 3

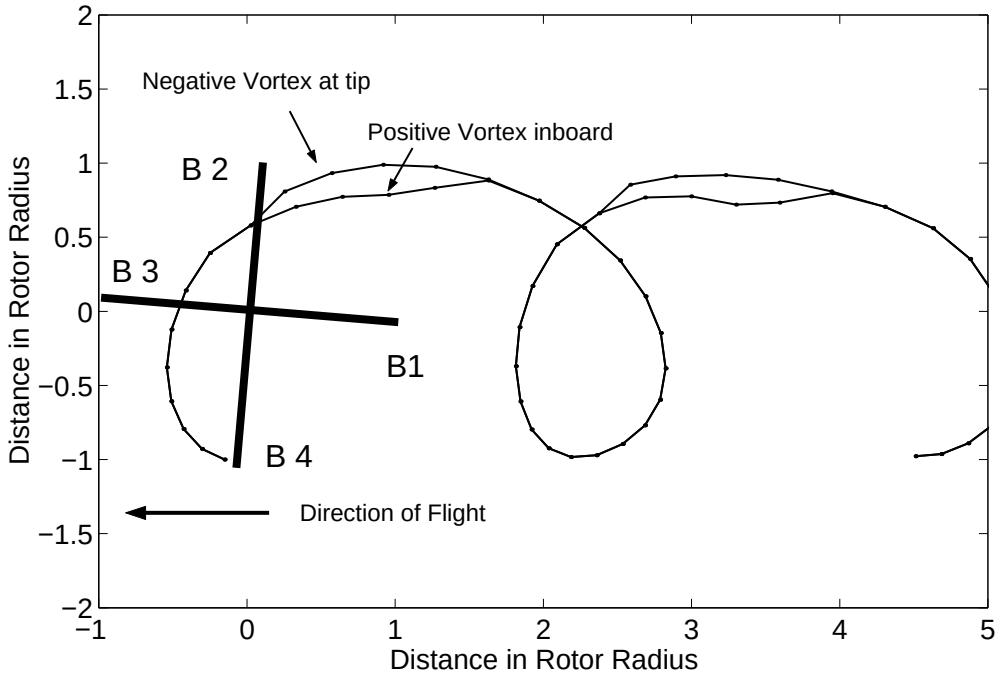

(b) Dual peak vortices from Blade 4

Figure 8: **Top View of Dual peak free wake geometries; UH-60A Flight C8534**

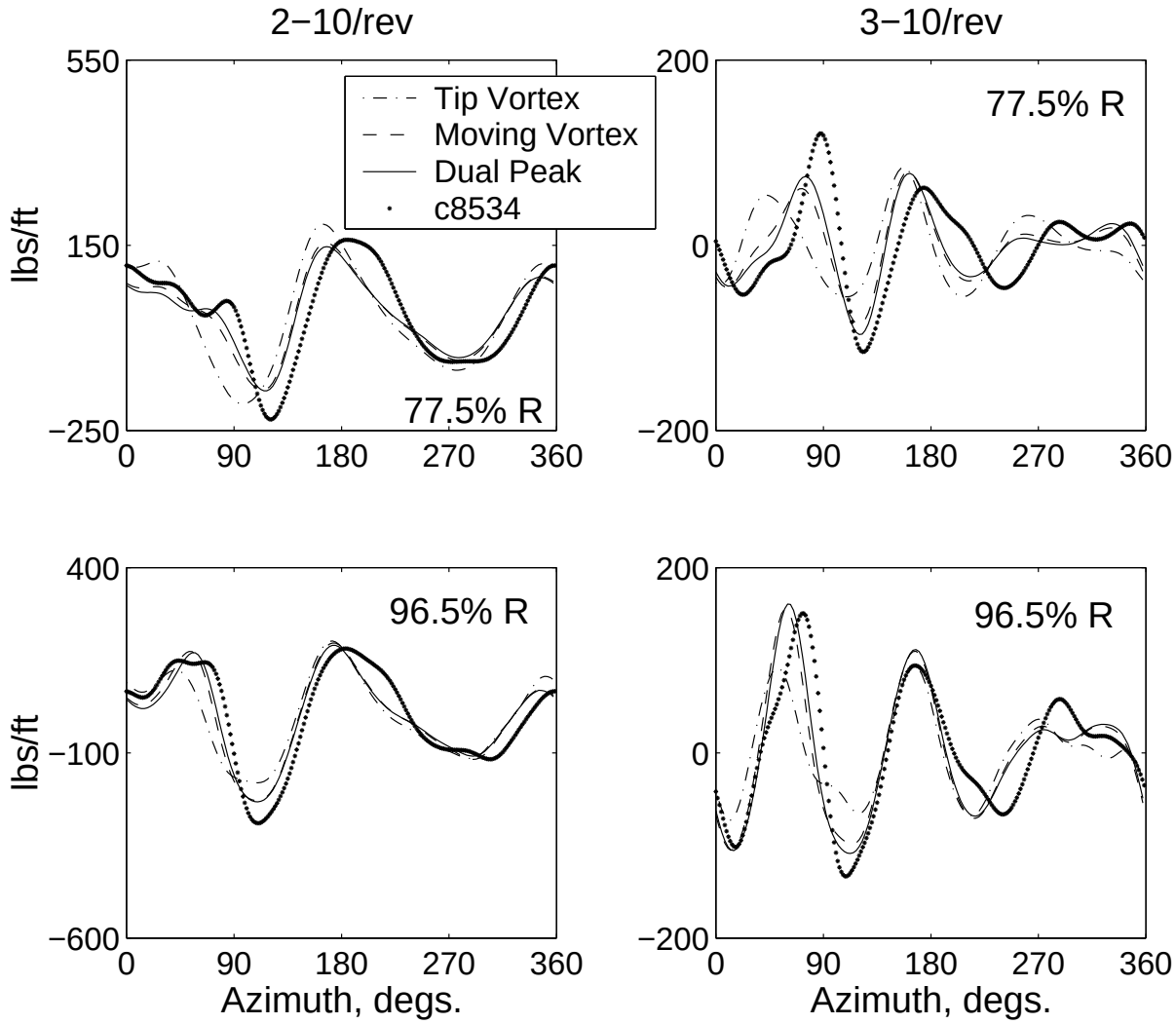

Figure 9: **Effect of free wake models on lifting-line predictions of blade lift using prescribed deformations ; UH-60A Flight C8534**

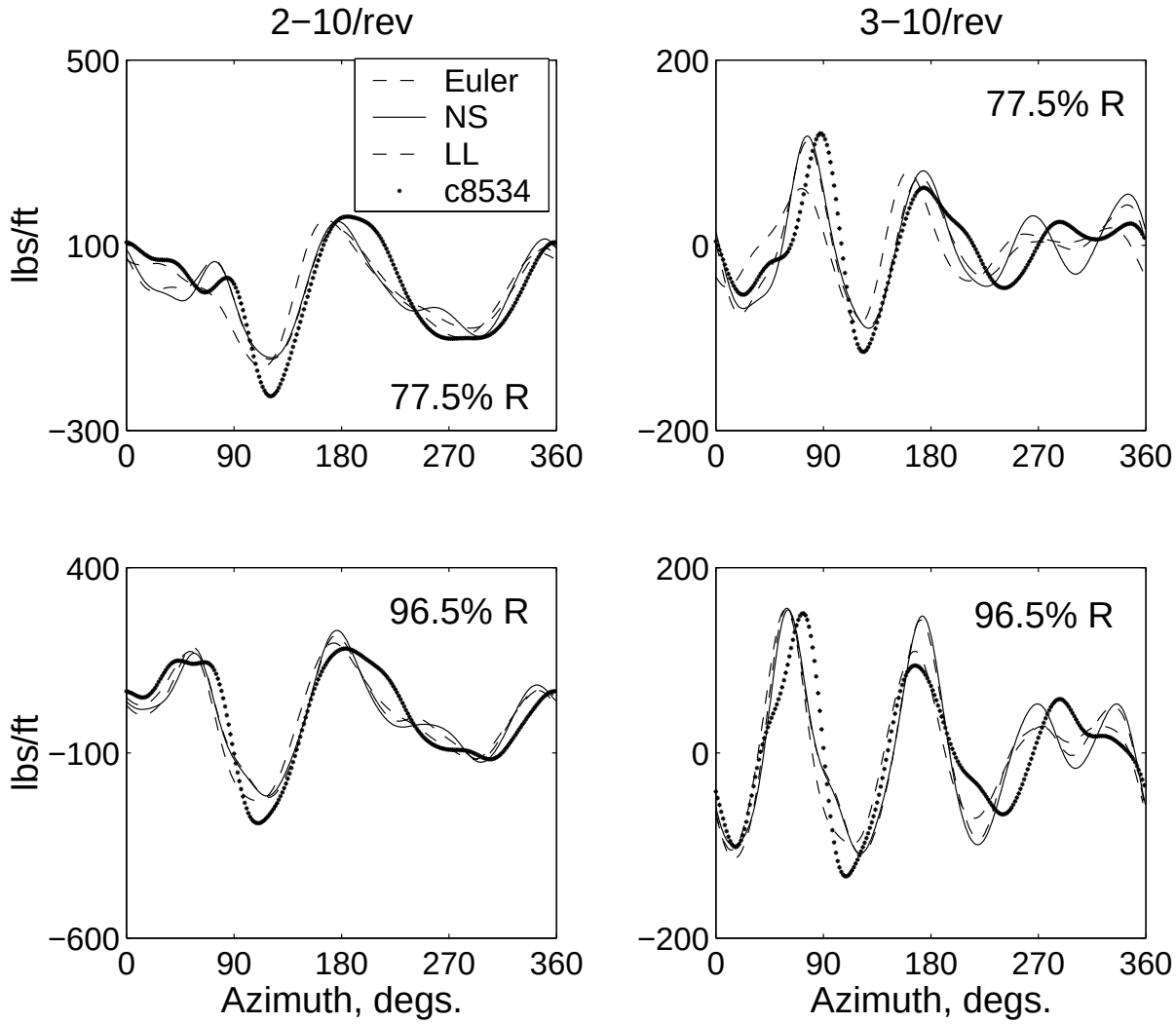

Figure 10: **Navier-Stokes, Euler and lifting-line predictions of blade lift; prescribed deformations and moving vortex free wake; UH-60A Flight C8534**

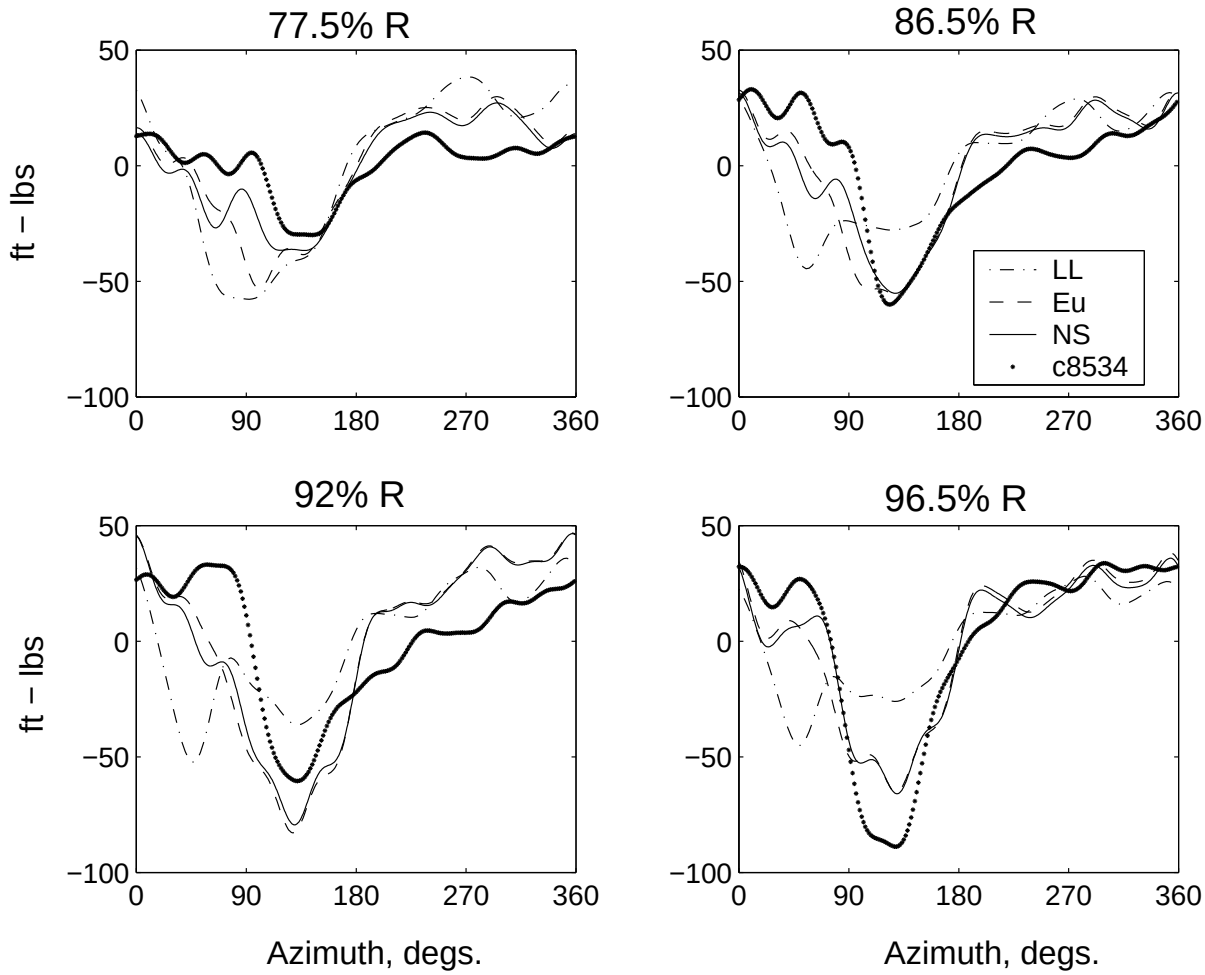

Figure 11: **Navier-Stokes, Euler and lifting-line predictions of quarter-chord pitching moments; prescribed deformations and moving vortex free wake; UH-60A Flight C8534**

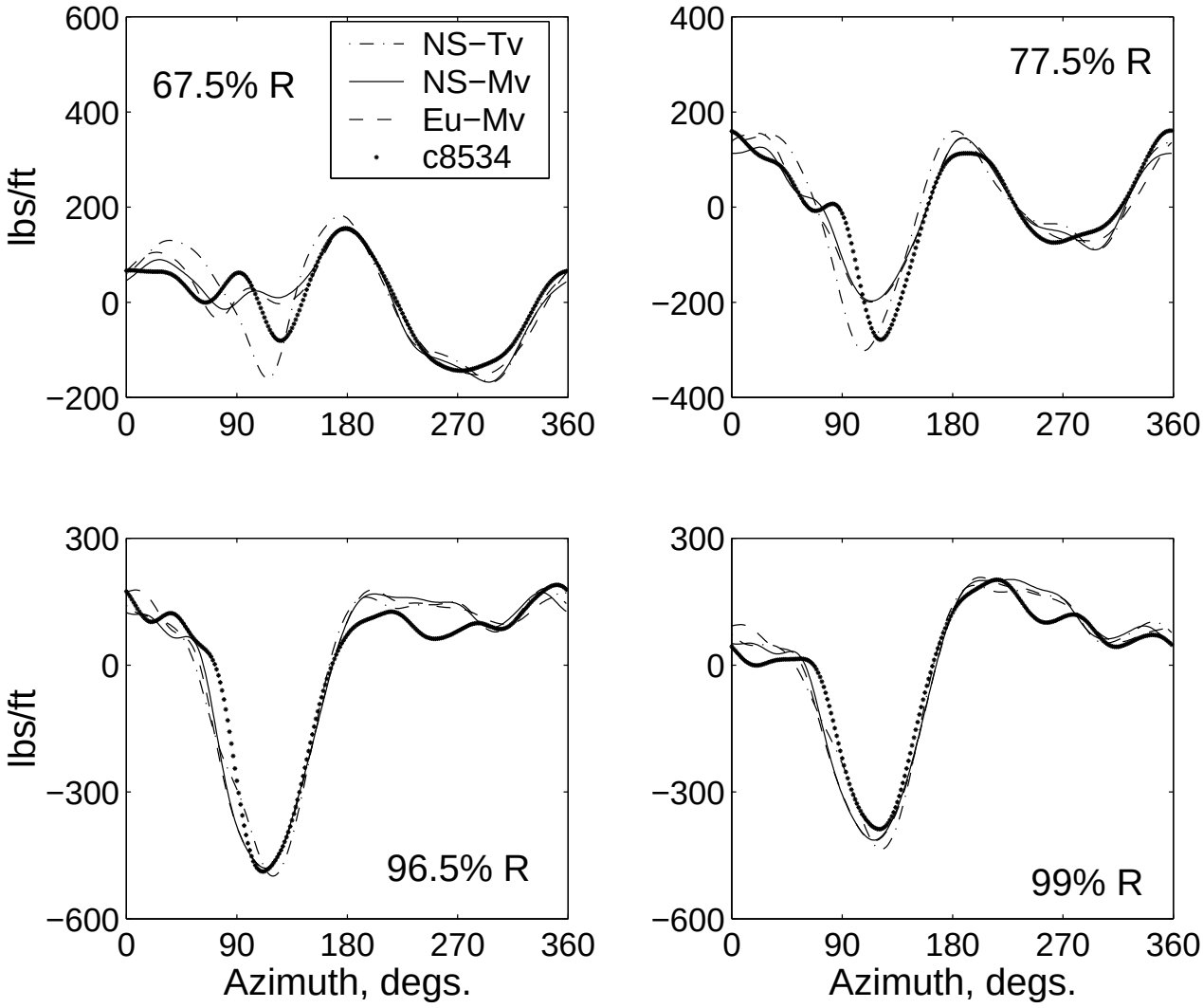

Figure 12: **Predicted UH-60A normal force (1-10/rev) using UMARC-TURNS loose coupling; Tv - Tip Vortex, Mv - Moving Vortex; NS - Navier-Stokes, Eu - Euler; UH-60A Flight C8534**

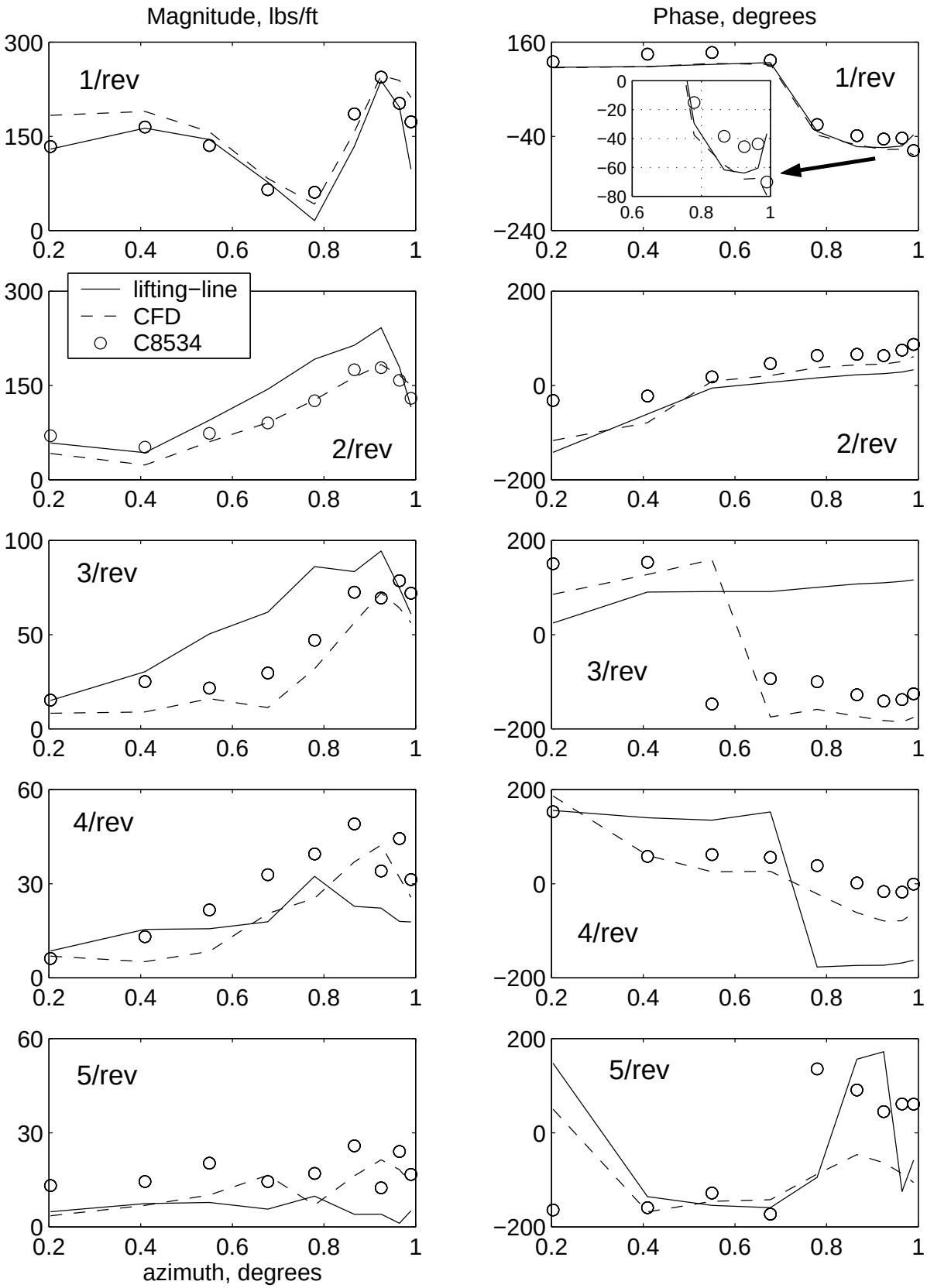

Figure 13: **Contribution of CFD in improving lift harmonics over blade span; CFD - NS with moving vortex, Lifting-line with moving vortex UH-60A Flight C8534**

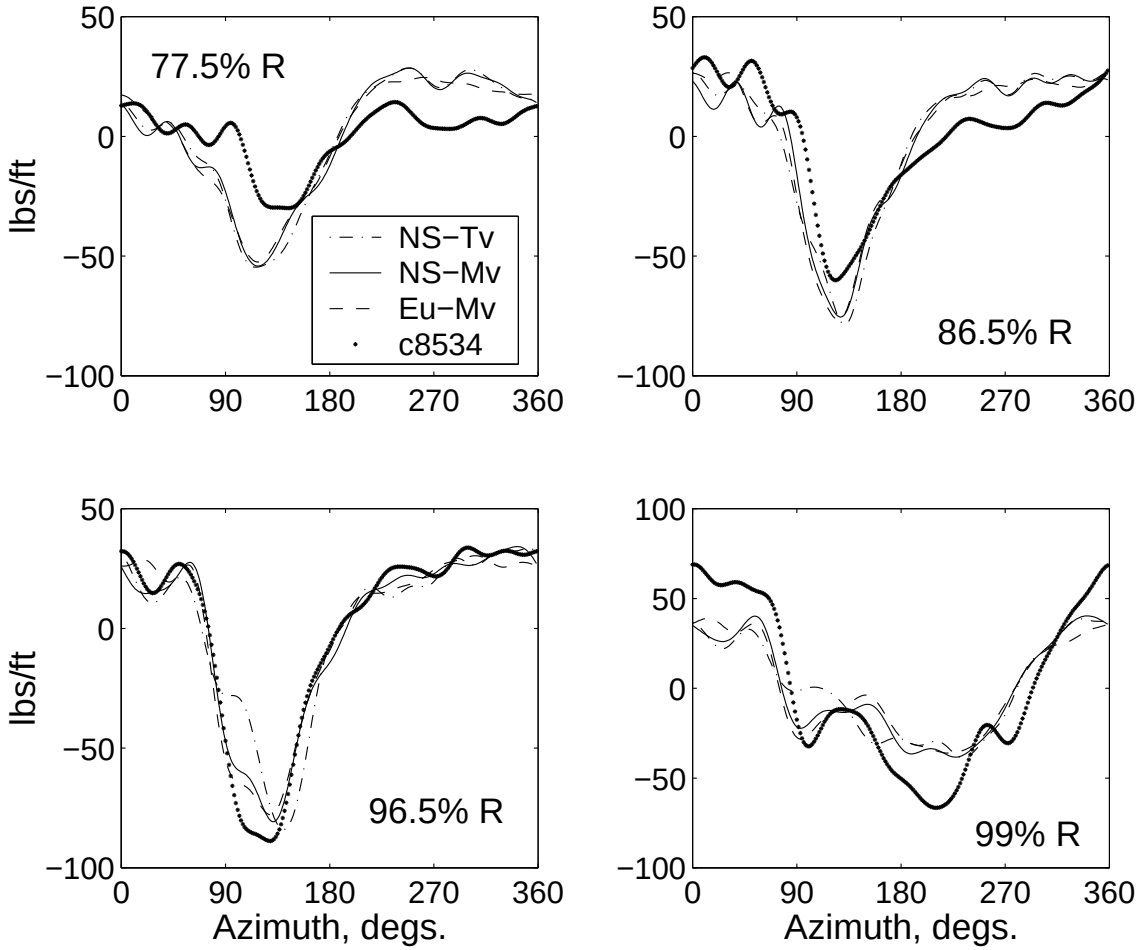

Figure 14: **Predicted UH-60A quarter-chord pitching moments (1-10/rev) using UMARC-TURNS loose coupling; Tv - Tip Vortex, Mv - Moving Vortex; NS - Navier-Stokes, Eu - Euler; UH-60A Flight C8534**

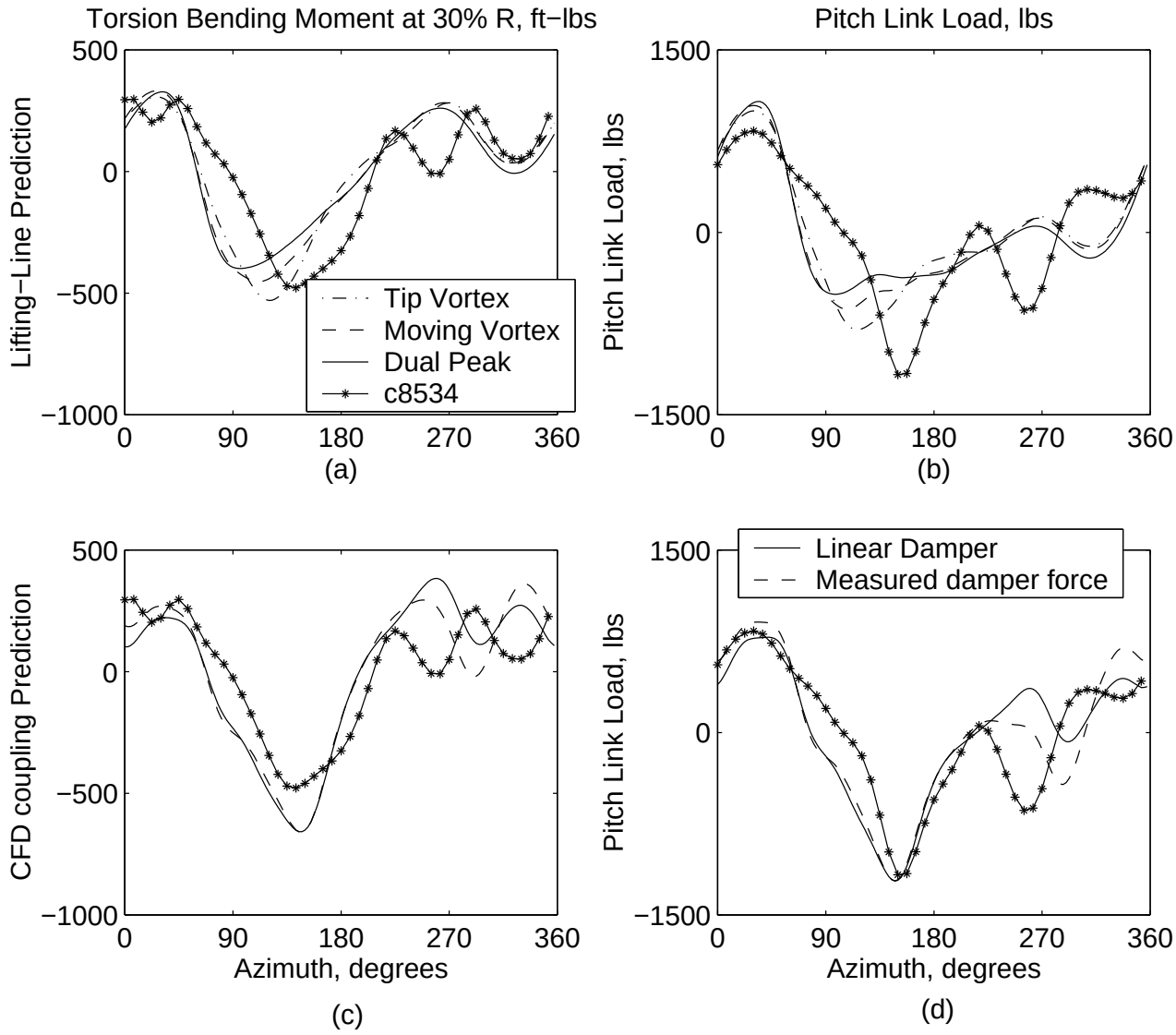

Figure 15: **Predicted torsion loads (1-10/rev); UMARC lifting-line compared with UMARC-TURNS; UMARC-TURNS uses the moving vortex model; UH-60A Flight C8534**

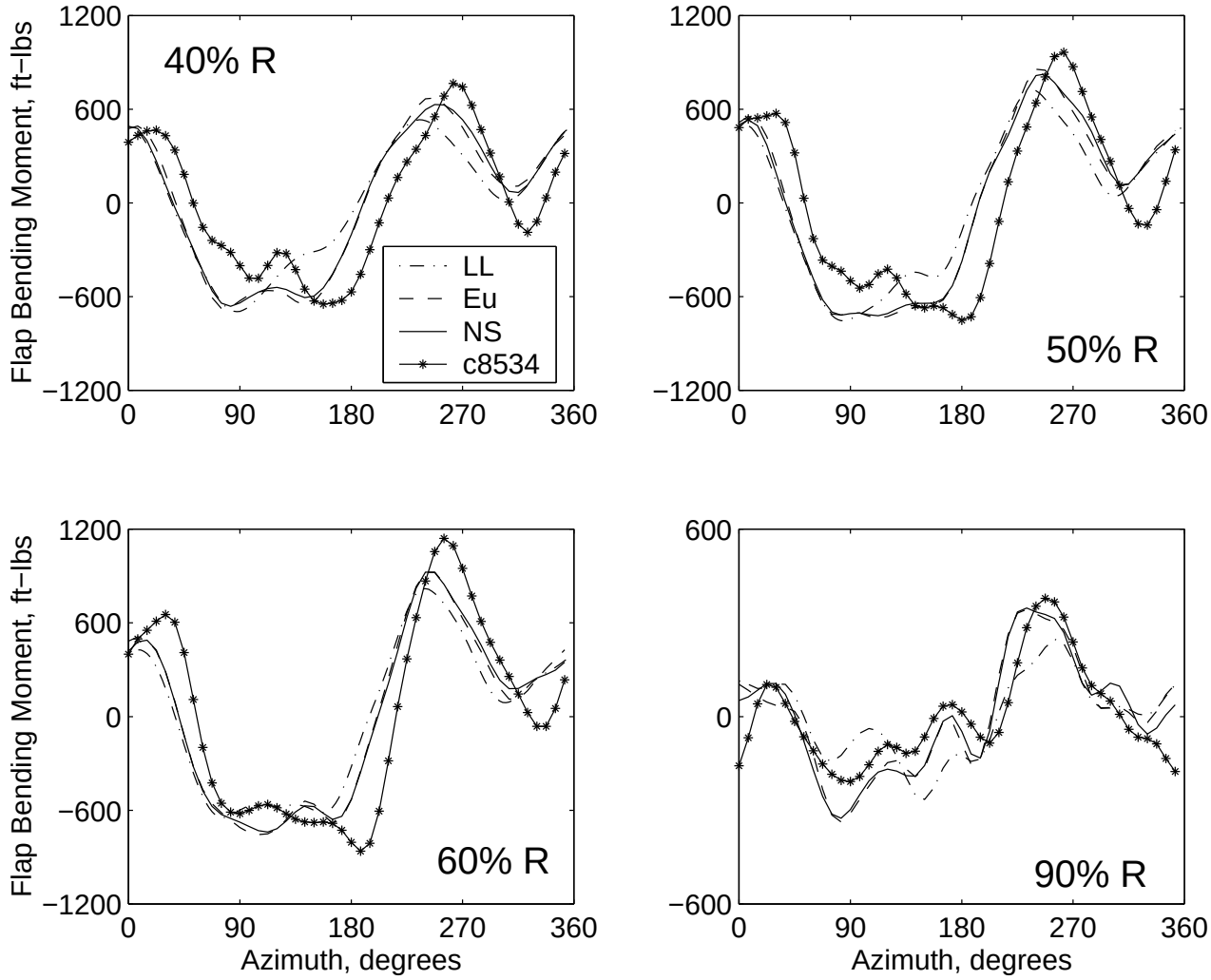

Figure 16: **Predicted flap bending moments (1-10/rev); UMARC lifting-line compared with UMARC-TURNS in NS and Euler modes; all three uses moving vortex free wake; UH-60A Flight C8534**

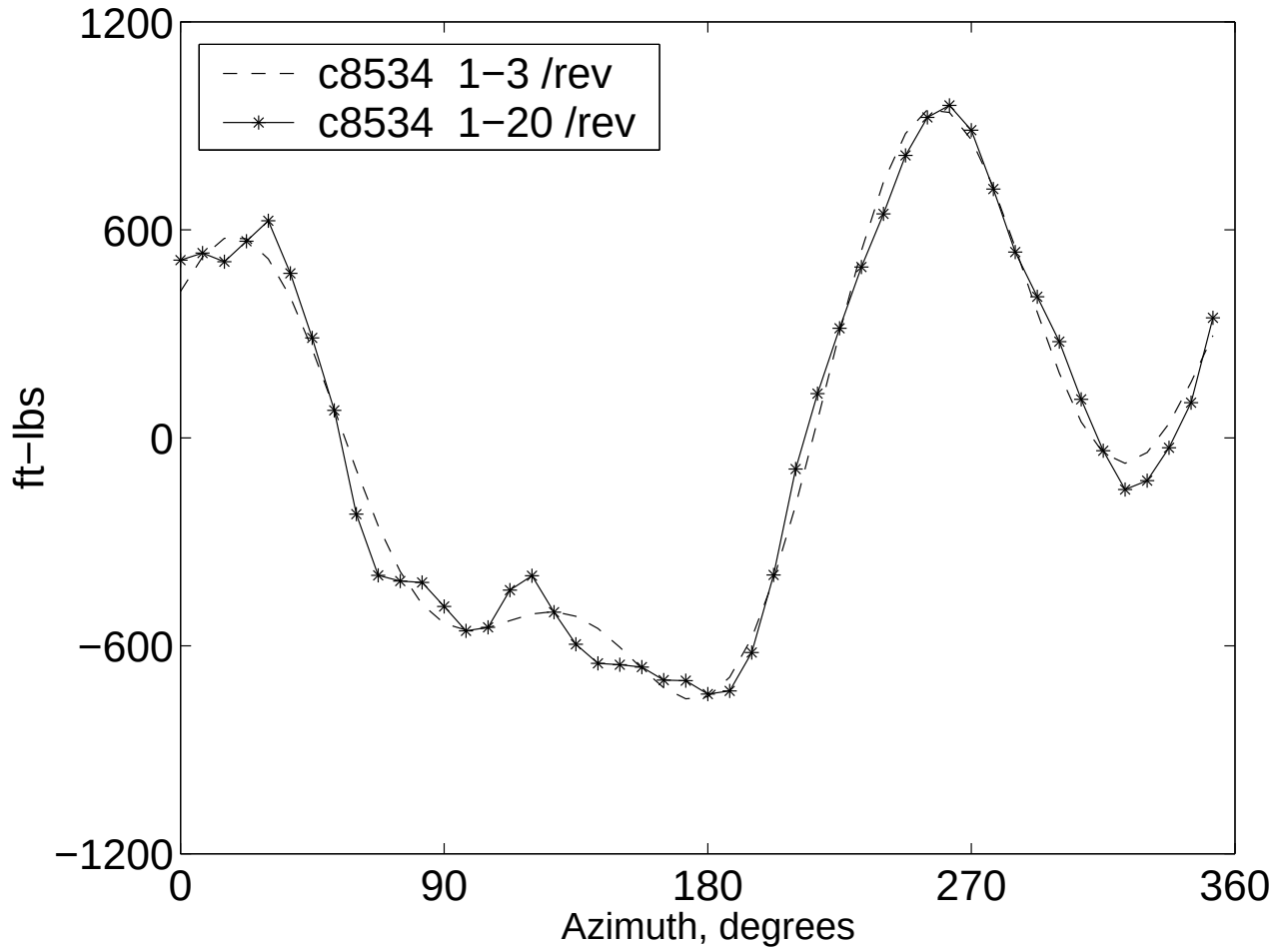

Figure 17: **Measured flap bending moment at 50% R; Waveform dominated by 1-3/rev harmonics; UH-60A Flight C8534**

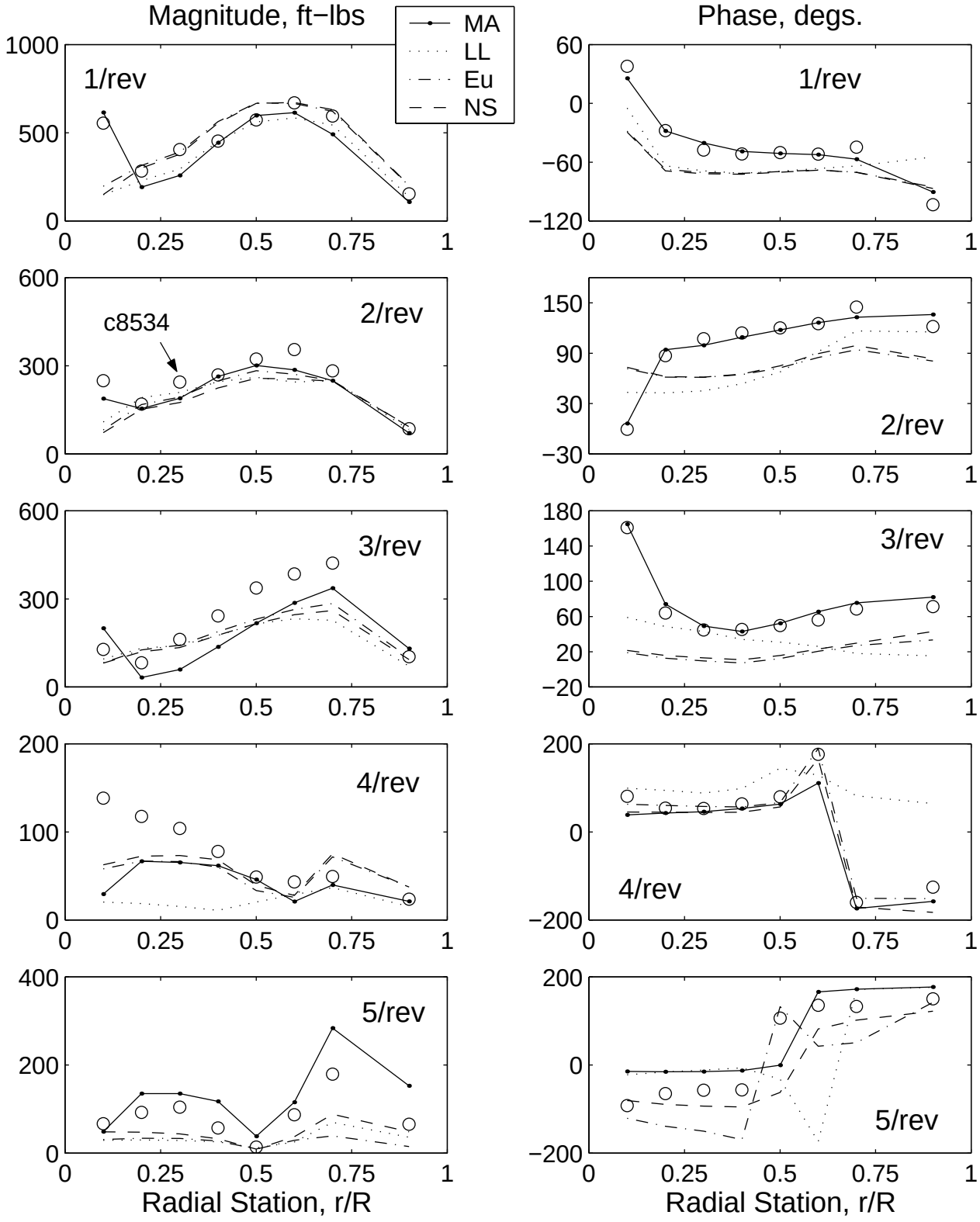

Figure 18: **Measured and predicted flap bending moment harmonics over blade span; UH-60A Flight C8534**

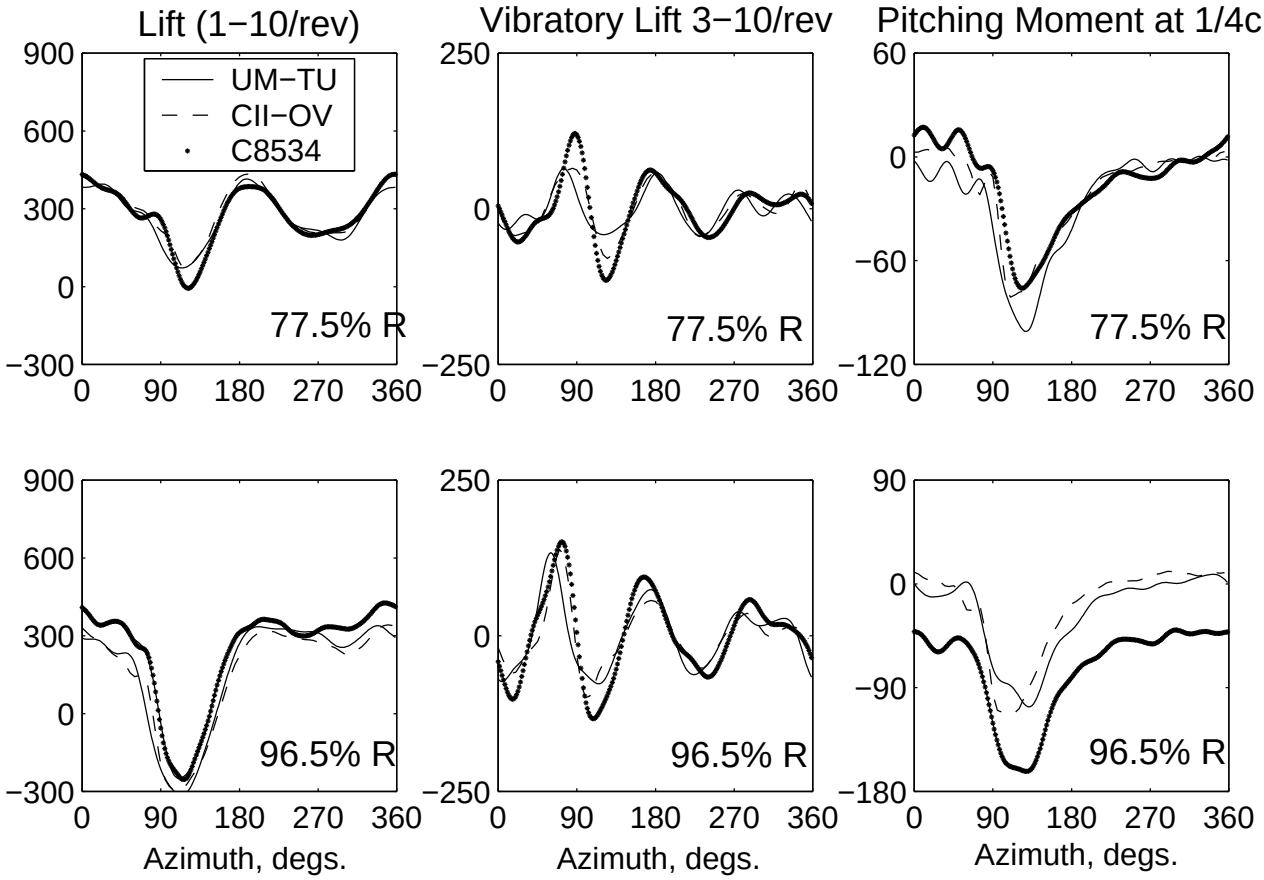

Figure 19: **State of art in predicted airloads using CFD/CSD loose coupling; UH-60A flight 8534; high speed level flight, $\mu = 0.368$, $C_w/\sigma = 0.0783$; CAMRAD II/OVERFLOW from Potsdam (Reference 23)**